CUMULATIVE EFFECTS OF OFFSHORE WIND FARMS ON DISPERSAL CORRIDORS FOR NON-INDIGENOUS SPECIES AND ECOSYSTEM INDICATORS

Scientific Report from DCE – Danish Centre for Environment and Energy No. 688 2026

AARHUS
UNIVERSITY
DCE – DANISH CENTRE FOR ENVIRONMENT AND ENERGY

CUMULATIVE EFFECTS OF OFFSHORE WIND FARMS ON DISPERSAL CORRIDORS FOR NON-INDIGENOUS SPECIES AND ECOSYSTEM INDICATORS

Scientific Report from DCE – Danish Centre for Environment and Energy No. 688 2026

Charlotte H. Clubley
Christian Mohn
Janus Larsen
Vibe Schourup-Kristensen
Ange P. Ishimwe
Eva Friis Møller
Karsten Dahl
Marie Maar

Aarhus University, Department of Ecoscience

AARHUS
UNIVERSITY
DCE – DANISH CENTRE FOR ENVIRONMENT AND ENERGY

Data sheet

Series title and no.:	Scientific Report from DCE – Danish Centre for Environment and Energy No. 688
Category:	Scientific advisory report
Title:	Cumulative effects of offshore wind farms on dispersal corridors for non-indigenous species and ecosystem indicators
Author(s):	Charlotte H. Clubley, Christian Mohn, Janus Larsen, Vibe Schourup-Kristensen, Ange P. Ishimwe, Eva Friis Møller, Karsten Dahl, Marie Maar
Institution(s):	Aarhus University, Department of Ecoscience.
Publisher:	Aarhus University, DCE – Danish Centre for Environment and Energy ©
URL:	http://dce.au.dk/en
Year of publication:	January 2026
Editing completed:	December 2025
Referee(s):	Christian Lønborg
Quality assurance, DCE:	Anja Skjoldborg Hansen
Linguistic QA:	Charlotte Kler
External comments:	The comments can be found here:
Financial support:	Danish Energy Agency
Please cite as:	Clubley CH, Mohn C, Larsen J, Schourup-Kristensen V, Ishimwe A, Møller EF, Dahl K, Maar M. 2026. Cumulative effects of offshore wind farms on dispersal corridors for non-indigenous species and ecosystem indicators. Aarhus University, DCE – Danish Centre for Environment and Energy, 73 pp. Scientific Report No. 688

Abstract:	This report provides a model assessment of the dispersal corridors of non-indigenous species and the interannual variability of ecosystem indicators in scenarios of offshore wind farm development in the North Sea and the Inner Danish waters.

Keywords:	Offshore wind, non-indigenous species, dispersal, interannual variability, ecosystem indicators, accumulated effects, hydrodynamics, biogeochemistry
Front page photo:	Colorbox
ISBN:	978-87-7648-011-0
ISSN (electronic):	2244-9981
Number of pages:	73

Contents

Preface

This report contributes to the project "*Environmental mapping and screening of areas for offshore wind in Denmark*" initiated in 2022 by the Danish Energy Agency. The project aims to support the long-term planning of offshore wind farms by providing a comprehensive overview of the combined offshore wind potential in Denmark. It is funded under the Finance Act 2022 through the programme "Investeringer i et fortsat grønnere Danmark" (Investing in the continuing greening of Denmark). The project is carried out by NIRAS, Danish Centre for Environment and Energy (DCE), Aarhus University (Department of Ecoscience) and Danish Technical University (DTU) Wind.

The overall project consists of four tasks defined by the Danish Energy Agency (https://ens.dk/energikilder/planlaegning-af-fremtidens-hav-vindmoelleparker):

1. Sensitivity mapping of nature, environmental, wind and hydrodynamic conditions.
2. Technical fine-screening of areas for offshore wind based on the sensitivity mapping and relevant technical parameters.
3. Assessment of potential cumulative effects from large-scale offshore wind development in Denmark and neighbouring countries.
4. Assessment of barriers and potentials in relation to coexistence.

This report addresses Task 3: Assessment of potential cumulative effects. In the first part of the study, 3D agent-based modelling is used to estimate potential dispersal corridors of non-indigenous species from offshore wind farms in the southern North Sea into Danish waters. In the second part, the interannual variability and accumulated effects over time of offshore wind farms on ecosystem indicators are assessed using 3D modelling within the North Sea and Inner Danish waters. The cumulative effects only consider the interaction between multiple offshore wind farms in Denmark and neighbouring areas in defined scenarios and not the cumulative effects of all pressures in the area. Other subjects within Task 3 - on marine mammals, seabirds and underwater noise will be presented in separate reports in early 2026.

The project management teams at both AU and NIRAS have contributed to the description of the background for the report and the relation to other activities in the preface. The report and the work contained within are solely the responsibility of the authors.

Sammenfatning

Denne rapport giver en modelbaseret vurdering af de kumulative effekter af havvindmølleparker på spredningskorridorer og den årlige variation af økosystemindikatorer i scenarier for udvikling af havvind i Nordsøen og de Indre Danske farvande. To modelscenarier vurderede effekten af i) den nuværende fordeling af havvindmølleparker og ii) en potentiel fremtidig fordeling i 2030 af havvindmølleparker i forhold til et scenarie uden vindmølleparker i Nordsøen og de Indre Danske farvande.

3D FlexSem modellen blev anvendt til at beskrive effekter af havvind på hydrodynamik og biogeokemi. Wake-effekten blev estimeret af DTU ved hjælp af en 3D atmosfærisk model med realistiske fordelinger og størrelser af vindmølleparker i havet og på land. Desuden ændrede møllefundamenternes vandmodstand lokalt havstrømmen og turbulensen i den hydrodynamiske model. De koblede hydrodynamiske-biogeokemiske modeller blev valideret med overvågningsdata. Den årlige variation blev vurderet for årene 2019 og 2020. År 2020 viste generelt lavere vindhastigheder om sommeren og højere om vinteren og var varmere end 2019.

I første del af undersøgelsen blev der anvendt en 3D hydrodynamisk-agentbaseret model til at estimere potentielle spredningskorridorer for ikke-hjemmehørende arter fra havvindmølleparker i den sydlige Nordsø og ind i de Indre Danske farvande. Alle modelscenarier viste, at de ikke-hjemmehørende arter driver langs en 'blå korridor' (ikke-tilfældige spredningsveje) fra den Tyske Bugt nordpå langs den danske vestkyst mod indgangen til Kattegat. Fra Kattegat driver agenterne overvejende sydpå langs den svenske vestkyst. Resultaterne fra begge modelscenarier og begge år (2019 og 2020) indikerer, at spredning af ikke-hjemmehørende arter fra Nordsøen gennem de Indre Danske farvande og ind i Østersøen er både mulig og sandsynlig over flere generationer af populationen.

I 2019 spredte de ikke-hjemmehørende arter sig over et relativt bredt geografisk område og fortsatte østpå mod Bornholm. Derimod viste scenariet for 2020 markant færre agenter, der drev syd for Sjælland, hvilket tyder på betydelig årlig variation i spredningsveje – sandsynligvis drevet af reducerede strømhastigheder det år. Samlet set kan havvindmølleparker fungere som spredningskorridorer ('stepping stones') for ikke-hjemmehørende arter både under nuværende forhold og i lyset af fremtidig udbygning af havvind.

I anden del af undersøgelsen blev den årlige variation og de akkumulerede effekter af havvindmølleparker på økosystemindikatorer vurderet ved hjælp af 3D hydrodynamisk-biogeokemisk modellering. Økosystemindikatorernes respons på havvind var markant forskellig mellem de to undersøgte år både i Nordsøen og de Indre Danske farvande. Dette resultat understreger vigtigheden af at tage højde for den årlige variation for fuldt ud at forstå og estimere effekterne af havvind på havmiljøet i forhold til den naturlige variation i økosystemet.

De akkumulerede effekter mellem år for visse økosystemindikatorer antyder en form for hukommelse i begge havøkosystemer med hensyn til påvirkninger fra havvind. Dette indebærer en potentiel langsigtet opvarmningstendens i begge bassiner forbundet med udviklingen af havvind. Ligeledes kan en faldende tendens i bundiltindhold være under udvikling i Nordsøen. I de Indre

Danske farvande synes havvindmølleparker at have forårsaget en rumlig omfordeling af bundiltindholdet, hvilket kan intensiveres over tid. For at kunne vurdere disse langsigtede økosystemreaktioner ud over den årlige variation ville det dog være nødvendigt at køre modellen for en længere periode.

Summary

This report provides a model assessment of cumulative effects of offshore wind farms on dispersal corridors and interannual variability of ecosystem indicators in scenarios of offshore wind farm development in the North Sea and the Inner Danish waters. Two model scenarios evaluated the impact of i) current distribution and ii) potential future distribution in 2030 of offshore wind farms relative to a scenario without wind farms in the North Sea and the Inner Danish waters.

The 3D FlexSem model system was used to describe the effects of offshore wind farms on hydrodynamics and biogeochemistry. The wake effect was estimated by DTU using a 3D atmospheric model with realistic distributions and sizes of onshore and offshore wind farms. The monopile drag effect changed the currents and turbulence in the hydrodynamic model. The coupled hydrodynamic-biogeochemical models were validated against monitoring data. The interannual variability was assessed for two years, 2019 and 2020. Year 2020 showed lower wind speeds during summer and higher during winter and was warmer than 2019.

In the first part of the study, 3D hydrodynamic–agent-based modelling was employed to estimate potential dispersal corridors for non-indigenous species from offshore wind farms in the southern North Sea into the Inner Danish waters. All model scenarios showed that model agents representing non-indigenous species drift along a 'blue corridor' (non-random dispersal pathway) from the German Bight northwards following the western Danish coastline towards the entrance to the Kattegat. From the Kattegat, non-indigenous species agents predominantly drifted southwards along the Swedish coastline. The results from both model scenarios and both years (2019 and 2020) indicate that, given multiple generations, the spread of non-indigenous species from the North Sea through the Inner Danish waters and into the Baltic Sea proper is both feasible and likely.

In 2019, non-indigenous species agents dispersed across relatively broad spatial scales, continuing eastward toward the island of Bornholm. In contrast, year 2020 showed significantly fewer agents drifting south of Zealand, suggesting substantial interannual variability in dispersal pathways—likely driven by reduced current speeds in that year. Overall, the offshore wind farms were found to act as stepping stones in facilitating the spread of non-indigenous species both under current conditions and in light of future offshore wind expansion.

In the second part of the study, the interannual variability and accumulated effects between years of offshore wind farms on ecosystem indicators (stratification index, temperature, current speed, primary production, Chlorophyll a (Chl *a*) and bottom oxygen) were assessed using 3D hydrodynamic-biogeochemical modelling. Ecosystem indicator responses to offshore wind were significantly different between the two considered years in the North Sea and Inner Danish waters. This result highlights the importance of considering the interannual variability to fully understand and estimate the effects of offshore wind on the marine environment in comparison to the natural variability of the ecosystem.

The found accumulated effects between years for certain ecosystem indicators suggest a form of ecological memory in both marine ecosystems regarding the impacts of offshore wind. This implies the potential for a long-term warming

trend in both basins associated with offshore wind development. Similarly, a declining temporal trend in bottom oxygen levels may be emerging in the North Sea. In the Inner Danish waters, offshore wind farms appear to have caused a spatial redistribution of oxygen content, which could intensify over time. However, to fully assess these long-term ecosystem responses beyond interannual variability, data spanning more than the considered two years would be necessary.

1 Introduction

1.1 Offshore wind farms as dispersal corridors for marine species

Danish marine waters support biodiversity-rich habitats that provide vital ecosystem services, including fisheries, tourism and carbon and nutrient sequestration. These waters also serve as donor areas of benthic species for the less diverse Baltic Sea, where lower salinities limit species richness (Ojaveer et al. 2010, Vuorinen et al. 2015). However, marine biodiversity in Danish waters is under pressure from eutrophication, overfishing, physical disturbance, climate change and the spread of non-indigenous species (Oesterwind et al. 2016, Andersen et al. 2020, Jensen et al. 2023). The planned expansion of the offshore wind industry in this area is also likely to introduce new, or exacerbate existing, pressures that must be accounted for in future environmental impact assessments. For example, in the Baltic Sea alone it is expected that an area of 11,000 km^2 will be dedicated to offshore wind by 2030 (Pettersen et al. 2023). Within offshore wind parks, turbine foundations and scour protection introduce artificial hard substrates that have the potential to support sessile species (i.e., those that are attached permanently to a surface) differing from those in surrounding natural habitats (Wilhelmsson and Malm 2008, Andersson and Öhman 2010).

Natural reef habitats with hard, stable surface substrates are particularly well-documented in the northeastern North Sea and Skagerrak, along the eastern coast of England and within the English Channel. Smaller reef occurrences have also been identified in areas such as the German Bight, notably within Natura 2000 sites such as Borkum Riffgrund and near Helgoland (EUSeaMap Broad-Scale Predictive Habitat Map for Europe; Vasquez et al. 2023). Boulder reef sites are, on the other hand, very common in the Kattegat and the Belt Sea area, and rocky shorelines prevail on most of the Skagerrak and Kattegat coastline along Norway and Sweden. However, in the southern North Sea bottom trawling has significantly degraded natural hard-bottom habitats, disturbing the seafloor, damaging biogenic habitats and causing mortality among benthic invertebrates (Rijnsdorp et al. 2016 and references therein). Such impacts can significantly reduce structural complexity, altering the composition and function of these benthic ecosystems (Thrush and Dayton 2002, van Denderen et al. 2015). The introduction of artificial hard substrates through offshore wind farms (e.g., monopiles, scour protection) has been suggested as a strategy to boost local biodiversity of marine flora and fauna in areas where these impacts are realised (ter Hofstede et al. 2022).

However, much of the North Sea seabed is characterised by surface sediments classified as well-sorted sandy deposits, with smaller areas mapped as mixed sediments, referring to unsorted deposits of glacial origin (Figure 1.1.1). Therefore, in many areas the construction of offshore wind farms is likely to introduce artificial hard substrates to areas naturally dominated by soft, sandy sediments, potentially negatively affecting the associated soft sediment communities (Degraer et al. 2013, Heery et al. 2017). In fact, in their recent report Göke et al. (2025) found 'infralittoral sand' to be the most affected broad habitat type in the North Sea by offshore wind constructions. Offshore wind construction may also conflict with the newly set threshold (maximum 2% loss and maximum 25% adversely affected) for broad-scale habitats according to the EU Marine Strategy Framework Directive (MSFD) Descriptor 6 "Sea-floor integrity".

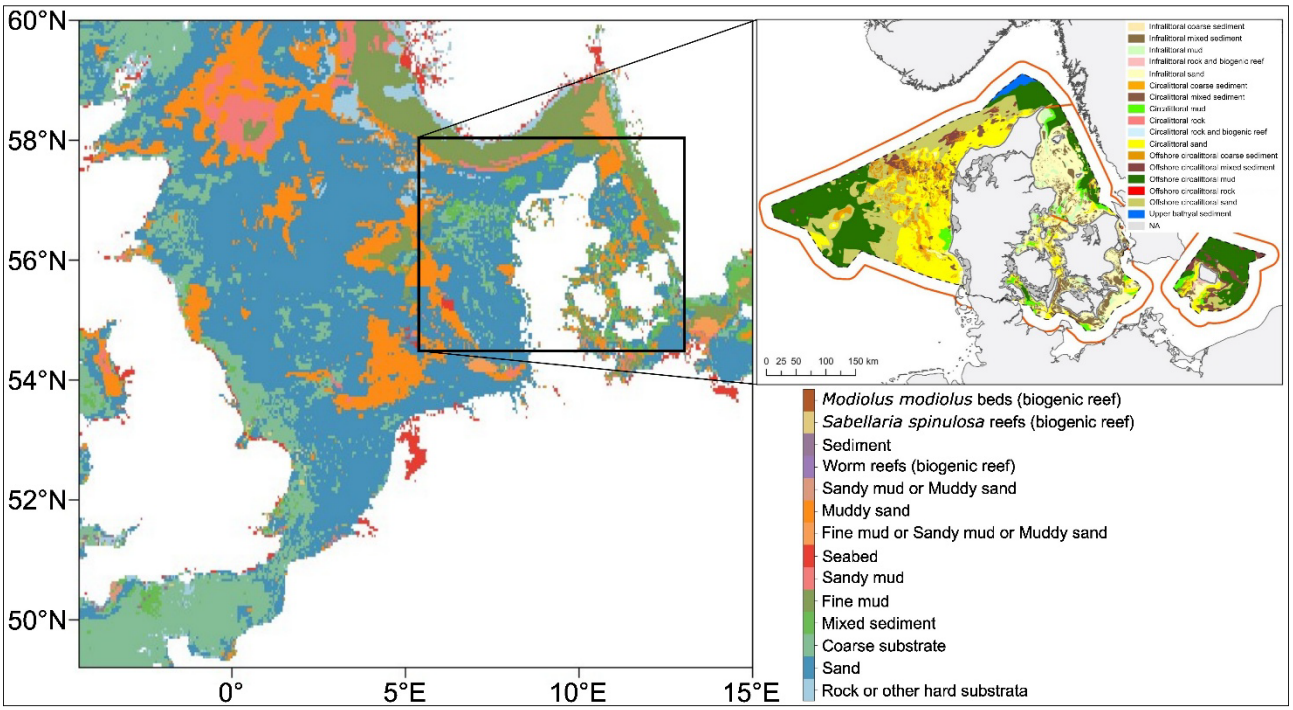

Figure 1.1.1. Broad-scale substrate classifications of the North Sea and Inner Danish waters. Data for the North Sea and Inner Danish waters were obtained from the European Marine Observation Data network (EMOD-net) EUSeaMap (Vasquez et al. 2023) and are at 100 m resolution. The inset map was taken from Göke et al. (2025) and shows the updated broad habitat types in the Danish Exclusive Economic Zone.

Of additional concern regarding the introduction of artificial hard substrates to previously soft sediment habitats is the potential facilitation of non-indigenous species (NIS) introduction and spread. Typically, NIS enter marine ecosystems through primary introductions such as ballast water, hull fouling, aquaculture and canal openings (Pergl et al. 2020), which are regulated under instruments like the Ballast Water Management Convention (IMO 2004) and the MSFD Descriptor 2 "Non-Indigenous Species". Conversely, despite representing the most common form of secondary spread (Pergl et al. 2020), secondary spread of NIS via natural dispersal processes (i.e. movement with ocean currents), is not easily managed. This is largely due to the species-specific natural dispersal properties, which depend on the species' biological traits (e.g., pelagic larval duration) and the environmental compatibility of new habitats (Seebens et al. 2013, Katsanevakis et al. 2013). Many NIS are associated with hard substrates or have sessile life stages, often attaching to ship hulls and artificial structures such as offshore wind turbines (Donelan et al. 2022, Bishop et al. 2017). Therefore, there is concern that future planned offshore wind farms will act as 'stepping stones' for NIS, facilitating spread to previously unreachable areas via dispersal along blue corridors (current-driven non-random particle dispersal routes) (Figure 1.1.2; Adams et al. 2014, De Mesel et al 2015).

Recent data indicate that 874 NIS have been recorded in European seas, with 250 in the Northeast Atlantic and 123 in Danish waters (Stæhr et al. 2022, Zenetos et al. 2022, Jensen et al. 2023). A recent review by Schourup-Kristensen et al. (2024) found that 249 sessile NIS (fauna and macroalgae) found in the southern North Sea could potentially spread to Danish waters by ocean currents. There is therefore concern that the construction of offshore wind farms could accelerate this spread, facilitating transport of these NIS to protected Natura 2000 reef sites in the Danish part of the Skagerrak. Should NIS reach and establish on boulder reefs in the Skagerrak, ocean currents could facilitate their rapid spread into Inner Danish waters and further into the Baltic Sea. If these species

were to become invasive (see Soto et al. (2024) for distinction between 'non-indigenous' and 'invasive'), they may dramatically alter sensitive reef habitats, disrupt food webs and influence biogeochemical processes (Tsirintanis et al. 2022). Although initial studies and public discussions have often focused on the ecological benefits of turbine-associated artificial habitats (e.g., Werner et al. 2024), more recent reviews highlight the potential negative effects on benthic ecosystems and underscore considerable uncertainties regarding the stepping-stone role of wind farms (Dannheim et al. 2020, Wood et al. 2021).

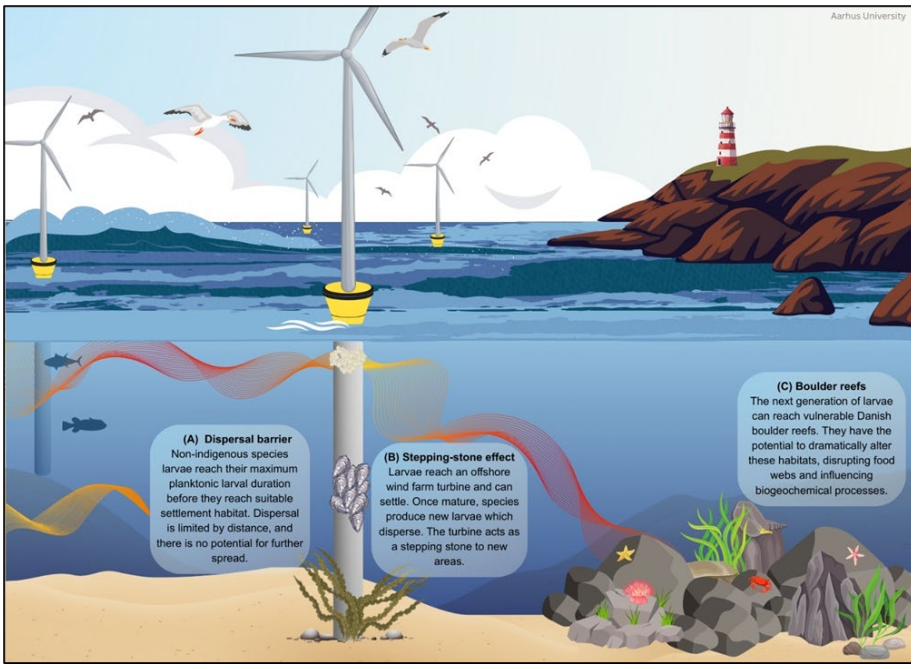

Figure 1.1.2. **(A)** If there is no hard substrate available to settle on at the end of their planktonic larval duration, non-indigenous species larvae will fail to settle and eventually die. Therefore, there is no risk of further spread and the dispersal of the species is said to be limited by distance. **(B)** If an offshore wind farm turbine is placed in an area where there was previously no hard substrate, artificial hard substrate is introduced, and non-indigenous species may settle on the turbine. If these species survive to maturity, they may produce larvae that can go on to disperse to new areas such as **(C)** previously unreachable Danish boulder reefs. In this scenario, the offshore wind turbine acts as a stepping stone to new areas. If the non-indigenous species settles on the Danish boulder reef, it can have negative effects on local native biodiversity.

1.2 Offshore wind farm effects on ecosystem indicators

In a recent 3D modelling study covering the North Sea and Inner Danish waters, Maar et al. (2025) demonstrated that offshore wind farms influence the physical and biogeochemical environment. The study applied two scenarios: current (2021) and future (2030) offshore wind farm development compared to a reference without any offshore or onshore wind farms. Maar et al. (2025) showed that the marine environment is affected through two mechanisms: changes in wind stress at the sea surface (wake effect) and increased friction (drag effect) around monopiles (Figure 1.2.1). Offshore wind farms extract kinetic energy from the atmospheric flow, which reduced the wind speed in their wake (Volker et al. 2017). This wake effect causes a reduced wind stress at the sea surface and was shown to decrease current speeds, increase stratification intensity, reduce bottom stress and increase surface temperatures (Daewel et al. 2024, Maar et al. 2025). The second mechanism, increased friction and turbulence caused by the monopiles themselves, leads to increased local turbulent mixing of the water column and local changes in current speed (Rennau et al. 2012, Christiansen et al. 2023, Mohn et al. 2025). Hence, the two mechanisms, wake and drag effect, are opposing forces with respect to the mixing/stratification of the water column. This highlights the importance of

including both the wind wake effect and the monopile drag effect in the modelling, making the responses highly complex in space and time in marine waters (Maar et al. 2025).

The North Sea and Inner Danish waters were shown to be affected differently by offshore wind farms (Maar et al. 2025). In the North Sea, stratification decreased at high current speeds in the offshore wind farm areas due to strong monopile mixing, whilst at lower current speeds stratification was strengthened by the wake effect. Conversely, in the Inner Danish waters stratification increased in a larger area both inside and outside the offshore wind farms due to the wake effect. The monopile mixing effect was found to dominate over the wake effect at average water current speeds > 0.25 m s^{-1} in both areas.

The resulting changes in stratification observed by Maar et al. (2025) influenced summer primary production in both areas, showing a negative correlation – primary production decreased with stronger stratification due to less nutrient transport from the bottom layer to the surface. Primary production increased with decreasing stratification because of monopile mixing bringing more nutrients up to the depleted surface waters. On average, primary production increased in the North Sea and decreased in the Inner Danish waters due to differences in stratification changes. Due to the wake effect extending over larger distances, the spatial effects showed a smooth pattern, reflecting cumulative effects from numerous offshore (and possible onshore) wind parks, including those outside the Danish Exclusive Economic Zone.

In the previous study, Maar et al. (2025) used meteorological forcing from just one year, 2019, due to the large computational effort of running the 3D atmospheric and ocean models with wake effects. The meteorological year 2019 was chosen as a typical year over the past 30 years according to wind speed, wind direction and atmospheric stability distributions (Hahmann et al. 2025). However, it is important to consider the inter-annual variability to fully understand and estimate the effects of offshore wind in comparison to the natural variability of the systems. Further, effects may accumulate over time and affect the following year(s), for example through heating/cooling of the water, changes in winter nutrient concentrations affecting primary production, and changes in organic matter content in the sediment affecting oxygen depletion. Only one study (Arneborg et al. 2024) has conducted a multi-year run for different offshore wind farm scenarios using a hydrodynamic model in the Baltic Sea and found that increases in bottom salinity and temperature evolve over the years due to offshore wind farms.

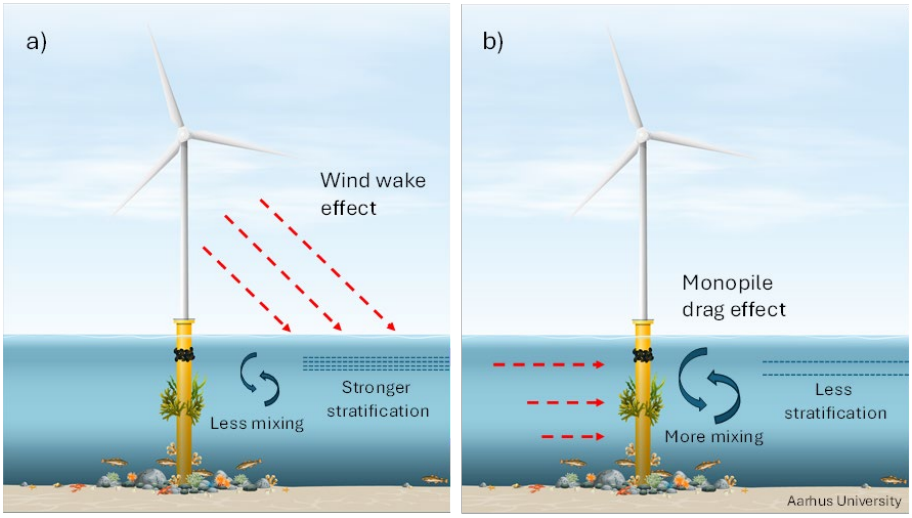

Figure 1.2.1. a) The wind wake causes reduced wind stress at the sea surface, less mixing and stronger stratification of the water column. b) The drag effect from monopiles causes increased local mixing and less stratification of the water column. Hence, the two effects from offshore wind are causing opposite effects on water column mixing and stratification operating on different temporal-spatial scales. Reproduced from Maar et al. (2025).

1.3 Aim of the study

In the present study, we compared the cumulative effects of offshore wind farms on dispersal corridors and ecosystem indicators for two consecutive years, 2019 and 2020. The two years differ with respect to wind speed, air temperature and wake effect. The cumulative effects were assessed as the combined effects of multiple offshore wind farms in Denmark and neighbouring countries. Cumulative effects from other pressures than offshore wind were not included in the present study. In future research, other pressures such as nutrient loading, fisheries, pollution and climate change will be important to consider together with the effects from offshore wind farms.

In the first part of the study, we hypothesise that offshore wind farms may serve as dispersal corridors, or stepping-stones, for NIS, allowing them to overcome natural barriers to dispersal, such as distance between suitable hard bottom habitats, and facilitating their expansion through the southern North Sea and Inner Danish waters. Dispersal is known to be of great importance to the functioning and stability of ecological networks (group of areas connected by ecological corridors; Boulanger et al. 2020, Clubley et al. 2024), and to the spread of NIS (Morel-Journel et al. 2018). To assess this risk, NIS dispersal potential was modelled using a combination of 3D hydrodynamic and agent-based particle tracking simulations, and the yearly variability in dispersal patterns for NIS was examined.

In the second part of the study, we hypothesise that the effects of offshore wind farms on ecosystem indicators vary between years and potentially accumulate over time. We compared the interannual variability of selected ecosystem indicators to offshore wind farms using 3D hydrodynamic-biogeochemical modelling. The selected ecosystem indicators are known to respond to offshore wind farms (Trifonova et al. 2022). These indicators were: stratification, surface temperature, current velocity, Chlorophyll *a* (Chl *a*) concentrations, primary production and bottom oxygen.

2 Methodology

2.1 Model scenarios and parameterisation of offshore wind farm effects

The offshore wind farm scenarios were developed by the Danish Energy Agency and DTU Wind and consisted of i) a reference scenario with no wind turbines on land or offshore (REF-NO-FARM), ii) current on- and offshore wind farm locations as of 2021 (CURRENT), and iii) future planned on- and offshore wind locations for 2030 (Y2030) (Table 2.1.1, Figure 2.1.1). The offshore wind capacity was 24.4 GW in the CURRENT scenario and 158 GW in the Y2030 scenario, while the onshore wind capacity was 50.4 GW in both scenarios. The scenarios are described in more detail in previous reports (see: Energistyrelsen 2024a, b, Hahmann et al. 2025a,b, Maar et al. 2025).

The parameterisation of offshore wind farm effects included the representation of wind wake effects resulting from local wind fields altered by operational wind turbines, estimated by the Weather Research and Forecasting (WRF) model (Hahmann et al. 2025, Maar et al. 2025). Further, the drag exerted by monopile structures within the water column was parameterised by adding drag and turbulent kinetic energy to the hydrodynamic model (Rennau et al. 2012). The drag produced by the monopiles slows the mean currents and generates increased turbulence in the wake of the monopile. The relatively coarse resolution of the model may underestimate the wind wake and drag effects compared to small-scale high-resolution modelling. However, the results from a high-resolution FlexSem flume proof-of-concept model demonstrated good agreement between a configuration with an existing monopile, a set-up featuring the monopile drag parameterisation (excluding the monopile), and measurements of the currents downstream of the monopile obtained from inside the Anholt offshore wind farm. All model configurations were run using the same high horizontal resolution (Mohn et al. 2025).

Table 2.1.1. Scenarios used in the wind and FlexSem simulations. The onshore wind farm capacity was 50.4 GW in CURRENT and Y2030 scenarios.

Scenario	Wind farm scenario	Meteorological years	Offshore wind farm capacity (GW)
REF-NO-FARM	No wind farms	2019 - 2020	-
CURRENT	Wind farms as of November 2021	2019 - 2020	24.4
Y2030	Wind farm scenario 2030	2019 - 2020	158

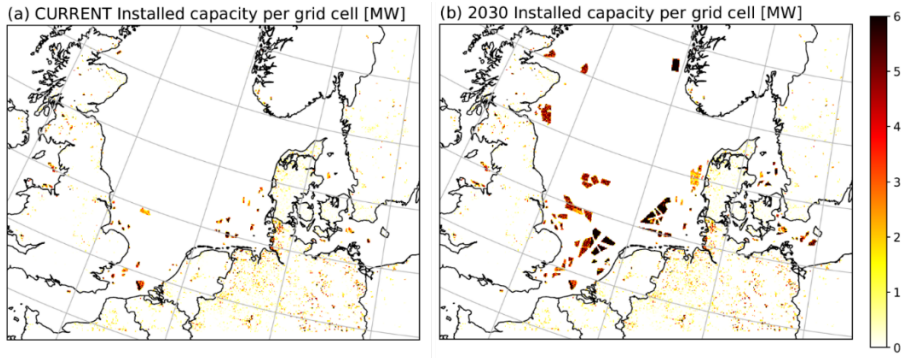

Figure 2.1.1. Installed wind farm capacity (MW km^{-2}) in the Weather Research and Forecasting (WRF) model in the a) CURRENT and b) Y2030 scenarios (Hahmann et al. 2025a,b).

2.2 Interannual variability

The interannual variability of offshore wind farm effects was assessed by comparing model results from the two years 2019 and 2020. The initial fields in the 2019 runs were obtained from Copernicus data for both scenarios (Table 2.1.2). For the 2020 runs, initial fields were obtained from the last time step in the two 2019 scenarios REF-NO-FARM and Y2030 (Table 2.1.2). In this way, not only differences in the meteorological and other forcing were assessed, but also the transfer of the signal from the offshore wind farms between years in Y2030. This 2020 run was named 2020-S (scenario initial fields).

To assess the importance of accumulated effects from offshore wind farms evolving from one year to the next relative to the interannual variability, the Y2030 scenario for 2020 (named 2020-R) used the reference initial fields from REF-NO-FARM (last time step in 2019) (Table 2.1.2). In this way, there was no transfer of the signal from the offshore wind farms between years. By comparing the outcome between 2020-S and 2020-R, the accumulated effects between years could be estimated.

Table 2.1.2. Interannual variability. Initial fields used in the FlexSem simulations for year 2019 and 2020 in the scenarios REF-NO-FARM and Y2030 to assess either the interannual variability (2020-S) or the accumulated effects (2020-R) of offshore wind farms.

	REF-NO-FARM	**Y2030**
	Initial field	**Initial field**
Interannual variability (2019)	Copernicus data	Copernicus data
Interannual variability (2020-S)	REF-NO-FARM 2019	Y2030 2019
Accumulated effects (2020-R)	REF-NO-FARM 2019	REF-NO-FARM 2019

2.3 Surface forcing

The WRF model provided surface forcing to the 3D hydrodynamic models of the North Sea and Inner Danish waters (Hahmann et al. 2025a,b). The meteorological forcing was 10 m (above surface) wind (u,v) components, 10 m (above surface) air temperature, cloud cover and specific humidity. A surface radiation model calculated the heat transfer through the ocean surface and modified the water temperature by calculating the short-wave radiation, the long-wave radiation, the sensible heat flux and the latent heat flux (heat evaporation). The latter three are surface layer effects, whereas the short-wave radiation penetrates the surface and attenuates throughout the upper water column (Larsen et al. 2020). Evaporation does not affect salinity in the model. The wind stress at the sea surface was described by a parameterisation of the difference between the wind speed and the water current speed and the ratio of the density of the atmosphere and the density of the water (Smith and Banke 1975).

Two years, 2019 and 2020, were chosen for the scenarios to account for interannual variability. The annual mean wind speed and mean air temperature of both years were compared with the average over five years (2019 – 2023). Year 2019 was closer to the 5-year average (-0.2%), while 2020 experienced higher wind speeds (~5%), particularly on the western side of the North Sea and in the Skagerrak (Figure 2.2.1c). Additionally, year 2020 showed higher temperature in the Inner Danish waters (Figure 2.2.1d).

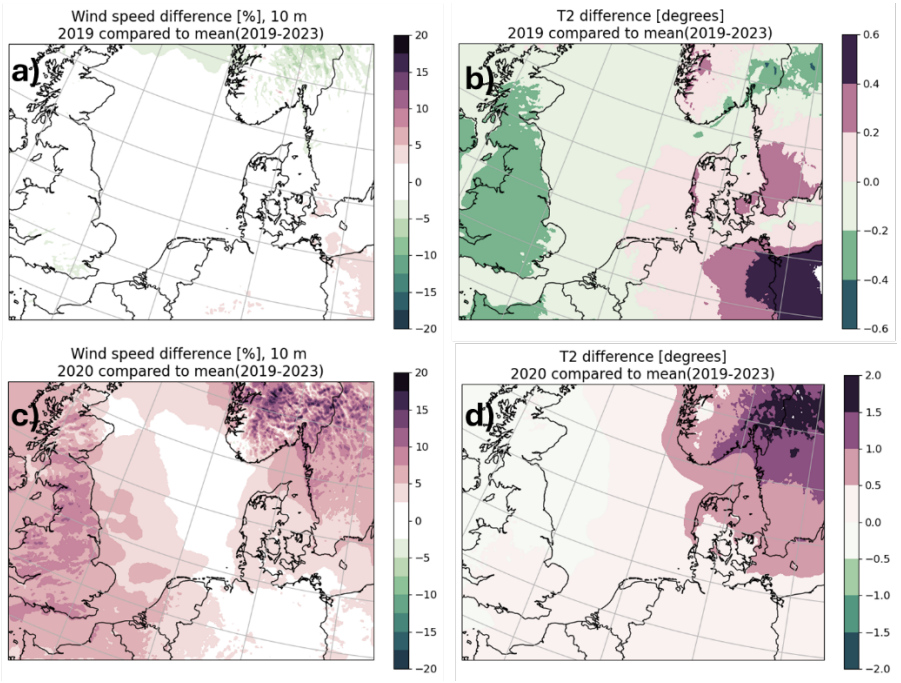

Figure 2.2.1. Annual mean wind speed difference (%) and annual mean air temperature difference (°C) for 2019 (a, b) and 2020 (c, d), respectively, compared to the 5-year mean (2019-2023).

In the North Sea model, summer (April to September) wind speeds varied from 3 to 9 m s^{-1} for 2019 in the Y2030 scenario including all the offshore wind farms and the wake effect (Figure 2.2.2a). For 2020, summer wind speeds were lower in the central part of the North Sea and higher in the English Channel and south-western North Sea and in the Danish part of the Skagerrak compared to 2019 (Figure 2.2.2b,c). Wind speeds were lower during summer, whereas annual wind speeds were higher in 2020 compared to 2019 in Y2030 (Table 2.2.1). The change in summer wind speed between years was highest within 40 km distance from the offshore wind farms (Table 2.2.1) and this distance was used in the analysis of effects in the North Sea. However, there was no significant difference between 20 km, 40 km and 60 km distance due to the high variability (Kruskal-Wallis tests, p>0.18). There was a significant difference between summer wind speed at 40 km distance and within the offshore wind farms (Kruskal-Wallis tests, p=0.04) and for the entire North Sea (Kruskal-Wallis tests, p<0.01).

Table 2.2.1. Changes (%) in wind speed between 2020 and 2019 in scenario Y2030 (including the wind wake) for the North Sea and Inner Danish waters (IDW) annually and summer period. A negative value means that wind speed was lower in 2020 relative to 2019. The wind speed changes were estimated for offshore wind farm areas (OWF), for 20 km, 40 km and 60 km distance from OWF and the entire area. The distance in bold was chosen for further analysis of effects. The changes are shown as the 25th, 50th (median) and 75th percentiles.

Basin and period	Area	25th perc. (m s^{-1})	Median (m s^{-1})	75th perc. (m s^{-1})
North Sea, annually	OWF	0.03	0.17	0.59
	<40 km	0.02	0.10	0.34
	Entire area	0.05	0.17	0.50
North Sea, summer	OWF	-0.59	-0.27	-0.15
	<20 km	-0.51	-0.24	-0.12
	<40 km	-0.59	**-0.25**	-0.10
	<60 km	-0.71	-0.24	-0.08
	Entire area	-0.55	-0.15	0.01
IDW, annually	OWF	0.05	0.15	0.26
	<20 km	0.01	0.04	0.19
	Entire area	0.02	0.06	0.19
IDW, summer	OWF	-0.62	-0.47	-0.21
	<20 km	-0.52	**-0.19**	-0.08
	<40 km	-0.45	-0.16	-0.05
	<60 km	-0.45	-0.15	-0.05
	Entire area	-0.27	-0.07	-0.02

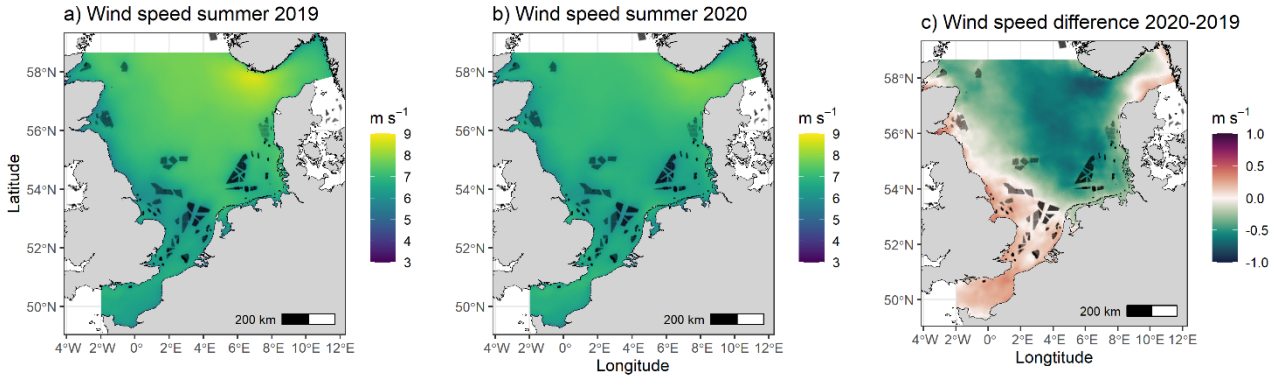

Figure 2.2.2. North Sea mean wind speed (m s^{-1}) during summer 2019 (a) and 2020 (b) in scenario Y2030 including the wake effect. Difference in wind speed (m s^{-1}) between 2020 and 2019 in scenario Y2030 (c).

For the Inner Danish waters, the 2019 summer wind speeds varied from 4 to 7 m s^{-1} in scenario Y2030 (Figure 2.2.3a). In 2020, the summer wind speeds were lower in most of the area, except for the Northern Kattegat, compared to 2019 (Figure 2.2.3b,c). On average for the entire area, wind speeds in Y2030 (including the wind wake) were lower during summer, whereas annual wind speeds were higher in Y2030 in 2020 compared to 2019 (Table 2.2.1). The change in summer wind speed between years was significantly highest within 20 km distance from the offshore wind farms compared to the other distances and for the entire area (Kruskal-Wallis tests, p<0.01). The 20 km distance was therefore used in the analysis of effects in the Inner Danish waters.

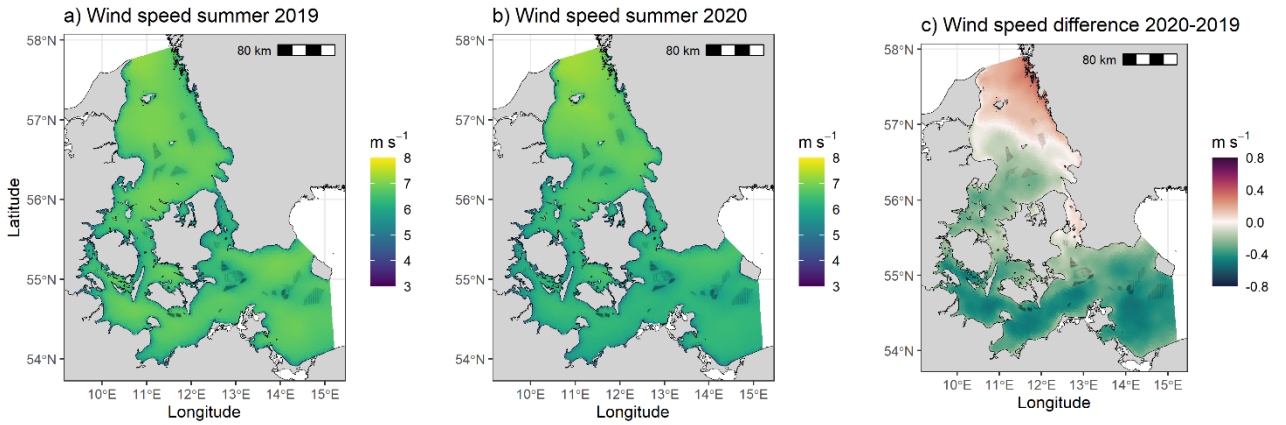

Figure 2.2.3. Mean wind speed (m s^{-1}) during summer 2019 (a) and 2020 (b) in scenario Y2030. Difference in wind speed (m s^{-1}) between 2020 and 2019 in scenario Y2030 (c).

2.4 The North Sea model set-up

A high-resolution hydrodynamic model of the Greater North Sea (OSPAR Region II) was developed using the open-source FlexSem modelling framework (Figure 2.3.1; Larsen et al. 2020, Schourup-Kristensen et al. 2024, Larsen et al. 2025). FlexSem is a three-dimensional ocean model that solves the Navier-Stokes equations on an unstructured grid allowing flexible spatial resolution and is particularly suited for complex coastal and estuarine environments. The model simulates key physical parameters such as salinity, temperature, current velocity and water column mixing.

The model domain stretches from the English Channel in the south to the Norwegian Trench and Skagerrak in the north, occupying an area of 484,087 km^2. The horizontal resolution varies from 7.8 km in the central North Sea to 2.5 km in shallow coastal zones such as the Wadden Sea. The model has 29 vertical layers with varying resolution (from surface to bottom: 10 layers of 5 m thickness, five layers of 10 m thickness, five layers of 20 m thickness and nine layers of 50 m thickness). The maximum water depth in the model domain is 682 m in the Norwegian Trench: The model implements wetting and drying. Shallow areas dry out during low tides, hence, there is no minimum depth in the model. The computational mesh consists of 12,721 polygons, comprising 121,474 computational cells.

A second-order advection-diffusion scheme was implemented to improve resolution of vertical and horizontal gradients, offering reduced numerical diffusion compared to earlier first-order approaches. To parameterise turbulent mixing, a k-epsilon model was used in the vertical (Burchard et al. 1998, Warner et al. 2005), and a Smagorinsky scheme in the horizontal (Smagorinsky 1963). The model operates with a two-minute time step and includes wetting and drying processes to realistically represent tidal dynamics across the region.

The hydrodynamic model was coupled to biogeochemical models for both the water column and sediment, simulating the cycling of nitrogen (N) and phosphorous (P) using Redfield ratios (Maar et al. 2011, Maar et al. 2016, Maar et al. 2022). The 10 state variables describe concentrations of inorganic nutrients (NO_3, NH_4, PO_4), two functional groups of phytoplankton (diatoms, flagellates), micro- and mesozooplankton, detritus, oxygen and suspension feeders. The model considers the processes of nutrient uptake, growth, grazing, respiration, excretion, recycling, mortality and settling of detritus and diatoms. For a comprehensive description of the North Sea model processes, setup,

boundary conditions and supplementary data sources, please refer to Maar et al. (2025). The model validation for 2020 is shown in appendix A.

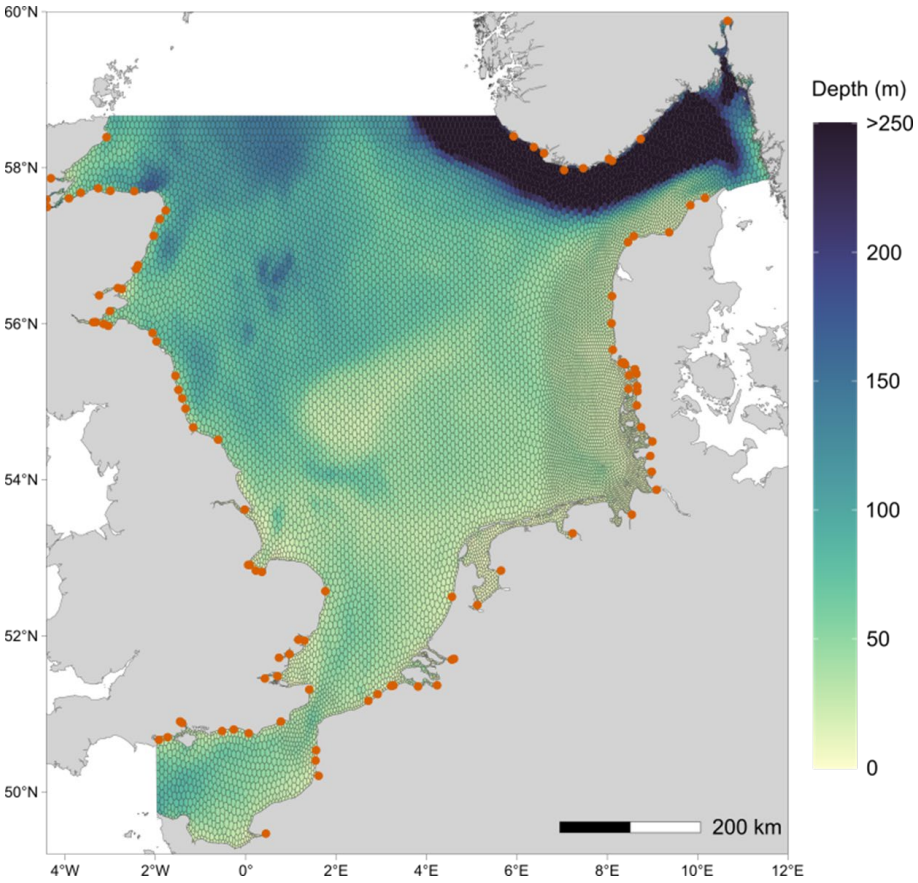

Figure 2.3.1. The North Sea model domain showing the bathymetry (color bar), model mesh (polygons) as well as position of freshwater sources (red dots) (maximum depth is 680 m in the Skagerrak.

2.5 Inner Danish waters model set up

The open-source FlexSem model framework was also applied to the Inner Danish waters (Figure 2.4.1). The model uses a 1.5-minute time step and an unstructured horizontal mesh. The horizontal resolution ranges from ~200 m in the Little Belt to 5 km in the northern Kattegat and western Baltic Sea. The maximum depth of the model is 84.5 m, divided into a 2 m surface layer and 84 vertical layers, each with 1 m depth (Maar et al. 2025). The surface layer is 2 m thick, and the free surface height can vary from -2m and up. Hence, the minimum bathymetry is 2 m, but the depth of the water in shallow areas can become infinitely small. The computational mesh is comprised of 11,244 polygons made up of 216,981 computational cells and covering a total area of 66,369 km^2.

Boundary conditions for temperature, salinity, sea surface height and velocity were provided by the Baltic Sea Physics Analysis and Forecast (SMHI/E.U. Copernicus, https://doi.org/10.48670/moi-00010). Freshwater and nutrient inputs came from the DK-QNP model (Danish rivers; Windolf et al. 2011) and the E-HYPE catchment model (Swedish and German rivers; Lindström et al. 2010). The biological model was updated with two classes of dissolved organic nitrogen (DON), a labile and refractory pool, based on the ERGOM model (Neumann et al. 2022). Initial and boundary conditions for nitrate, ammonium, phosphate and oxygen were taken from a NEMO-ERGOM Baltic set up (https://doi.org/10.48670/moi-00012), while DON conditions were based on Kattegat and Arkona Basin observations (www.odaforalle.au.dk). The model validation for 2020 is shown in appendix A.

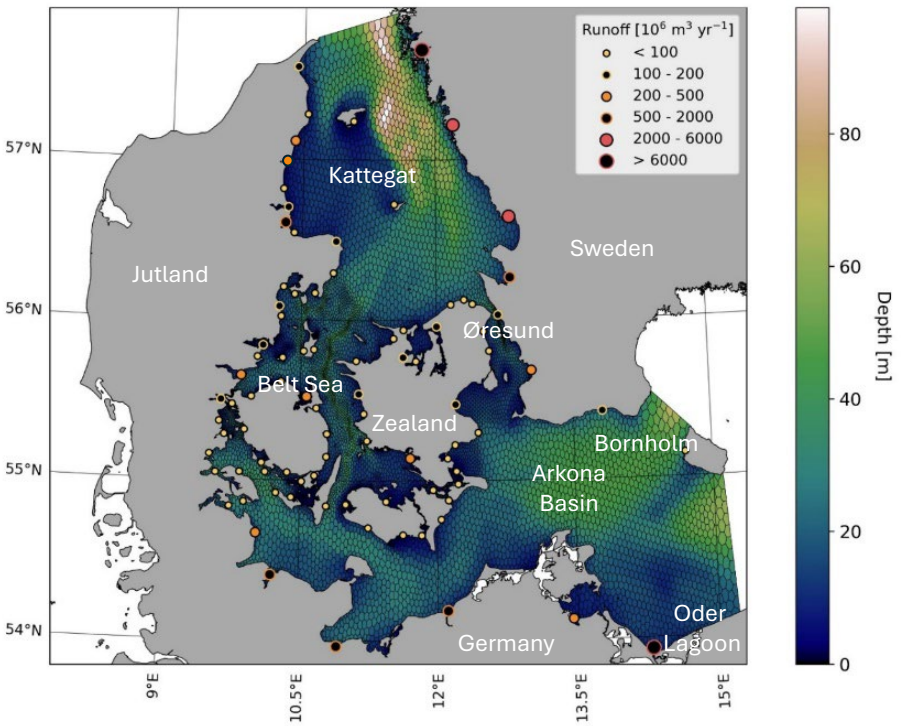

Figure 2.4.1. The Inner Danish waters model domain showing the bathymetry (color bar), model mesh (polygons) as well as position and strength of freshwater sources (dots).

2.6 Larval dispersal modelling

2.6.1 Agent-based model

To investigate the risk of non-indigenous species' (NIS) spread from the southern North Sea to the Inner Danish waters, the main dispersal routes ('blue corridors') of non-indigenous species (NIS) from areas of hard substrate (both natural and artificial/man-made) in the southern North Sea (defined as areas below 55°N, following Cameron et al. 1992) and the Inner Danish waters were modelled. Using an agent-based model (ABM; Larsen et al. 2020, Pastor et al. 2021) forced by the FlexSem model outputs for the respective regions, we simulated dispersal of NIS for 2019 and 2020 under both current and future offshore wind scenarios (Table 2.1.1). In brief, the ABM consists of a given number of virtual particles that represent one or more individuals that are released from a given set of locations at a specified time and allowed to disperse passively for a set duration with the ocean currents provided by the hydrodynamic model. The longitude and latitude of these particles are stored at set time intervals (timesteps).

2.6.2 Selection of locations from which to release particles

Species settling and surviving on offshore wind turbines are likely to be those that settle and live primarily on hard substrata. Therefore, we focused our study on the dispersal of agents from areas of natural and artificial (man-made) hard substrates. We defined areas of artificial hard substrate using the locations of the offshore wind turbines in the two scenarios, CURRENT and Y2030. We defined areas of natural hard substrate using substrate classification data obtained from the European Marine Observation Data network (EMOD-net) EUSeaMap (Figure 1.1.1; Vasquez et al. 2023). These data had a spatial resolution of 100 m and were cropped to include only those areas categorised as 'Rock or other hard substrata'.

For the southern North Sea, we defined particle release locations by creating a uniform 10 km × 10 km grid of the ocean area and selecting the centroid coordinates of those grid cells that contained either 'Rock or other hard substrata' as determined by the EUSeaMap or an offshore wind turbine. This resulted in two sets of release coordinates, one for the CURRENT scenario and one for the Y2030 scenario. Four ABMs were run, one for the CURRENT and one for the Y2030 scenario for both 2019 and 2020. For the CURRENT scenarios, particles were released from 380 coordinates (Figure 2.6.1a), and for the Y2030 scenarios particles were released from 637 coordinates (Figure 2.6.1b).

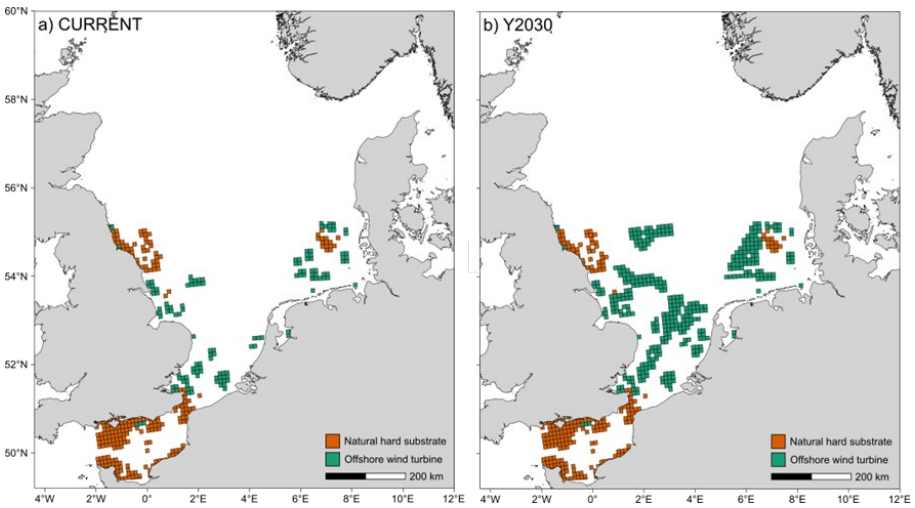

Figure 2.6.1. 10 km × 10 km grid cells in the southern North Sea containing either natural hard substrata or an offshore wind turbine. The centroid of each grid cell comprised the release coordinates for particles representing non-indigenous species in the North Sea agent-based models. In a) offshore wind turbine locations represent the CURRENT scenario, and in b) offshore wind turbine locations represent the Y2030 scenario.

Our aim was to investigate the risk of spread of NIS from the southern North Sea to the Inner Danish waters. Therefore, for the Inner Danish waters ABMs we released particles from a set of 30 evenly spaced coordinates along a transect at the northern open boundary of the FlexSem model (Figure 2.6.2). The transect was placed 5 km (one polygon) away from the open boundary to minimise any potential error caused by the boundary conditions. These particles represented the potential further dispersal of particles from the southern North Sea ABMs that travelled to the opening of the Kattegat into the Inner Danish waters. Four ABMs were run, one for the CURRENT and one for the Y2030 scenario for both 2019 and 2020. The location and number of release coordinates remained the same for all scenarios.

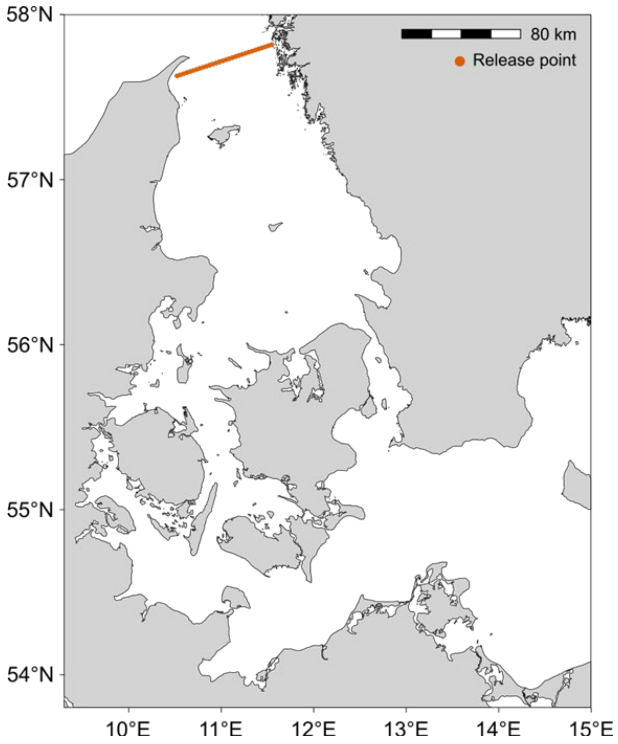

Figure 2.6.2. Release locations for particles representing non-indigenous species in the Inner Danish waters agent-based models. Release coordinates were the same for both the CURRENT and Y2030 scenarios. Please note, release coordinates are so close together they appear as a straight 'line'.

2.6.3 Model parameters

In all models, NIS particles were released from the locations outlined above once a day from 1 March to 30 April (i.e., 60 days), coinciding with the phytoplankton spring bloom in north-west Europe, when many NIS are likely to undergo reproduction and spawning (Sverdrup 1953, Wiltshire and Manly 2004). All particles were released at midnight, which coincided with different points in the tidal cycle and therefore accounted for the effects of tidal state on dispersal.

In the North Sea ABMs, particles from areas of natural hard substrate were released at 40 m depth, or the maximum depth of the model cell, as NIS on hard substrates would be present at the seabed and therefore larval release would likely occur at depth. For areas where an offshore wind turbine was present, particles were released at 1 m depth intervals from 0 – 40 m to reflect the fact that offshore wind monopiles are present throughout the water column, and therefore NIS may also be present and reproducing throughout the water column. We used this depth range, as it is representative of general patterns in vertical distribution of pelagic larvae noted by Correll et al. (2012) in the Baltic Sea. For the CURRENT scenario, this resulted in the release of 271,020 particles in total for both 2019 and 2020 (380 coordinates × depth layers × 60 days). For the Y2030 scenario, 819,180 particles were released in total for both 2019 and 2020 (637 coordinates × depth layers × 60 days).

In the Inner Danish waters ABMs, particles were released at 1 m depth intervals from 0 – 40 m (or the maximum depth of the model cell) for each of the 30 transect coordinates, resulting in 62,040 particles released in total for both the CURRENT and Y2030 scenarios for both 2019 and 2020. In this way, we account for the continued dispersal of particles arriving at any depth from the North Sea to the Kattegat.

In all models, we allowed the NIS particles to disperse for a period of six months (~183 days), representing the maximum pelagic period (residence

time) of NIS in the North Sea area (Vandendriessche et al. 2008, Hansen et al. 2021). This provides a 'worst-case scenario' of the potential for downstream offshore wind farms to contribute to the spread of NIS to the Inner Danish waters as they are colonised by particles arriving from other areas. The ABMs had an internal timestep of 2-minutes and the particle positions (longitude, latitude and depth) were saved at daily intervals.

2.6.4 Comparison of dispersal pathways for scenarios and years

For all model outputs, we calculated the distance distribution of agents. We calculated distance as the great-circle distance (shortest path between two points on a sphere) between the starting and ending positions of each agent measured in km. We compared distance distributions separately for the North Sea and Inner Danish waters models between model scenarios (CURRENT – Y2030) to assess the effect of offshore wind farm development on the potential distance travelled by non-indigenous species larvae and between years (2019 – 2020) to test for interannual variation. To formally test for differences in distance distributions, we used a Kruskal-Wallis test followed by a Dunn's post hoc test with Benjamin-Hochberg adjustment to control for type I error. The Kruskal-Wallis test is a non-parametric method used to determine whether there are statistically significant differences between the medians of three or more independent groups.

Dispersal pathways of NIS particles for the CURRENT and Y2030 scenarios for 2019 and 2020 for both the North Sea and Inner Danish waters ABMs were illustrated by density maps showing both the tracking and settlement densities. Tracking density illustrates the 'blue corridors' within the model domain by highlighting those areas where non-indigenous species larvae most frequently travel. This metric was calculated as the total number of agents that travelled through a given grid cell at any point in the model divided by the area of the grid cell (North Sea: 100 km; Inner Danish waters: 25 km). Settlement density illustrates the areas most likely to receive a large volume of non-indigenous species larvae based on currents alone. This metric was calculated as the total number of agents contained within a given grid cell at the end of that agents' planktonic larval duration divided by the area of the grid cell. For the North Sea, both tracking density and settlement density were calculated using a 10 km × 10 km grid of the ocean areas, whilst for the Inner Danish waters a 5 km × 5 km grid was used.

The likelihood that non-indigenous species larvae spawning in the North Sea and arriving at the entrance to the Kattegat would go on to further disperse in the Inner Danish waters was assessed for both the North Sea and Inner Danish waters models. The likelihood was calculated and mapped as the average age (in days) of agents that pass through a given grid cell at any point in the model. Further, for the North Sea model we examined the age distribution of agents in those grid cells at the eastern boundary, where the Skagerrak meets the Kattegat, representing the opening to the Inner Danish waters. We formally tested for differences in the ages of agents in this area between both years and scenarios using a Kruskal-Wallis test followed by a Dunn's post hoc test with Benjamin-Hochberg adjustment to control for type I error.

2.7 Interannual effects of offshore wind farms on ecosystem indicators

2.7.1 Indicators of change

The spatio-temporal effects of offshore wind farms on the environment were estimated for two years, 2019 and 2020. The two years differed with respect to wind speed, wind wake effect and air temperature (section 2.2). We compared the responses of selected ecosystem indicators known to respond to offshore wind farms (Trifonova et al. 2022). The indicators were stratification, surface temperature, horizontal current speed, Chl *a* concentrations, primary production and bottom oxygen.

Stratification. The water column can be stratified due to differences in salinity and/or temperature and thereby limit the vertical exchange of nutrients and oxygen, which are important for biogeochemical processes and marine life. The stratification index was estimated as the Potential Energy Anomaly (PEA, J m^{-3}), indicating the amount of energy needed to mix the water column (Simpson and Bowers 1981). In the North Sea, the southern tidal and coastal areas are mostly mixed, while the strength of stratification increases towards the Skagerrak in the northeast (Maar et al. 2025). The seasonal development of temperature stratification begins in April and lasts until end of September. In the Inner Danish waters, the water column is generally more stratified than in the North Sea due to salinity stratification. During summer, temperature stratification also contributes to overall stratification.

In a previous study, Maar et al. (2025) found that PEA responded strongly to offshore wind farms through the wind wake and monopile mixing effects. Other modelling studies have shown that PEA is crucial for predicting changes in the abundance of marine species at both lower and higher trophic levels on a regional scale (Trifonova et al. 2022). Additionally, PEA can capture subtle spatial and temporal changes within specific habitat types and seasons, underscoring its importance as an indicator of physical processes that affect the entire trophic chain and overall ecosystem functioning (Trifonova et al. 2022). Year-to-year variability in stratification can therefore be important for the ecosystem responses to offshore wind.

Temperature. Sea water temperature is a major driver of marine ecosystems. It is important for the seasonal stratification of the water column and affects many biogeochemical, physiological and ecological processes that can induce changes in distributions, abundance and richness of marine species (Trifonova et al. 2022). Temperature is an indicator of climate warming, and increasing temperatures can increase hypoxia (Bendtsen and Hansen 2013). Maar et al. (2025) observed a modest increase of surface temperature to offshore wind farm development. However, there may be accumulated responses (e.g., warming) and year-to-year variability in sea temperatures over time that could be important to consider.

Horizontal Current Speed. Local and regional current speeds can influence primary productivity and occupancy patterns of mobile animals by increasing food availability and abundance (Trifonova et al. 2022). Hydrodynamic characteristics have been hypothesized to aggregate, disaggregate and disorient prey, affecting prey availability and foraging efficiency. Recent findings on very fine spatial scales (< 500 m) demonstrate that man-made structures (e.g., decommissioned tidal turbines) and physical features (e.g., eddies and boils) generate wake features that attract top predators, which has implications for

the distribution of species and identification of foraging hotspots (Benjamins et al. 2017, Lieber et al. 2019). In a previous report, Maar et al. (2025) demonstrated that surface current speeds decreased both locally within the wind farm areas, but also on regional scales in the Y2030 scenario. However, the year-to-year variability has not been assessed.

Primary Production and Chl *a*. Pelagic primary producers (phytoplankton) play a fundamental role in marine ecosystems, sustaining the rest of the trophic levels, and are strongly linked to the structure and functioning of ecosystems (Tomczak et al. 2013, Schlenger et al. 2019). Spatial patchiness of phytoplankton biomass (expressed as Chl *a* concentrations) and primary production are important for a predator's ability to find food, and the timing of phytoplankton blooms is crucial for energy flows in the marine food web and productivity of higher trophic levels (Trifonova et al. 2022). However, excessive nutrient input (eutrophication) can increase phytoplankton production and biomass, thereby decreasing water clarity. Additionally, once dead phytoplankton sinks to the seabed and oxygen is consumed during degradation, it potentially leads to hypoxia, thus contributing to the mortality of benthic organisms. In a previous modelling exercise, Maar et al. (2025) found that summer primary production generally decreased with increasing stratification, although modified by current speed due to offshore wind farm development.

Bottom Oxygen. Oxygen depletion (i.e., hypoxia) has negative effects on many marine organisms, such as large-scale mortality and behavioural responses, as well as variations of species distributions, biodiversity, physiological stress and other sub-lethal effects (e.g. on growth and reproduction). In the Inner Danish waters, strong stratification and limited bottom water transport from neighbouring areas during the summer season in combination with high primary production causes frequent episodes of extensive hypoxia. It has been found that hypoxic events in open waters covary with nitrogen loadings from land, wind during late summer and surface temperatures (Conley et al. 2007). The North Sea is highly dynamic, and low oxygen events are not common in the central North Sea but may occur at the Oyster Ground (Daewel et al. 2022). Future climate warming may enhance hypoxic conditions through increased biological respiration and stratification.

In a previous report, Maar et al. (2025) found a small decrease in the median of bottom oxygen response to offshore wind farm development in the North Sea and Inner Danish waters due to lower primary production and lower bottom temperatures. The response of bottom oxygen (hypoxia) is, however, complex, as it depends on various hydrodynamic and biogeochemical processes. Maar et al. (2025)'s model showed only small changes (< 3%) in bottom oxygen in both areas, but only one year (2019) was considered. This response may be intensified over time if there is accumulative organic matter content in the sediment and bottom waters, increasing temperatures or stronger stratification.

2.7.2 Analysis of interannual variability

The ecosystem indicator responses (%) were estimated as the difference between each scenario (*SCE*=Y2030 for 2019, 2020-S, 2020-R) and the REF-NO-FARM scenario (*REF*) divided by the mean of *REF* and multiplied by 100% for each grid cell (Daewel et al. 2022):

$$Response_i = \frac{\int_{i=1}^{n}(SCE_i - REF_i)}{mean(REF)} \times 100\% \qquad \text{(eq. 1)}$$

The scenarios were defined in Table 2.1.2. The response was estimated for each day=*i* during the year (*n*=365 days) and summer period from April to September (*n*=180 days). The summer period is important to consider because stratification, warming, productivity and oxygen depletion show the highest signals during the year. Data was extracted from the model for the elements (polygons) with offshore wind farms and from the areas up to 40 km and 20 km outside of the offshore wind farms in the North Sea and Inner Danish waters, respectively. The two distances were chosen because of the highest change in the wind speeds (Table 2.2.1). The responses were compared using combined box-violin plots for each scenario. The box plots show the minimum, maximum, 25th, 50th (median) and 75th percentiles and potential outliers. The violin plots show the distribution of the data. We tested for differences in indicator responses between both years and scenarios using a Kruskal-Wallis test (type 2 error=5%) followed by a Dunn's post hoc test with Benjamin-Hochberg adjustment to control for type I error.

3 Results & Discussion

3.1 Offshore wind farms as dispersal corridors for non-indigenous species

3.1.1 The North Sea

Dispersal distance. For the North Sea, the distance distribution of agents differed significantly between all scenarios ($\chi^2(3) = 198033$, $p < 0.001$). For both 2019 and 2020, distances between the start and end point of agents were greater in the Y2030 than the CURRENT scenario (with the exception of maximum distance for 2019), suggesting the expansion of offshore wind significantly increases the potential dispersal distance of non-indigenous species larvae (Table 3.1.1; Figure 3.1.1).

Comparing between years, for the CURRENT scenario there was little to no difference in the median distance between start and end locations of agents between 2019 and 2020, however, the maximum distance for the 2019 model was 127 km (16%) greater than for the 2020 model (Table 3.1.1; Figure 3.1.1), perhaps due to lower wind speeds in the central North Sea in 2020 (Figure 2.2.2). For the Y2030 scenario, there was again little to no difference in median distance between the two years.

The 75th percentile distance was greater in 2019 than 2020, however, for the maximum distance the opposite was true (2020 greater than 2019; Table 3.1.1; Figure 3.1.1). This would suggest that for the Y2030 scenario, in 2020 a smaller proportion of agents travelled over large distances than in 2019, likely due to slower current speeds in the Y2030 scenario (Maar et al. 2025). These differences highlight the importance of considering interannual variability in the potential dispersal patterns of non-indigenous species.

Table 3.1.1. The distance distribution of agents that dispersed in the four North Sea agent-based models. Distances were measured between the start and end coordinates of each agent and are measured in kilometres (km).

Scenario	Year	Min.	25th percentile	Median	75th percentile	Max.
CURRENT	2019	0	0	5.33	25.00	834.46
Y2030	2019	0.01	6.42	20.42	61.82	809.58
CURRENT	2020	0	0	5.15	21.54	707.46
Y2030	2020	0.01	7.24	20.05	49.98	834.67

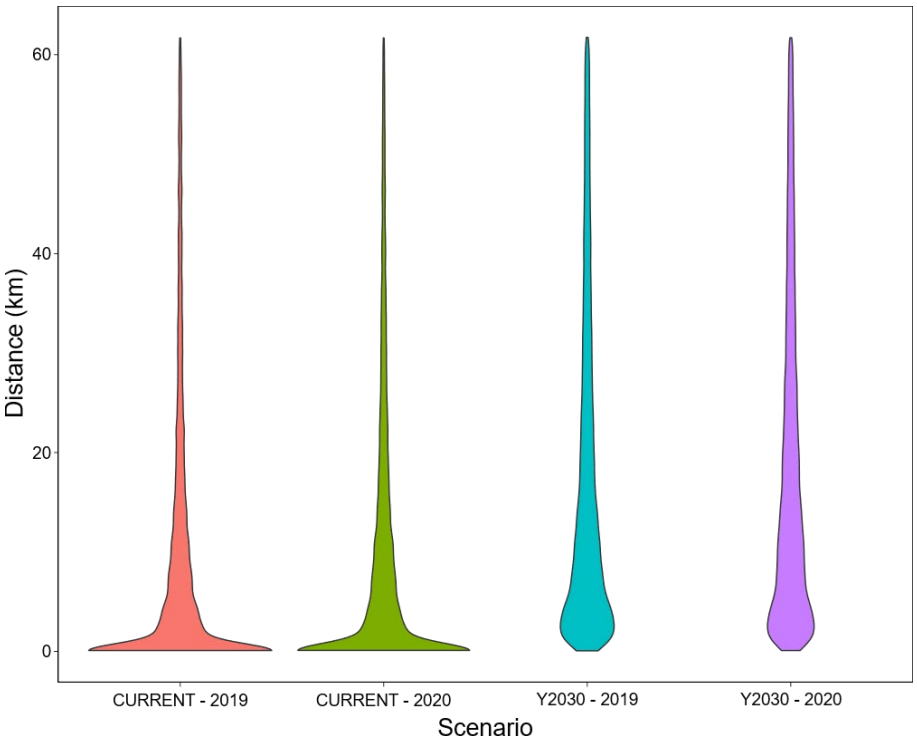

Figure 3.1.1. North Sea violin plot of the distance (km) between the start and end locations of agents in the agent-based models for each scenario. The distance has been limited to the maximum 75th percentile value across scenarios (61.8 km) to aid in interpretation. See Table 3.1.1 for the true maximum distance between agent start and end locations.

Tracking Density (Blue corridors). In all model scenarios, agents dispersed over broad spatial scales, covering a latitudinal range from the Skagerrak to the English Chanel (Figure 3.1.2). All models show that agents drift along a 'blue corridor' from the German Bight northwards following the western Danish coastline towards the entrance to the Kattegat, and for both 2019 and 2020 this drift appeared more substantial in the Y2030 than the CURRENT scenario (Figure 3.1.2). This would suggest that future planned offshore wind development is likely to increase the supply of non-indigenous species to the Kattegat, providing greater opportunity for further spread of these species into the Inner Danish waters. In particular, in the Y2030 scenarios for both 2019 and 2020 there is apparent connectivity between offshore wind farms in the Southern Bight and the eastern coast of England with those present in the German Bight, indicated by greater tracking densities between these areas (Figure 3.1.2b, d) – a link which is noticeably much weaker in the CURRENT scenarios. This indicates that under future offshore wind development, a number of locations that were previously isolated may become new sources of NIS to the Inner Danish waters, increasing the potential for introduction and spread of these species.

Despite having perhaps the greatest spatial cover of natural hard substrate within the model domain (Figure 2.6.1), model simulations for both offshore wind scenarios in both years suggest that in a single generation, a dispersal event the English Channel does not form a strong blue corridor for the spread of NIS to the Greater North Sea and beyond (Figure 3.1.2). This may be a result of the numerous ocean gyres that circulate water in this area (Ménesguen and Gohin 2006), potentially causing NIS to become 'trapped' within the area of the gyre rather than spreading beyond it. For example, the western Irish Sea seasonal gyre has been demonstrated to increase the likelihood that passive larvae are retained within the western Irish Sea (Phelps et al. 2015).

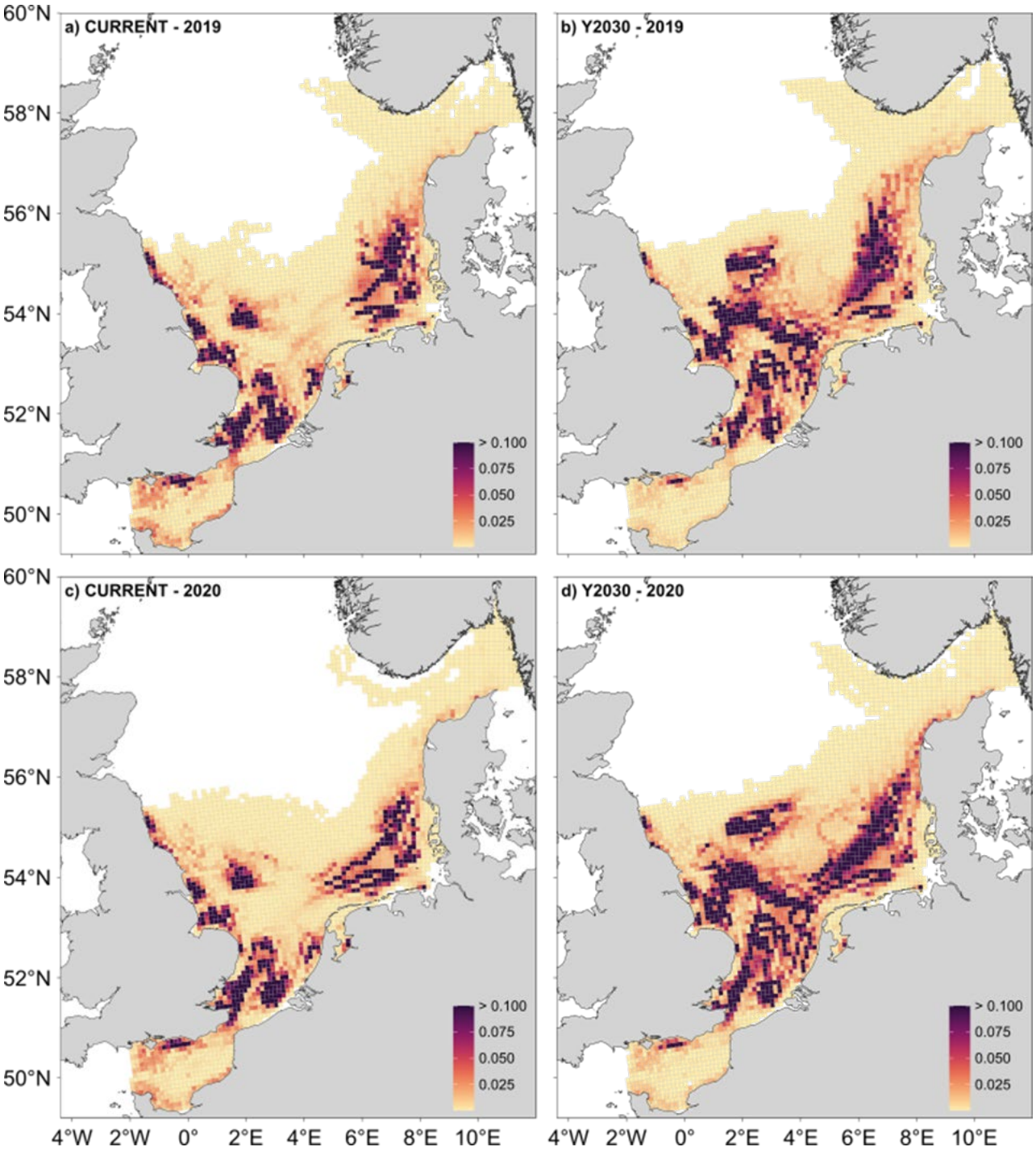

Figure 3.1.2. Tracking density of agents (i.e., Blue Corridors) in 10 km × 10 km grid cells in the North Sea for a) CURRENT scenario in 2019, b) Y2030 scenario in 2019, c) CURRENT scenario in 2020, and d) Y2030 scenario in 2020. Tracking density has been normalised between 0 and 1 and capped at a maximum value of 0.1 to aid interpretation.

Settlement Density. For all model scenarios, high settlement densities (i.e., number of agents within a grid cell at the end of their dispersal period) were observed on the western coast of Denmark, but these densities were greater in the Y2030 scenario than the CURRENT scenario in both years (Figure 3.1.3). Other areas with consistently high settlement densities were the German Bight, the Southern Bight and the eastern coast of England.

Considering 2019 only, in the CURRENT scenario high settlement densities were concentrated in those areas from which agents were released, suggesting dispersal was localised and that the majority of agents did not disperse over

large distances, as is evident from Figure 3.1.1. In fact, in the CURRENT scenario for 2019, 50% of agents were present within the same 10 km × 10 km grid cell from which they were released at the end of their planktonic larval duration (local retention). In contrast, for the Y2030 scenario in 2019, the local retention was 22% and settlement densities covered a greater spatial area (n = 2224 grid cells in the CURRENT scenario and n = 2718 grid cells in the Y2030 scenario), particularly along the Danish coastline and into the Skagerrak (Figure 3.1.3a, b). These differences likely reflect both the increased number of release locations of agents in the Y2030 scenario, which allows greater variability in dispersal pathways and changes in current speed caused by the introduction of additional turbines.

The same is largely true for the 2020 simulations. In the CURRENT scenario, settlement density is largely concentrated in those locations from which agents were released and the areas immediately surrounding those locations (Figure 3.1.3c). On the other hand, under the Y2030 scenario settlement densities cover a much larger spatial area (Figure 3.1.3d), and there is a lesser degree of local retention (51% in the CURRENT scenario and 21% in the Y2030 scenario).

These results would suggest that future development of offshore wind is likely to reduce the number of NIS that are retained within the wind farms in which they are already present, rather promoting connectivity to other, previously uncolonized areas. Similar results were demonstrated by Wood et al. (2021) for the North Sea surrounding England, where the inclusion of offshore wind farms as spawning locations for the non-native Pacific oyster substantially increased the extent of their spread. Equally, the number of NIS arriving to the western coast of Denmark is likely to increase under future offshore wind development regardless of variability in currents between years, from which point, given multi-generational spread, they may use these areas as a 'stepping stone' to the Inner Danish waters.

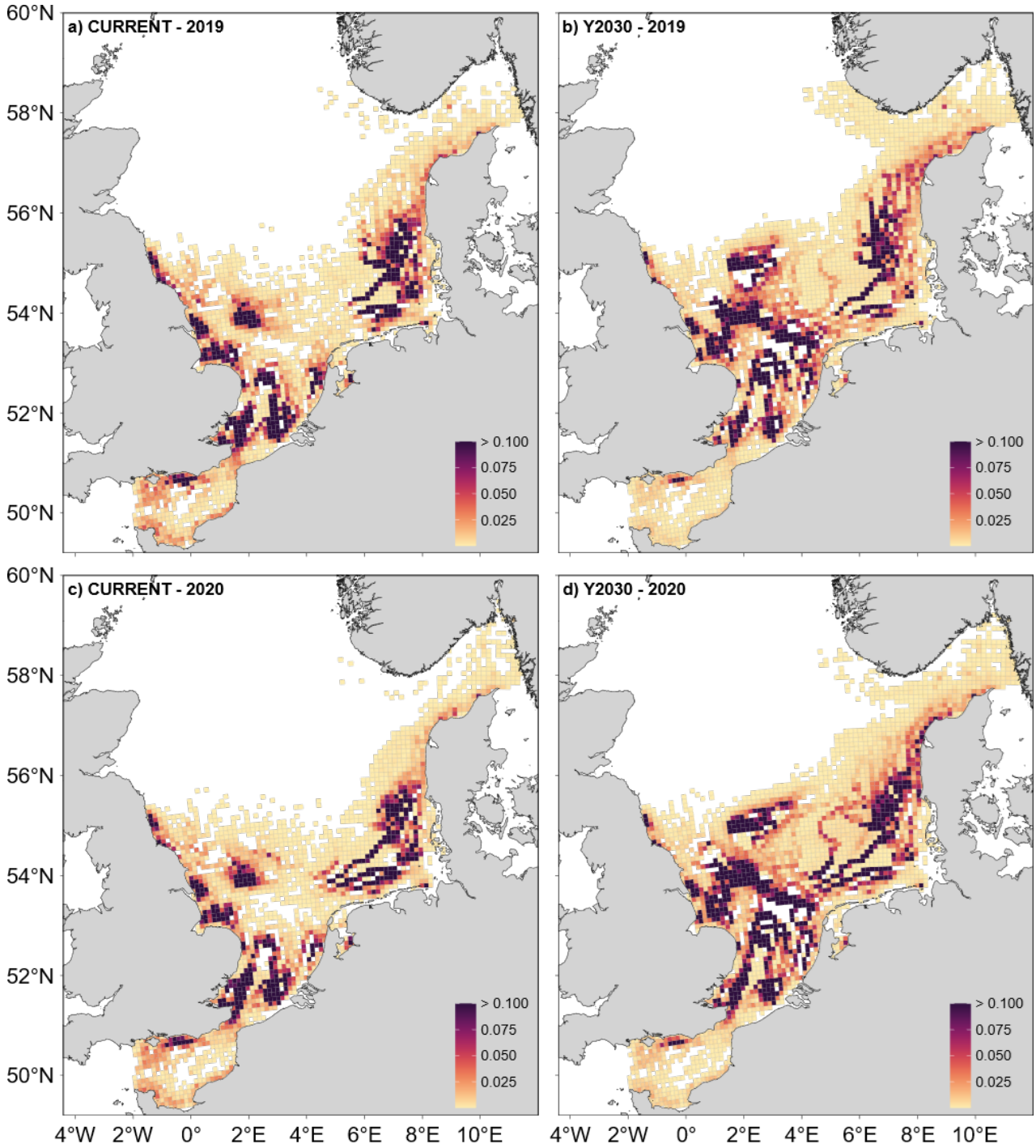

Figure 3.1.3. Settlement density of agents in 10 km × 10 km grid cells in the North Sea for a) CURRENT scenario in 2019, b) Y2030 scenario in 2019, c) CURRENT scenario in 2020, and d) Y2030 scenario in 2020. Settlement density has been normalised between 0 and 1 and capped at a maximum value of 0.1 to aid interpretation.

Age of Agents. The age of agents was calculated as the number of days for which they had been dispersing. Across all model scenarios, agents were youngest in the central North Sea and, on average, towards the end of their planktonic larval duration (183 days) by the time they reached the Danish coast, Skagerrak, and entrance to the Kattegat (Figure 3.1.4). This was especially evident when we examined the ages of agents within the 10 km × 10 km grid cells at the eastern border of the model, representing the opening to the Kattegat and Inner Danish waters.

Within these seven grid cells, the age distribution of agents differed significantly between model scenarios ($\chi^2(3) = 3869.8$, $p < 0.001$). For both years, the

median age of agents was greater in the Y2030 scenario than in the CURRENT scenario (Figure 3.1.5), likely as a result of lower current speeds in the Y2030 scenario, meaning it takes agents longer to disperse to this area (Maar et al. 2025). The median age of agents was lower in 2020 than 2019 for both the CURRENT and Y2030 scenarios, reflecting the higher wind speeds we observed in 2020 (Figure 3.1.5). Consequently, the minimum age of any one agent from all model scenarios was just 12 days and came from the CURRENT scenario for 2020, where greater current speeds and higher wind speeds enabled agents to rapidly reach the entrance to the Kattegat after dispersing from other areas. As for the distance distribution of agents, these differences highlight the importance of considering interannual variability in the potential dispersal patterns of non-indigenous species.

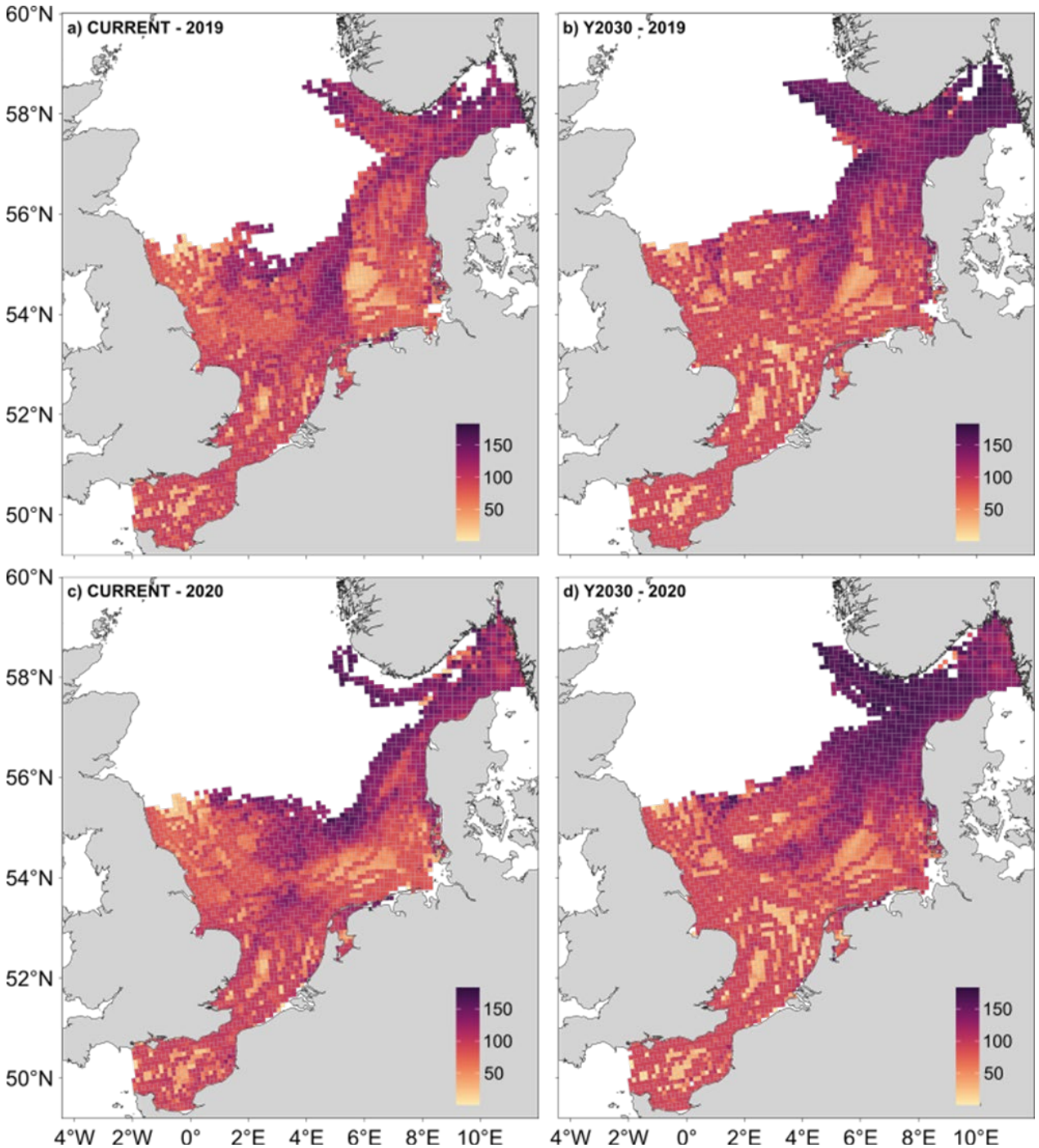

Figure 3.1.4. Average age (days) of agents in 10 km × 10 km grid cells in the North Sea for a) CURRENT scenario in 2019, b) Y2030 scenario in 2019, c) CURRENT scenario in 2020, and d) Y2030 scenario in 2020.

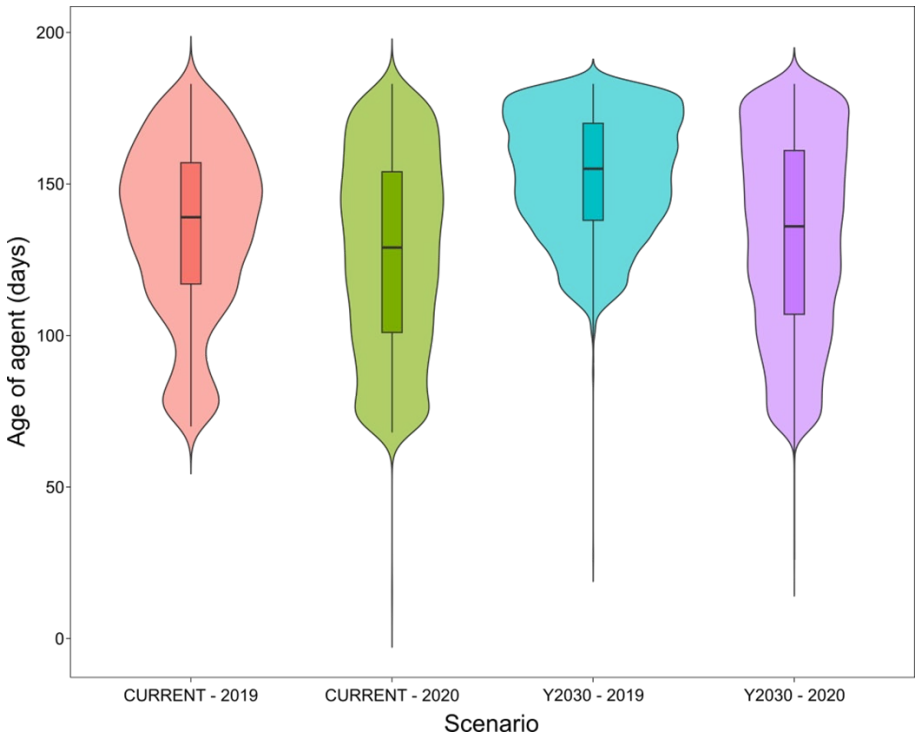

Figure 3.1.5. North Sea box and violin plots of the age (in days) of agents present in grid cells (10 km × 10 km) at the boundary to the Kattegat and Inner Danish waters at any point during the models for each of the four scenarios. Box plots show the minimum, maximum, 15th, 50th (median) and 75th percentiles of the age data. Violin plots show the distribution of the data.

3.1.2 Inner Danish waters

Dispersal Distance. For the Inner Danish waters, the distance distribution of agents did not significantly differ between the CURRENT and Y2030 scenarios for either 2019 or 2020 (Z= -1.79, p = 0.09 and Z = -1.33, p = 0.18, respectively). For both years, this would suggest little effect of the expansion of offshore wind on the potential dispersal distance of NIS within the Inner Danish waters (Table 3.1.2; Figure 3.1.6). On the other hand, the distance distributions of agents within the CURRENT and Y2030 scenarios significantly differed between the two years ($\chi^2(3) = 1888.9$, $p < 0.001$), with agents in the 2019 models travelling greater distances than the 2020 models (Table 3.1.2; Figure 3.1.6). This is unsurprising given the lower wind speeds observed in 2020 compared to 2019 (Figure 2.2.3). There was a greater degree of local retention in the 2020 models, with ~7% of agents retained in both scenarios compared to ~3% in the 2019 models. As for the North Sea models, this highlights the importance of considering interannual variability in the potential dispersal patterns of NIS.

Table 3.1.2. The distance distribution of agents that dispersed in the four Inner Danish waters agent-based models. Distances were measured between the start and end coordinates of each agent and are measured in kilometres (km).

Scenario	Year	Min.	25th percentile	Median	75th percentile	Max.
CURRENT	2019	0.30	10.31	33.70	65.31	384.67
Y2030	2019	0.38	10.36	34.95	67.05	396.14
CURRENT	2020	0.38	5.75	13.12	36.43	367.71
Y2030	2020	0.38	5.84	13.55	37.09	370.93

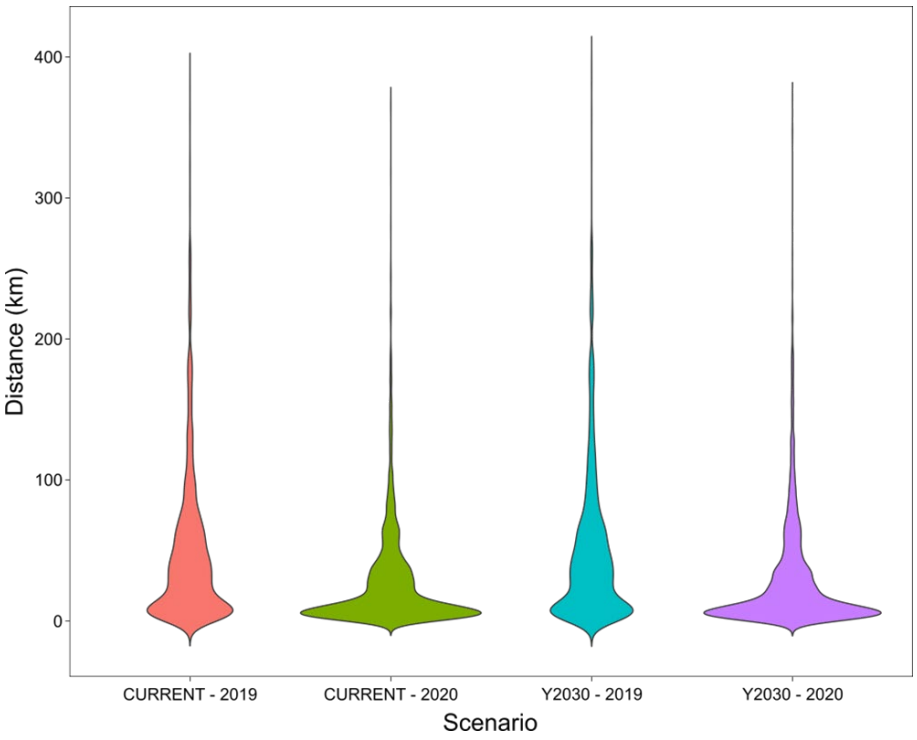

Figure 3.1.6. Inner Danish waters violin plot of the distance (km) between the start and end locations of agents in the agent-based models for each scenario.

Tracking Density (Blue corridors). In both scenarios for both years, agents predominantly drifted southwards along the Swedish coastline (Figure 3.1.7). For the 2019 models, agents in both scenarios then dispersed over relatively broad spatial scales, drifting both east and west of Zealand through the Sound and the Great Belt and continuing eastwards towards the island of Bornholm (Figure 3.1.7a, b). Conversely, for both scenarios in 2020, much fewer agents drifted south of Zealand (Figure 3.1.7c, d), which would suggest large inter-annual variability in dispersal pathways, likely resulting from the lower current speeds in 2020.

The tracking density of agents between the CURRENT and Y2030 scenarios for 2019 were largely similar, with the exception of the areas south of Funen and Bornholm, within which agents drifted in the Y2030 scenario, but not the CURRENT scenario (Figure 3.1.7a, b). In the 2020 models, agents in the Y2030 scenario drifted eastwards towards Bornholm, whilst in the CURRENT scenario agents did not drift past the area to the east of Møn (Figure 3.1.7c, d). For both years, this would suggest that future construction of offshore wind will alter blue corridors for NIS in the Inner Danish waters, facilitating eastward spread potentially into the Baltic Sea.

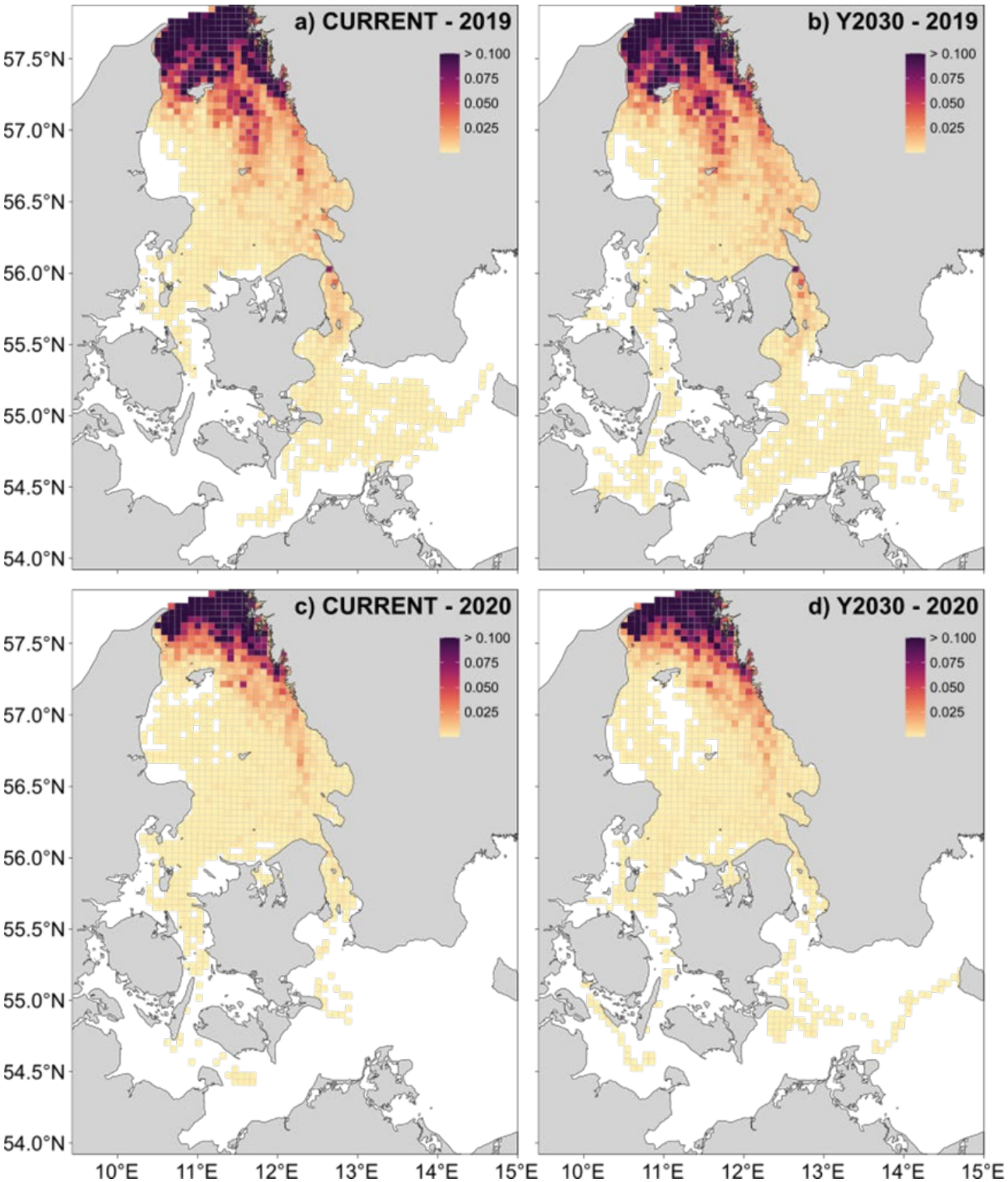

Figure 3.1.7. Tracking density (i.e., Blue Corridors) of agents in 5 km × 5 km grid cells in the Inner Danish waters for a) CURRENT scenario in 2019, b) Y2030 scenario in 2019, c) CURRENT scenario in 2020, and d) Y2030 scenario in 2020. Tracking density has been normalised between 0 and 1 and capped at a maximum value of 0.1 to aid interpretation.

Settlement Density. For all model scenarios, high settlement densities were observed along the northern part of the west coast of Sweden and at the boundary to the Kattegat (Figure 3.1.8). However, in both 2019 models there were also high settlement densities along the northern part of the east coast of Jutland, Denmark and around the island of Læsø, which were either not present or appeared significantly weaker in both 2020 models.

Settlement densities remained relatively similar between the CURRENT and Y2030 scenarios within either year. For the 2019 models, a 'hot-spot' for NIS settlement was evident between Elsinore (Denmark) and Helsingborg (Sweden) (Figure 3.1.8a, b). Whilst settlement occurred in the same area in both of the 2020 models, larvae did not arrive in as great a number as in 2019, evidenced by lower settlement density for both scenarios that year (Figure 3.1.8c, d). Additionally, settlement of agents in the 2019 models in the Arkona basin and towards Bornholm reflects the greater wind speeds observed that year (Figure 2.2.3), as such areas remained largely unreached in the 2020 models (Figure 3.1.8).

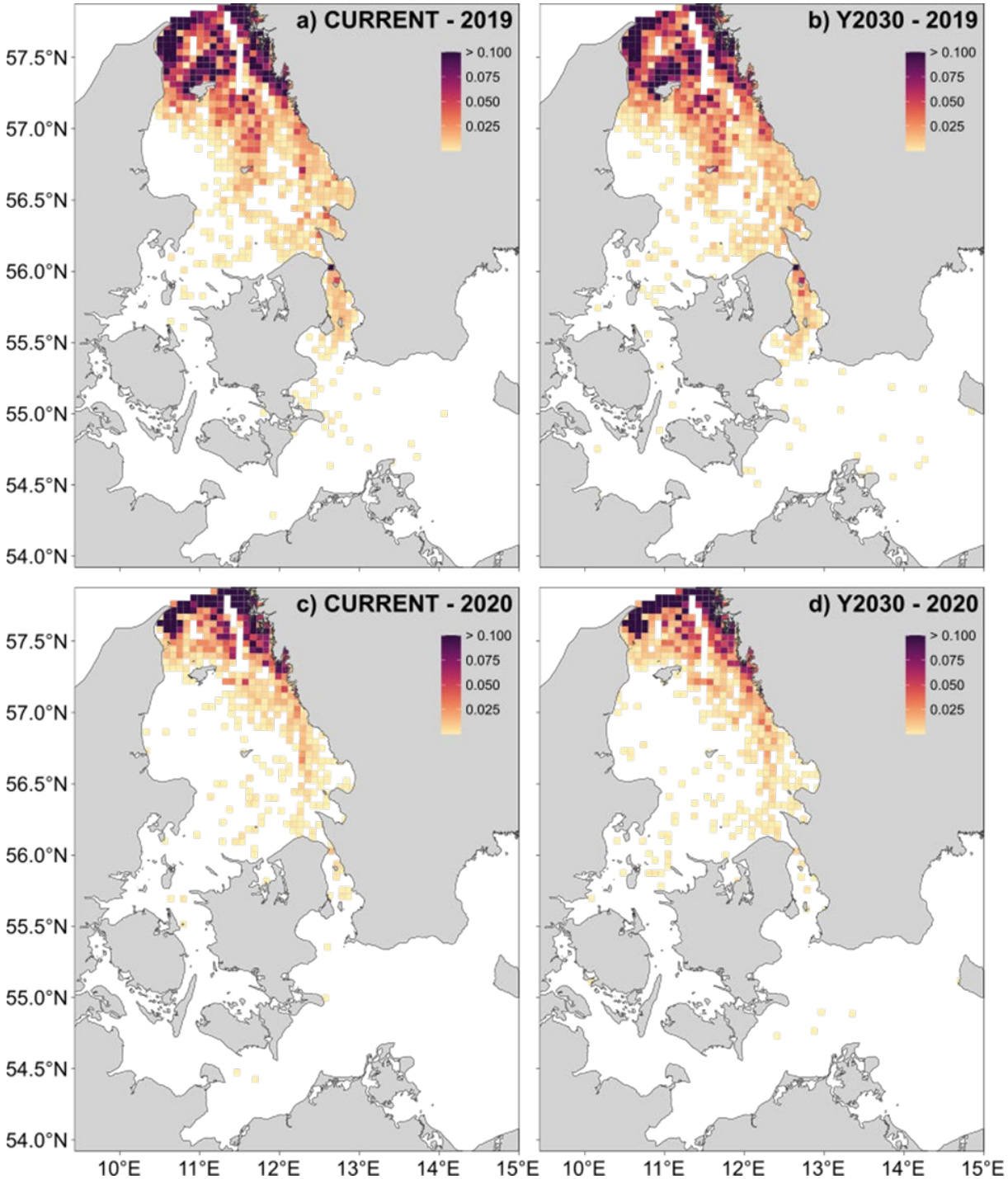

Figure 3.1.8. Settlement density of agents in 5 km × 5 km grid cells in the Inner Danish waters for a) CURRENT scenario in 2019, b) Y2030 scenario in 2019, c) CURRENT scenario in 2020, and d) Y2030 scenario in 2020. Settlement density has been normalised between 0 and 1 and capped at a maximum value of 0.1 to aid interpretation.

Age of Agents. As agents were released at the border between the Skagerrak and Kattegat, the average age of agents in this area is relatively low across all scenarios (Figure 3.1.9). For both the CURRENT and Y2030 scenarios, agents dispersing in 2019 appeared to be marginally younger on average when they reached the northern coast of Zealand than those in the 2020 models (Figure 3.1.9). This difference becomes more evident when considering those agents drifting through the Sound and southeast towards Bornholm, with agents in the 2019 models visibly younger than those in the 2020 models (Figure 3.1.9).

As a whole, these results would suggest that NIS spread from the southern North Sea into the Inner Danish waters is unlikely to occur within one generation for both the CURRENT and Y2030 offshore wind scenarios in 2020, as agents arriving from the North Sea to the entrance of the Kattegat are likely to be at least ~130 days old (based on the median age of agents in this area; Figure 3.1.5), and to reach areas south of Zealand would require ~100 additional days of dispersal (Figure 3.1.9). To put this into perspective, ~80% of shallow water invertebrate species will not survive a dispersal period of more than 8 weeks, or 56 days (Thorson 1961). However, the 2019 models' agents travelled further south through the Kattegat over a shorter period, which may suggest that dispersal from the southern North Sea to the Inner Danish waters is more likely in this year (Figure 3.1.9) and perhaps feasible for NIS capable of longer planktonic larval durations, such as the non-indigenous bryozoan *Watersipora subtorquata*, which has been shown to survive up to 15 weeks in a laboratory environment (Sams et al. 2015).

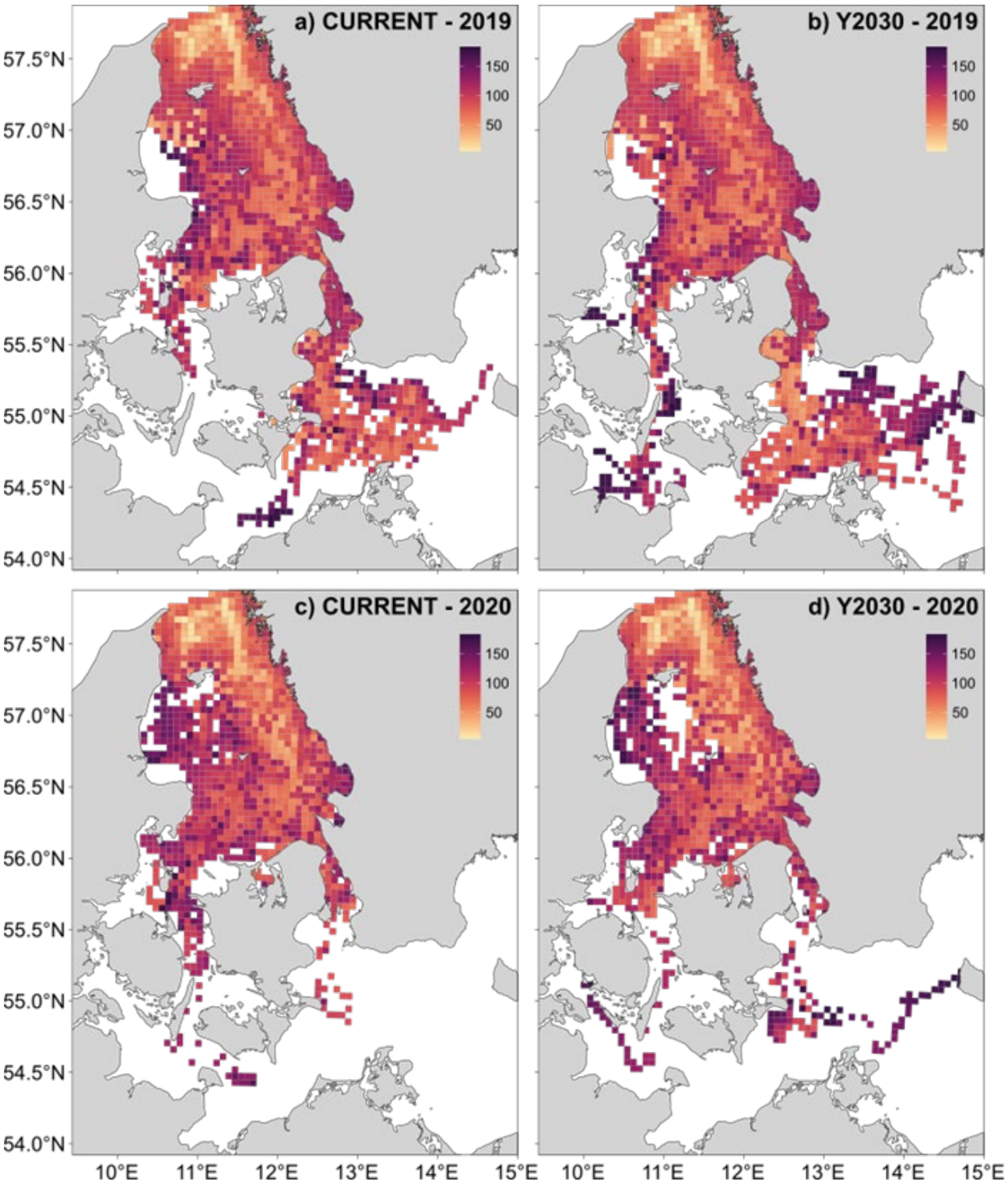

Figure 3.1.9. Average age (days) of agents in 5 km × 5 km grid cells in the Inner Danish waters for a) CURRENT scenario in 2019, b) Y2030 scenario in 2019, c) CURRENT scenario in 2020, and d) Y2030 scenario in 2020.

3.1.3 Model uncertainties and potential future development of ABMs

The aim of this work was to document the main dispersal pathways, or 'blue corridors' within the North Sea and Inner Danish waters as driven by the predominant ocean currents. Therefore, we chose to model passive agents with no biological traits. The process of larval dispersal is complex, and both inter-species and inter-individual heterogeneity in biological traits, such as larval mortality (Rumrill 1990), vertical swimming behaviour (James et al. 2023), settlement dynamics (Hunt and Scheibling 1997) and planktonic larval duration

(Shanks 2009), can dramatically alter dispersal outcomes (Bowler and Benton 2005, Nanninga and Berumen 2014). Whilst our decision to model passive agents with no mortality, a set PLD (six months), and without restrictions on settlement was appropriate given the aims of the study, it necessitates that the results of the models are not intended to form detailed or quantitative predictions of NIS dispersal or spread. In another ongoing project, species biological traits will be added to the ABMs.

Our approach emulates the dispersal of NIS with a pelagic larval phase, which, whilst representing the majority of non-indigenous species in this region (Quell et al. 2021), is therefore not applicable to those with alternative dispersal mechanisms, such as brooded larvae or direct development (Paulay and Meyer 2006). For example, the non-indigenous amphipod *Caprella mutica*, broods developing embryos that hatch as fully formed juveniles (Cook et al. 2007), whilst the sea squirt *Didemnum vexillum* reproduces both sexually (larvae) and asexually through fragmentation (Stefaniak and Whitlatch 2014). As such, the results of the models presented here should be interpreted with caution in relation to NIS whose primary mechanism of dispersal is not pelagic larvae.

The movement of agents in the ABMs was directly influenced by the velocity fields and turbulence simulated by the hydrodynamic model and, consequently, uncertainties in the hydrodynamic model propagate into the ABMs. The hydrodynamic model has been rigorously calibrated using an extensive dataset and performs well in reproducing sea surface height dynamic observations from the Danish Meteorological Institute, which provide a strong constraint on horizontal transport processes and overall circulation patterns. However, the Inner Danish waters represent a highly complex hydrodynamic environment and, despite the model's robust performance, an absence of direct current measurements within the three major straits - Little Belt, Great Belt and the Sound - introduces a degree of uncertainty in the simulated flow fields. This affects the accuracy of agent trajectories and, therefore, of the predicted spread of NIS. Thus, whilst the model provides a reliable framework for understanding transport dynamics, some uncertainty in agent movement and dispersal pathways must be acknowledged.

Finally, our aim was to characterise the primary dispersal corridors of NIS larvae within the two model regions that had set extents and boundaries. As such, agents that dispersed to areas outside of the model boundaries were not considered. However, in the case of the eastern-most open boundary of the North Sea, the model may have provided additional insights into the supply of NIS to the Inner Danish waters. Examining the proportion of agents leaving the model domain and the age at which they left could be a focus of future research to strengthen predictions on the likelihood of spread of NIS from the southern North Sea to the Inner Danish waters.

3.2 Interannual effects of offshore wind farms on ecosystem indicators

3.2.1 Interannual variability

Model scenario. The interannual variability is governed by the different meteorological forces affecting the heat fluxes and wind stress at the sea surface. Year 2019 was considered a 'normal' year compared to the recent 5-year mean (2019-2023). Year 2020 contrasted with the 5-year mean, with greater annual wind speed and warmer temperatures (Figure 2.2.1), but with lower wind speed during summer (Table 2.2.1). Further, the open boundary conditions to the North Atlantic and the initial fields vary between years and can influence water level, current patterns, etc. Indicator responses to offshore wind farms in scenario Y2030 relative to REF-NO-FARM were tested for two years (equation 1). Scenario 2020-S used the respective initial fields from the two scenarios REF-NO-FARM and Y2030 (Table 2.6.1). Hence, the 2020-S scenario included the signal from the offshore wind farms evolving from one year to the next in the simulations.

The North Sea. The indicator responses to offshore wind farms differed significantly between the two years during summer, except for stratification (Table 3.2.1). Stratification (PEA) inside the offshore wind farms did not differ between years, probably due to the strong monopile mixing effect. On the contrary, stratification was stronger outside the offshore wind farm areas in 2020-S (Figure 3.2.1a,b) due to the weaker summer wind speed in 2020 compared to 2019. Surface temperature was warmer both outside and inside the offshore wind farms in 2020-S compared to 2019 due to the stronger stratification and lateral transport (Figure 3.2.1c,d). Surface current speeds decreased both years due to offshore wind farms, but the effect was significantly different between the two years (Figure 3.2.1e,f).

Primary production, Chl *a* concentrations and bottom oxygen responses were all significantly different between 2020-S and 2019 in Y2030 (Figure 3.2.2). Chl *a* concentrations decreased even more in 2020-S compared to 2019, probably due to the combination of higher temperatures, stronger stratification, nutrient limitation and grazing pressure. Bottom oxygen concentrations showed less response to offshore wind farms than in 2019. Although the median responses of all indicators were below 1% in Table 3.2.1, the variability (percentiles) was much higher, as seen in the box-violin plots (Figures 3.2.1 and 3.2.2). The annual indicator responses were similar to the summer responses (Table 3.2.2).

The Inner Danish waters. Indicator responses to offshore wind during summer differed significantly between the two years, except for primary production and Chl *a* concentrations inside the offshore wind farms (Table 3.2.3). Summer stratification (PEA) was stronger both inside and outside the offshore wind farms (<20 km) in 2020-S relative to 2019 (Figure 3.2.3a,b). The stronger stratification agreed with the weaker summer wind speed in 2020 compared to 2019. Surface temperature was warmer in 2020-S both outside and inside the offshore wind farms due to the stronger stratification and lateral transport

(Figure 3.3.3c,d). Current speeds decreased both in 2019 and 2020-S, although to a lesser extent in 2020-S (Figure 3.3.3e,f).

The responses in primary production and Chl *a* concentrations decreased to a lesser extent outside the offshore wind farms in 2020-S compared to 2019 (Figure 3.3.4a-d). Bottom oxygen decreased inside but increased outside the offshore wind farms in 2020-S compared to 2019 (Figure 3.3.4e,f). This pattern was most likely due to spatial changes in bottom stress causing a redistribution of organic matter and associated oxygen consumption. Although the median responses were below 9% for all variables in Table 3.2.3, the variability (percentiles) was much higher, as seen in the box-violin plots (Figures 3.2.3 and 3.2.4). The annual indicator responses were similar to the summer responses in 2020-S, except that current speed (inside) and primary production (outside) showed no significant change relative to 2019 (Table 3.2.4).

Table 3.2.1. North Sea summer median responses (%) between scenarios Y2030 and REF-NO-FARM for 2019 and 2020 and the difference between the two years. "OWF" = offshore wind farm area; "< 40 km" = area up to 40 km from the OWF. The responses between 2019 and 2020-S (interannual variability) are indicated as significant difference (*) or no difference (-). Cumulative effects (between 2020-S and 2020-R) were assessed as significant (√) or not (). A significant difference was assessed by a Kruskal-Walli's test.

North Sea Summer	Area	2019 (%)	2020-S (%)	Difference between years	2020-R (%)	Cumulative effects
PEA	OWF	-0.04	0.16	-	0.20	
PEA	<40 km	0.18	0.31	*	0.34	√
Surface temp.	OWF	0.19	0.43	*	0.37	√
Surface temp	<40 km	0.23	0.32	*	0.29	√
Current speed	OWF	-0.81	-0.70	*	-0.72	
Current speed	<40 km	-0.14	-0.19	*	-0.19	
Primary prod.	OWF	0.67	0.37	*	0.16	√
Primary prod.	<40 km	0.24	0.07	*	0.13	
Surface Chl *a*	OWF	-0.21	-0.52	*	-0.41	
Surface Chl *a*	<40 km	-0.01	-0.18	*	-0.03	√
Bottom oxygen	OWF	0.19	0.08	*	0.10	√
Bottom oxygen	<40 km	0.03	-0.01	*	0.00	√

Table 3.2.2. North Sea annual median responses (%) between scenarios Y2030 and REF-NO-FARM for 2019 and 2020 and the difference between the two years. "OWF" = offshore wind farm area; "< 40 km" = area up to 40 km from the OWF. The responses between 2019 and 2020-S (interannual variability) are indicated as significant difference (*) or no difference (-). Cumulative effects (between 2020-S and 2020-R) were assessed as significant (√) or not (). A significant difference was assessed by a Kruskal-Walli's test.

North Sea Annually	Area	2019 (%)	2020-S (%)	Difference between years	2020-R (%)	Cumulative effects
PEA	OWF	0.08	0.11	-	0.12	
PEA	<40 km	0.02	0.08	*	0.08	
Surface temp.	OWF	0.32	0.54	*	0.41	√
Surface temp	<40 km	0.25	0.36	*	0.26	√
Current speed	OWF	-0.89	-0.91	-	-0.94	
Current speed	<40 km	-0.11	-0.12	*	-0.12	
Primary prod.	OWF	0.15	0.07	*	0.04	
Primary prod.	<40 km	0.03	0.00	*	0.01	√
Surface Chl *a*	OWF	-0.07	-0.19	*	-0.04	√
Surface Chl *a*	<40 km	-0.02	-0.07	*	0.01	√
Bottom oxygen	OWF	-0.02	-0.08	*	-0.02	√
Bottom oxygen	<40 km	-0.03	-0.07	*	-0.03	√

Discussion of interannual variability. The interannual variability in indicator responses was significantly different between the two years for most indicators in both the North Sea and the Inner Danish wates. Year 2020 was a warmer year with less wind speed during summer compared to 2019. In general, the responses to offshore wind farms showed that stratification was stronger and surface temperatures higher in 2020-S compared to 2019 for both basins. The responses in current speeds, primary production, Chl *a* and bottom oxygen concentration varied inside and outside the offshore wind farms and between basins. The significant differences between the two years highlight the importance of considering the interannual variability to fully understand and estimate the effects of offshore wind on the marine environment.

3.2.2 Accumulated effects between years

Model scenarios. Indicator responses in Y2030 relative to REF-NO-FARM were compared for 2020 in two different settings (equation 1, Table 2.6.1). Scenario 2020-R used the same initial fields from REF-NO-FARM-2019, whereas scenario 2020-S used the respective initial fields from the REF-NO-FARM-2019 and Y2030-2019 (Table 2.6.1). The cumulative effects over time were assessed by comparing 2020-S (different initial fields from scenarios) and 2020-R (same initial fields from reference). If the two runs were different, this would indicate that there was a transfer of the signal from offshore wind farms from one year to the next.

The North Sea. There were significant accumulated effects during summer for PEA (only outside the wind farms), surface temperatures, primary production (only inside the wind farms), Chl *a* (only outside the wind farms) and bottom oxygen (Table 3.2.1). On an annual basis, there were significant accumulated effects for surface temperature, primary production (only outside the wind farms), Chl *a* concentrations and bottom oxygen (Table 3.2.2).

The Inner Danish waters. For the summer, there were accumulated effects for primary production, Chl *a* (both only outside the wind farms) and bottom oxygen (Table 3.2.3). On annual basis, there were significant accumulated effects for surface temperature, primary production, Chl *a* concentrations (for all three indicators only outside the wind farms) and bottom oxygen (Table 3.2.4).

Discussion of accumulated effects. These results suggest that there was some memory in the marine system regarding the effects of offshore wind farms. Hence, there could be a warming trend over more years due to offshore wind in both basins. Likewise, there could be a decreasing temporal trend in bottom oxygen for the North Sea. In the Inner Danish waters, there was a spatial redistribution of oxygen content due to offshore wind farms that could be reinforced over time. Primary production and Chl *a* concentrations showed a tendency towards accumulated effects outside the offshore wind farms, with a decrease in the North Sea and an increase in the Inner Danish waters over time. However, it would require data from a longer period (>5 years) to fully explore the cumulated ecosystem response on top of the interannual variability.

Stratification (PEA) only showed cumulative effects during summer in the North Sea outside the offshore wind farms, indicating more mixing over time. The signal from offshore wind farms on stratification between years was probably diluted by the winter mixing and storm events. Also, responses in current speed did not show any cumulative effect (annually or summer) over time, indicating that this effect was more an immediate response to offshore wind farms.

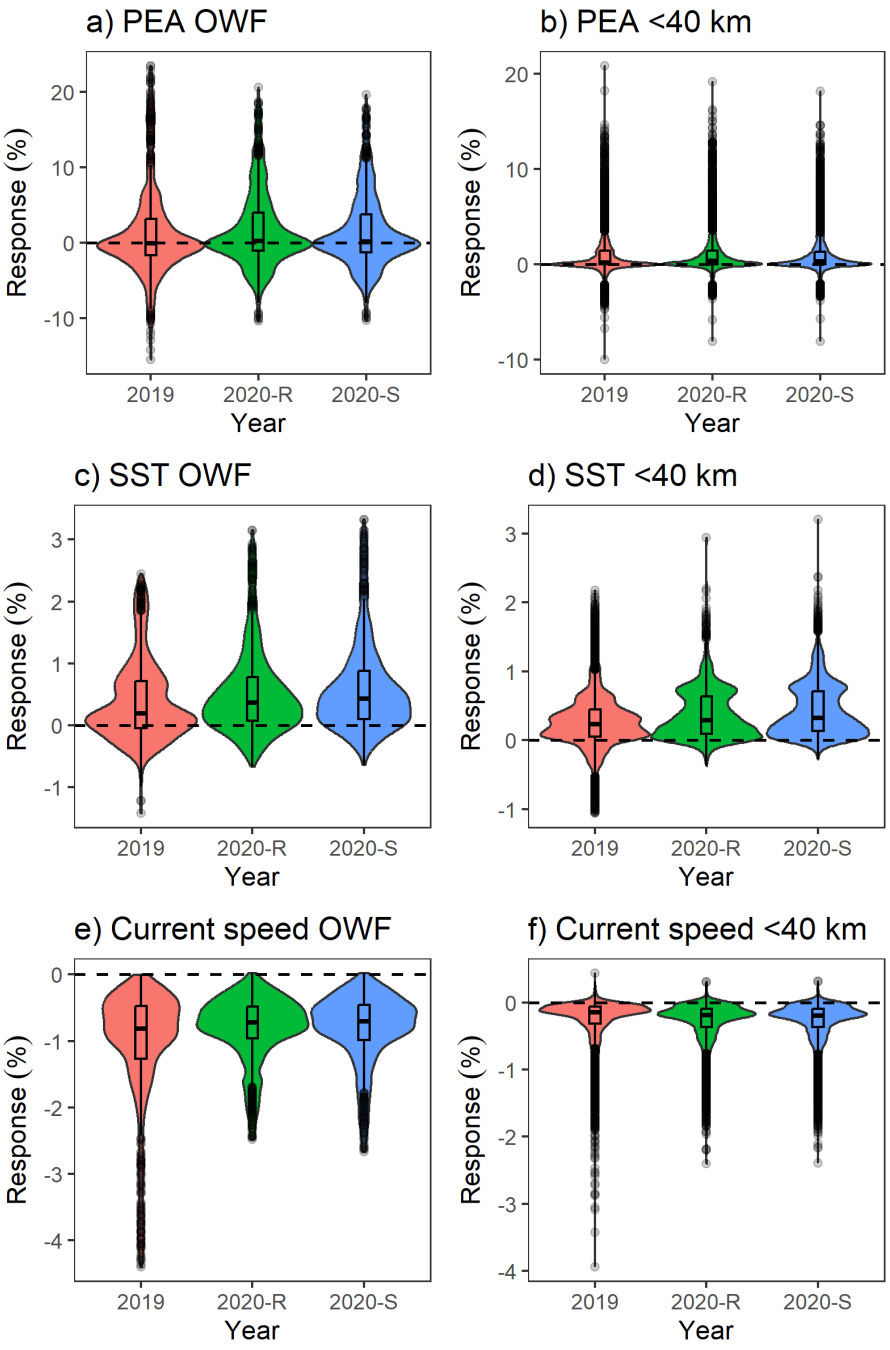

Figure 3.2.1. North Sea box-violin plots of physical indicators of change. The summer median responses (%) of a-b) PEA, c-d) Sea surface temperature (SST), and e-f) Surface current speed for the offshore wind farm areas (OWF) and up to 40 km from the OWF (< 40 km), respectively, in Y2030 relative to the REF-NO-FARM. The results are shown for 2019, 2020-R (same initial fields) and 2020-S (different initial fields). The box plots show the minimum, maximum, 25th, 50th (median) and 75th percentiles and potential outliers. The violin plots show the distribution of the data.

Figure 3.2.2. North Sea box-violin plots of ecosystem indicators of change. The summer median responses (%) of a-b) Primary production, c-d) Chl *a*, and e-f) Bottom oxygen for the offshore wind farm areas (OWF) and up to 40 km from the OWF (< 40 km), respectively, in Y2030 relative to REF-NO-FARM. The results are shown for 2019, 2020-R (same initial reference fields) and 2020-S (different initial fields). The box plots show the minimum, maximum, 25th, 50th (median) and 75th percentiles and potential outliers. The violin plots show the distribution of the data.

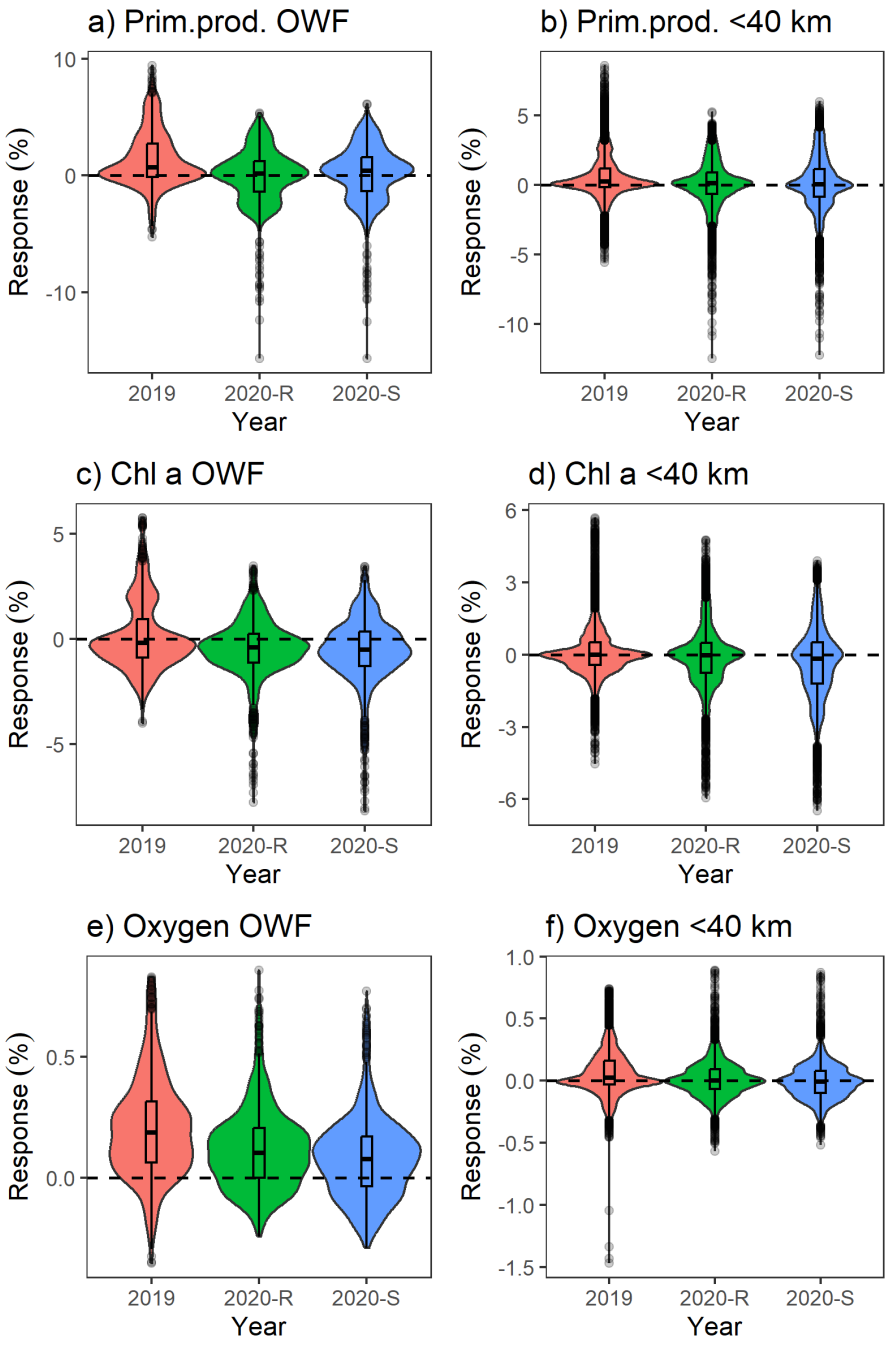

Table 3.2.3. The Inner Danish waters summer median responses (%) between scenarios Y2030 and REF-NO-FARM for 2019 and 2020. "OWF" = offshore wind farm area; "<20 km" = area up to 20 km from the OWF. The responses between 2019 and 2020-S (interannual variability) are indicated as significant difference (*) or no difference (-). Cumulative effects (between 2020-S and 2020-R) were assessed as significant (√) or not (). A significant difference was assessed by a Kruskal-Walli's test.

Inner Danish waters Summer	Area	2019 (%)	2020-S (%)	Difference between years	2020-R (%)	Cumulative effects
PEA	OWF	5.58	8.39	*	8.48	
PEA	<20 km	3.18	4.29	*	4.36	
Surface temp.	OWF	1.05	1.14	*	1.13	
Surface temp	<20 km	0.20	0.29	*	0.29	
Current speed	OWF	-3.74	-3.44	*	-3.47	
Current speed	<20 km	-0.67	-0.51	*	-0.50	
Primary prod.	OWF	-3.20	-4.48	-	-4.43	
Primary prod.	<20 km	-1.03	-0.45	*	-0.50	√
Surface Chl *a*	OWF	-1.88	-2.08	-	-2.07	
Surface Chl *a*	<20 km	-0.96	-0.66	*	-0.69	√
Bottom oxygen	OWF	-0.03	-0.32	*	-0.03	√
Bottom oxygen	<20 km	-0.12	-0.07	*	-0.12	√

Table 3.2.4. Inner Danish waters annual median responses (%) between scenarios Y2030 and REF-NO-FARM for 2019 and 2020. "OWF" = offshore wind farm area; "<20 km" = area up to 20 km from the OWF. The responses between 2019 and 2020-S (interannual variability) are indicated as significant difference (*) or no difference (-). Cumulative effects (between 2020-S and 2020-R) were assessed as significant (√) or not (). A significant difference was assessed by a Kruskal-Walli's test.

Inner Danish waters Annually	Area	2019 (%)	2020-S (%)	Difference between years	2020-R (%)	Cumulative effects
PEA	OWF	4.16	4.59	*	4.77	
PEA	<20 km	1.44	2.09	*	1.97	
Surface temp.	OWF	0.10	0.37	*	0.31	
Surface temp	<20 km	0.05	0.14	*	0.08	√
Current speed	OWF	-3.42	-3.28	-	-3.24	
Current speed	<20 km	-0.52	-0.45	*	-0.44	
Primary prod.	OWF	-0.30	-0.47	-	-0.46	
Primary prod.	<20 km	-0.01	0.00	-	-0.03	√
Surface Chl *a*	OWF	0.09	-0.07	*	-0.11	
Surface Chl *a*	<20 km	0.02	0.03	*	-0.05	√
Bottom oxygen	OWF	-0.19	-0.31	*	-0.19	√
Bottom oxygen	<20 km	-0.09	-0.05	*	-0.09	√

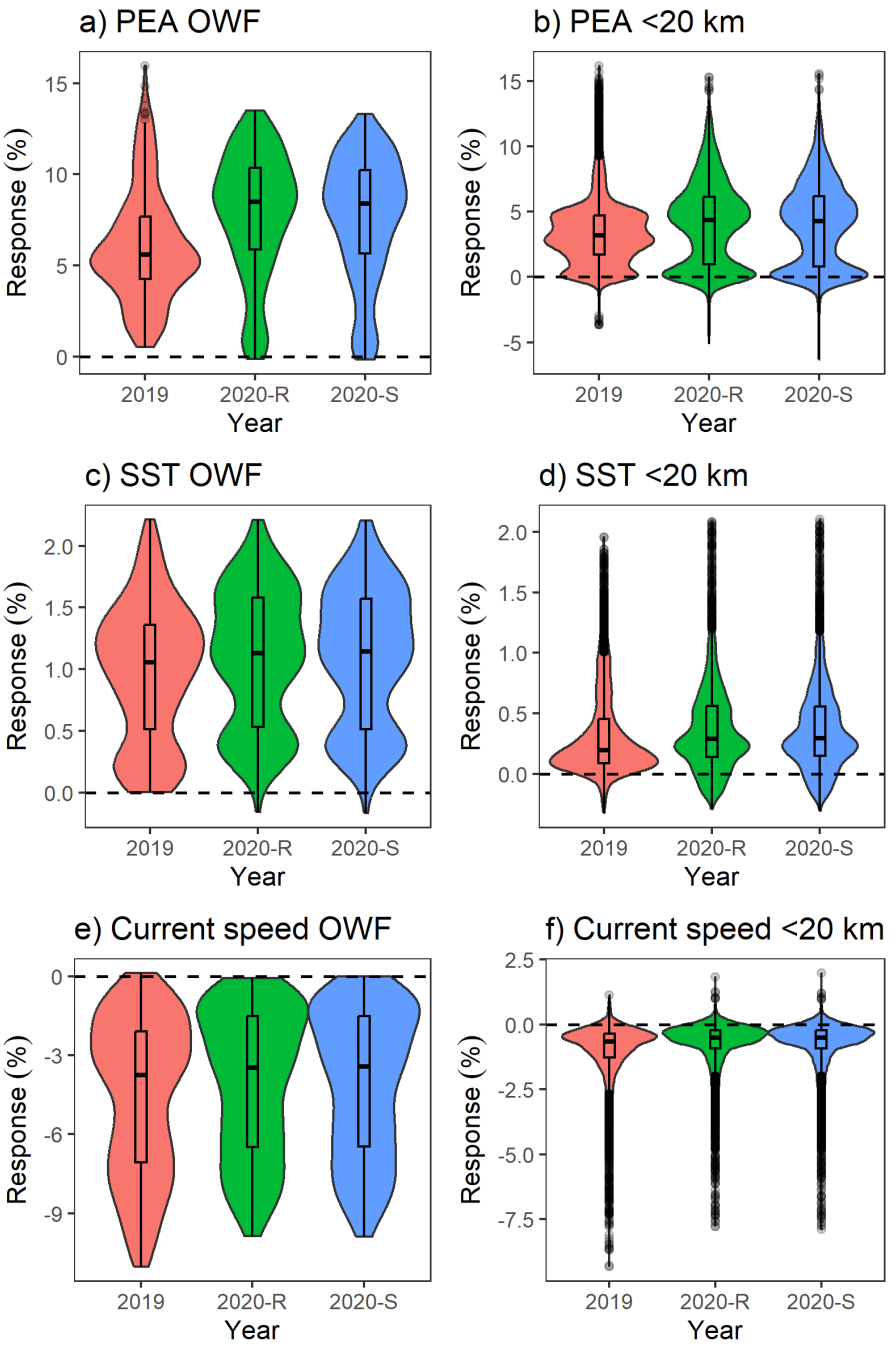

Figure 3.2.3. Inner Danish waters box-violin plots of physical indicators of change. The annual median responses (%) of a-b) PEA, c-d) Sea surface temperature (SST), and e-f) Surface current speed for the offshore wind farm areas (OWF) and up to 20 km from the OWF (<20 km), respectively, in Y2030 relative to the REF-NO-FARM. The results are shown for 2019, 2020-R (same initial fields) and 2020-S (different initial fields). The box plots show the minimum, maximum, 25th, 50th (median) and 75th percentiles and potential outliers. The violin plots show the distribution of the data.

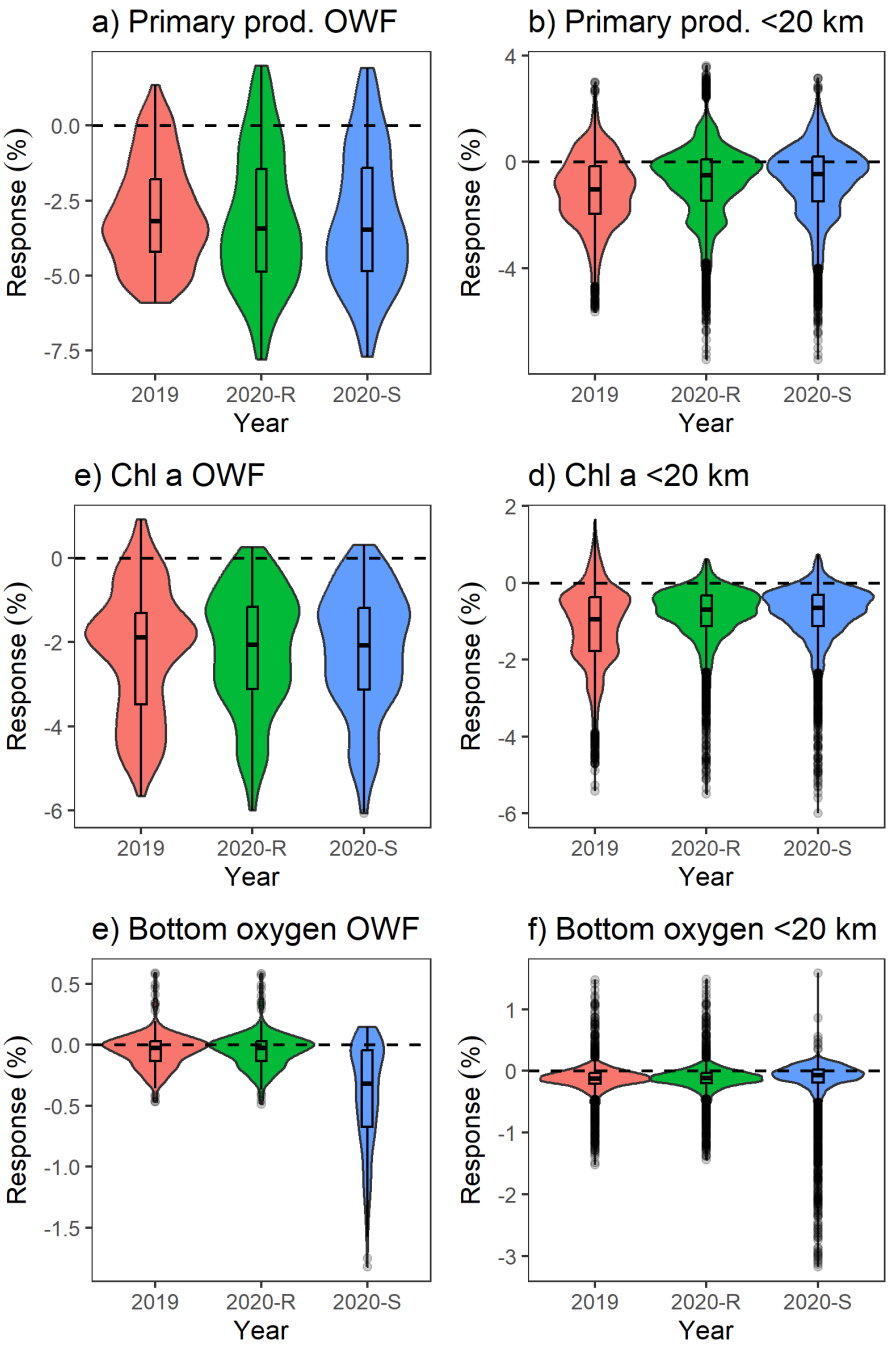

Figure 3.2.4. Inner Danish waters box-violin plots of ecosystem indicators of change. The annual median responses (%) of a-b) primary production, c-d) Chl *a* concentration, and e-f) bottom oxygen concentration for the offshore wind farm areas (OWF) and up to 20 km from the OWF (<20 km), respectively, in Y2030 relative to the REF-NO-FARM. The results are shown for 2019, 2020-R (same initial fields) and 2020-S (different initial fields). The box plots show the minimum, maximum, 25th, 50th (median) and 75th percentiles and potential outliers. The violin plots show the distribution of the data.

3.2.3 Biogeochemical model uncertainties and potential future development

Despite the valuable insights provided by 3D coupled hydrodynamic-biogeochemical models in understanding marine ecosystem dynamics, several sources of uncertainty must be acknowledged when interpreting model outputs and projecting future scenarios.

The scenarios were conducted for two years with different weather conditions, but more years would be needed to assess the full range of observed natural variability as seen in the atmospheric models. Further, since some of the effects were found to accumulate over time and the offshore wind farms are expected to be operational for many years, accumulated effects over several years would be appropriate to consider in the future rather than only two years.

The North Sea and Inner Danish water models were not coupled in the applied set-up but used the same open boundary conditions as in the reference simulations. The effects of offshore wind farms on the different indicators could be diluted by inflow of new water coming in from the open boundary in the Skagerrak.

Model structure and process representation pose a fundamental source of uncertainty. The biogeochemical model groups organisms into plankton functional types, which mask species-specific traits, adaptive behaviors and community shifts. Many biogeochemical processes, such as plankton and detritus interactions, sediment-water nutrient fluxes and species-specific physiological responses, are often simplified due to computational constraints or limited empirical data. This simplification can limit the model's ability to capture ecological responses to environmental stressors and anthropogenic pressures. These simplifications can lead to biased estimates of key ecosystem indicators, such as primary production, oxygen dynamics and nutrient cycling.

The coupling between physical and biogeochemical components introduces further complexity. Errors in hydrodynamic simulations, such as those related to temperature, salinity and stratification, can directly influence biogeochemical processes leading to misrepresentation of biological productivity and hypoxia events. Coarse grids may fail to capture localized phenomena correctly, such as monopile mixing effects and wake effects. The study used the best available atmospheric forcing data and monopile drag parameterization from similar studies. The FlexSem model set-ups of the North Sea and Inner Danish waters are two relatively new model systems, and continued calibration and improvement of physical-biogeochemical processes are foreseen. The models showed good to reasonable performance according to the cost functions, correlation coefficient's and normalized standard deviations in comparison to monitoring data from 2020 in the appendix A and the previous study for 2019 (Maar et al. 2025).

4 Summary

4.1 Dispersal corridors for NIS

All model scenarios show that agents drift along a 'blue corridor' from the German Bight northwards following the western Danish coastline towards the entrance to the Kattegat. Further, future offshore wind development in the Southern Bight and the eastern coast of England may transform previously isolated locations in the German Bight into new sources of NIS introductions to the Inner Danish waters, thereby increasing the potential for their spread. In contrast, the English Channel does not appear to form a strong blue corridor for NIS dispersal into the Greater North Sea and beyond.

Settlement density modelling indicates that future offshore wind expansion is likely to reduce the retention of NIS within existing wind farms, instead enhancing connectivity to other, potentially uncolonized areas. Notably, the number of NIS arriving to the Inner Danish waters is expected to increase under future offshore wind scenarios, regardless of interannual variability in ocean currents. These areas may then serve as 'stepping stones' for multi-generational spread into the Inner Danish waters.

After entering the Kattegat, agents predominantly drifted southwards along the Swedish coastline. In 2019, agents dispersed over relatively broad spatial scales, drifting both east and west of Zealand through the Sound and the Great Belt and continuing eastwards towards the island of Bornholm. Conversely, in 2020 much fewer agents drifted south of Zealand, which would suggest large interannual variability in dispersal pathways, likely resulting from the lower current speeds in 2020. Future construction of offshore wind was shown to alter blue corridors for NIS in the Inner Danish waters, facilitating a larger eastward spread potentially into the Baltic Sea.

Overall, these results would suggest that NIS spread from the southern North Sea into the Inner Danish waters is unlikely to occur within one generation for both the CURRENT and Y2030 offshore wind scenarios in 2020, as agents arriving from the North Sea to the entrance of the Kattegat are likely to be at least ~130 days old. However, the 2019 models' agents travelled further south through the Kattegat over a shorter period, which may suggest that dispersal from the southern North Sea to the Inner Danish waters is more likely in this year.

Regardless, the degree of spread demonstrated in both model scenarios for 2019 and 2020 demonstrates that, given multiple generations, non-indigenous species spread from the North Sea through the Inner Danish waters and towards the Baltic Sea proper is both feasible and likely. Therefore, the stepping-stone role of offshore wind in extending the spread of these species is of concern both now and given the future expansion of offshore wind.

4.2 Interannual variability and accumulated ecosystem effects

Ecosystem indicator responses to offshore wind were significantly different between the two considered years in the North Sea and Inner Danish waters. These results highlight the importance of considering the interannual variability to fully understand and estimate the effects of offshore wind on the marine environment in comparison to the natural variability of the ecosystem. To identify the robustness of the found patterns with respect to different weather conditions and interannual variations, additional analyses and simulations are required.

The accumulated effects observed in certain ecosystem indicators between years suggest a form of ecological memory in both marine ecosystems regarding the impacts of offshore wind. This implies the potential for a long-term warming trend in both basins associated with offshore wind development. Similarly, a declining temporal trend in bottom oxygen levels may be emerging in the North Sea. In the Inner Danish waters, offshore wind farms appear to have caused a spatial redistribution of oxygen content, which could intensify over time.

Primary production and chlorophyll-a concentrations also exhibited signs of cumulative effects outside the offshore wind farm areas, with a decreasing trend in the North Sea and an increasing trend in the Inner Danish waters. However, to fully assess these long-term ecosystem responses beyond interannual variability, data spanning more than the considered two years would be necessary. To further investigate the robustness of these patterns, their propagation through the food web and the implications for ecosystem services and management, it is essential to repeat the simulation experiments using a food web modelling approach and multi-annual simulations.

5 References

Adams T.P., Miller R.G., Aleynik D., & Burrows M.T. (2014). Offshore marine renewable energy devices as stepping stones across biogeographical boundaries. *Journal of Applies Ecology, 51*(2), p. 330-338. https://doi.org/10.1111/1365-2664.12207

Andersen J.H., Al-Hamdani Z., Harvey E.T., Kallenbach E., Murray C., & Stock A. (2020). Relative impacts of multiple human stressors in estuaries and coastal waters in the North Sea–Baltic Sea transition zone. *Science of the Total Environment, 704*. https://doi.org/10.1016/j.scitotenv.2019.135316

Andersson M.H., & Öhman M.C. (2010). Fish and sessile assemblages associated with wind-turbine constructions in the Baltic Sea. *Marine and Freshwater Research, 61*(6), p. 642-650. https://doi.org/10.1071/MF09117

Arneborg L., Pemberton P., Grivault N., Axell L., Saraiva S., Mulder E., & Fredriksson S. (2024). Hydrographic effects in Swedish waters of future offshore wind power scenarios. *Department of Research and Development, SMHI*, 37 pp. – Report Oceanography No. 77.

Bendsten J., & Jansen J.L.S. (2013). Effects of global warming on hypoxia in the Baltic Sea–North Sea transition zone. *Ecological Modelling, 264*, p. 17-26. https://doi.org/10.1016/j.ecolmodel.2012.06.018

Benjamins S., van Geel N., Hastie G., Elliott J., & Wilson B. (2017). Harbour porpoise distribution can vary at small spatiotemporal scales in energetic habitats. *Deep Sea Research Part II: Tropical Studies in Oceanography, 141*, p. 191-202. https://doi.org/10.1016/j.dsr2.2016.07.002

Bishop M.J., Mayer-Pinto M., Airoldi L., Firth L.B., Morris R.L., Loke L.H.L., Hawkins S.J., Naylor L.A., Coleman R.A., Chee S.Y., & Dafforn K.A. (2017). Effects of ocean sprawl on ecological connectivity: impacts and solutions. *Journal of Experimental Marine Biology and Ecology, 492*, p. 7-30. https://doi.org/10.1016/j.jembe.2017.01.021

Bowler D.E., & Benton T.G. (2005). Causes and consequences of animal dispersal strategies: relating individual behaviour to spatial dynamics. *Biological Reviews, 80*(2), p. 205-225.
https://doi.org/10.1017/S1464793104006645

Boulanger E., Dalongeville A., Andrello M., Mouillot D., & Manel S. (2020). Spatial graphs highlight how multi-generational dispersal shapes landscape genetic patterns. *Ecography, 43*(8), p. 1167-1179.
https://doi.org/10.1111/ecog.05024

Burchard H., Petersen O., & Rippeth T.P. (1998). Comparing the performance of the Mellor-Yamada and the κ-ε two-equation turbulence models. *Journal of Geophysical Research: Oceans, 103*(C5), p. 10543-10554. https://doi.org/10.1029/98JC00261

Cameron T.D.J., Crosby A., Balson P.S., Jeffery D.H., Lott G.K., Bulat J., & Harrison D.J. (1992). United Kingdom offshore regional report: the geology of the southern North Sea. London: HMSO for the British Geological Survey.

Christiansen N., Carpenter J.R., Daewel U., Suzuki N., & Schrum C. (2023). The large-scale impact of anthropogenic mixing by offshore wind turbine foundations in the shallow North Sea. *Frontiers in Marine Science, 10*, 1178330. https://doi.org/10.3389/fmars.2023.1178330

Clubley C.H., Silva T.A.M., Wood L.E., Firth L.B., Bilton D.T., O'Dea E., & Knights A.M. (2024). Multi-generational dispersal and dynamic patch occupancy reveals spatial and temporal stability of seascapes. *Science of the Total Environment, 952*, 175762. https://doi.org/10.1016/j.scitotenv.2024.175762

Conley D.J., Carstensen J., Ærtebjerg G., Bondo Christensen P., Dalsgaard T., Hansen J.L.S., & Josefson A.B. (2007). Long-Term Changes and Impacts of Hypoxia in Danish Coastal Waters. *Ecological Applications, 17*(5), *Supplement: Nutrient Enrichment and Estuarine Eutrophication*, p. S165-S184.

Cook E.J., Jahnke M., Kerckhof F., Minchin D., Faasse M., Boos K., & Ashton G. (2007). European expansion of the introduced amphipod *Caprella mutica* Schurin 1935. *Aquatic Invasions, 2*(4), p. 411-421. https://doi.org/10.3391/ai.2007.2.4.11

Corell H., Moksnes P-O., Engqvist A., Döös K., & Jonsson P.R. (2012). Depth distribution of larvae critically affects their dispersal and the efficiency of marine protected areas. *Marine Ecology Progress Series, 467*, p. 29-46. https://doi.org/10.3354/meps09963

Daewel U., Akhtar N., Christiansen N., & Schrum C. (2022). Offshore wind farms are projected to impact primary production and bottom water deoxygenation in the North Sea. *Communications Earth & Environment, 3*, 292. https://doi.org/10.1038/s43247-022-00625-0

Dannheim J., Bergström L., Birchenough S.N.R., Brzana R., Boon A.R., Coolen J.W.P., Dauvin J-C., De Mesel I., Derweduwen J., Gill A.B., Hutchinson Z.L., Jackson A.C., Janas U., Martin G., Raoux A., Reubens J., Rostin L., Vanaverbeke J., Wilding T.A., Wilhelmsson D., & Degraer S. (2020). Benthic effects of offshore renewables: identification of knowledge gaps and urgently needed research. *ICES Journal of Marine Science, 77*(3), p. 1092-1108. https://doi.org/10.1093/icesjms/fsz018

Degraer S., Brabant R., & Rumes B. (Eds). (2013). Environmental impacts of offshore wind farms in the Belgian part of the North Sea: Learning from the

past to optimise future monitoring programmes. *Royal Belgian Institute of Natural Sciences, Operational Directorate Natural Environment, Marine Ecology and Management Section*. 239 pp.

De Mesel I., Kerckhof F., Norro A., Rumes B., & Degraer S. (2015). Succession and seasonal dynamics of the epifauna community on offshore wind farm foundations and their role as stepping stones for non-indigenous species. *Hydrobiologia, 756*, p. 37-50. https://doi.org/10.1007/s10750-014-2157-1

Donelan S.C., Whitman Miller A., Muirhead J.R., & Ruiz G.M. (2022). Marine species introduction via reproduction and its response to ship transit routes. *Frontiers in Ecology and the Environment, 20*(10), p. 581-588. https://doi.org/10.1002/fee.2551

Energistyrelsen. (2024a). Notat om scenarier for havvindudbygning frem mod 2030. 9 pp. – J nr. 2022 – 25260

Energistyrelsen. (2024b). Notat om scenarier for havvindudbygning frem mod 2050. 12 pp. – J nr. 2022 – 25260.

Göke C., Robinson B.J.O., & Dahl K. (2025). Environmental mapping and screening of the offshore wind potential in Denmark. Sensitivity mapping: Benthic habitats and associated biological communities. *Aarhus University, DCE – Danish Centre for Environment and Energy*, 75 pp. – Scientific Report No. 642.

Gosselin L.A., & Qian P-Y. (1997). Juvenile mortality in benthic marine invertebrates. *Marine Ecology Progress Series, 146*, p. 265-282. https://doi.org/10.3354/meps146265

Hahmann A.N., Imberger M., Fischereit J., Alonso-de-Linaje N.G., & Badger J. (2025a). Environmental Mapping and Screening of the Offshore Wind Potential in Denmark. Sensitivity mapping: Wind. DTU Public report number DTU E-0255 2025.

Hahmann A.N., Imberger M., Fischereit J., Alonso-de-Linaje N.G., & Badger J. (2025b). Environmental Mapping and Screening of the Offshore Wind Potential in Denmark. Comparison of new and old simulations. DTU Public report number DTU E-262 2025.

Hansen, F.T., Gabellini A.P., Lindegren M., Munk P., Christensen A., & Edelvang K. (2021). Dispersal corridors for marine non-indigenous species in Danish waters – analysing modelled settling areas and observed occurrences. *DTU Aqua.* DTU Aqua-rapport No. 386-2021.

Heery E.C., Bishop M.J., Critchley L.P., Bugnot A.B., Airoldi L., Mayer-Pinto M., Sheehan E.V., Coleman R.A., Loke L.H.L., Johnston E.L., Komyakova V., Morris R.L., Strain E.M.A., Naylor L.A., & Dafforn K.A. (2017). Identifying the consequences of ocean sprawl for sedimentary habitats. *Journal of Experimental*

Marine Biology and Ecology, 492, p. 31-48. https://doi.org/10.1016/j.jembe.2017.01.020

Hunt H.L., & Scheibling R.E. (1997). Role of early post-settlement mortality in recruitment of benthic marine invertebrates. *Marine Ecology Progress Series, 155*, p. 269-301. https://doi.org/10.3354/meps155269

James M.K., Polton J.A., Mayorga-Adame C.G., Howell K.L., & Knights A.K. (2023). Assessing the influence of behavioural parameterisation on the dispersal of larvae in marine systems. *Ecological Modelling, 476*. https://doi.org/10.1016/j.ecolmodel.2022.110252

Jensen K.R., Andersen P., Andersen N.R., Bruhn A., Buur H., Carl H., Jakobsen H., Jaspers C., Lundgreen K., Nielsen R., Strandberg B., & Stæhr P.A.U. (2023). Reviewing Introduction Histories, Pathways, Invasiveness, and Impact of Non-Indigenous Species in Danish Marine Waters. *Diversity, 15*(3), 434. https://doi.org/10.3390/d15030434

Katsanevakis S., Zenetos A., Belchior C., & Cardoso A.C. (2013). Invading European Seas: Assessing pathways of introduction of marine aliens. *Ocean & Coastal Management, 76*, p. 64-74. https://doi.org/10.1016/j.ocecoaman.2013.02.024

Larsen J., Mohn C., Pastor A., & Maar M. (2020). A versatile marine modelling tool applied to arctic, temperate and tropical waters. *PLoS ONE, 15*(4), e0231193. https://doi.org/10.1371/journal.pone.0231193

Larsen J. (2025). FlexSem source code. *Zenodo*. https://doi.org/10.5281/zenodo.15695485

Lieber L., Nimmo-Smith W.A.M., Waggitt J.J., & Kregting L. (2019). Localised anthropogenic wake generates a predictable foraging hotspot for top predators. *Communications Biology, 2*, 123. https://doi.org/10.1038/s42003-019-0364-z

Lindström G., Pers C., Rosberg J., Strömqvist J., & Arheimer B. (2010). Development and testing of the HYPE (Hydrological Predictions for the Environment) water quality model for different spatial scales. *Hydrology Research, 41*(3-4), p. 295-319. https://doi.org/10.2166/nh.2010.007

Maar M., Friis Møller E., Larsen J., Skovgaard Madsen K., Wan Z., She J., Jonasson L., & Neumann T. (2011). Ecosystem modelling across a salinity gradient from the North Sea to the Baltic Sea. *Ecological Modelling, 222*, p. 1696-1711. https://doi.org/10.1016/j.ecolmodel.2011.03.006

Maar M., Larsen J., & Schourup-Kristensen V. (2022). FlexSem Biogeochemical model with mussel farming (version V10). *Zenodo*. https://doi.org/10.5281/zenodo.7114589

Maar M., Markager S., Skovgaard Madsen K., Windolf J., Moltke Lyngsgaard M., Estrup Andersen H., & Friis Møller E. (2016). The importance of local versus external nutrient loads for Chl *a* and primary production in the Western Baltic Sea. *Ecological Modelling, 320*, p. 258-272. https://doi.org/10.1016/j.ecolmodel.2015.09.023

Maar M., Schourup-Kristensen V., Mohn C., Ishimwe A.P., Friis Møller E., Clubley C.H., & Larsen J. (2025). Spatial impacts of offshore wind farms on hydrodynamics and biogeochemical environment. *Aarhus University, DCE – Danish Centre for Environment and Energy*, 70 pp – Scientific Report No. 658.

Ménesguen A., & Gohin F. (2006). Observation and modelling of natural retention structures in the English Channel. *Journal of Marine Systems, 63*(3-4), p. 244-256. https://doi.org/10.1016/j.jmarsys.2006.05.004

Mohn C., Maar M., & Larsen J. (2025). Ocean currents and water mass properties inside the Anholt Offshore Wind Farm (Kattegat, Denmark). *Aarhus University, DCE – Danish Centre for Environment and Energy*, 30 pp. – Technical Report No. 341.

Morel-Journel T., Assa C.R., Mailleret L., & Vercken E. (2019). It's all about connections: hubs and invasion in habitat networks. Ecology Letters, 22(2), p. 313-321. https://doi.org/10.1111/ele.13192

Nanninga G.B., & Berumen M.L. (2014). The role of individual variation in marine larval dispersal. *Frontiers in Marine Science, 1*. https://doi.org/10.3389/fmars.2014.00071

Neumann T., Radtke H., Cahill B., Schmidt M., & Rehder G. (2022). Non-Redfieldian carbon model for the Baltic Sea (ERGOM version 1.2) – implementation and budget estimates. *Geoscientific Model Development, 15*, p. 8473-8540. https://doi.org/10.5194/gmd-15-8473-2022

Oesterwind D., Dewitz B.v., Döring R., Eero M., Goti L., Kotta J., Nurske K., Ojaveer H., Rau A., Skov H., Stepputtis D., & Zaiko A. (2016). Review on patterns and dynamics of drivers of biodiversity (species, communities, habitats) across Baltic Sea ecosystems in space and time in-cluding socio-economy. *BIO-C3 Deliverable, D3.1. EU Bonusprojekt BIO-C3*, 102 pp. https://oceanrep.geomar.de/id/eprint/33168/

Ojaveer H., Jaanus A., MacKenzie B.R., Martin G., Olenin S., Radziejewska T., Telesh I., Zettler M.L., & Zaiko A. (2010). Status of biodiversity in the Baltic Sea. *PLoS one, 5*(9), e12467. https://doi.org/10.1371/journal.pone.0012467

Paris C.B., Chérubin L.M., & Cowen R.K. (2007). Surfing, spinning, or diving from reef to reef: effects on population connectivity. *Marine Ecology Progress Series, 347*, p. 285-300. https://doi.org/10.3354/meps06985

Pastor A., Larsen J., Thorbjørn Hansen F., Simon A., Bierne N., & Maar M. (2021). Agent-based modeling and genetics reveal the Limfjorden, Denmark, as a well-connected system for mussel larvae. *Marine Ecology Progress Series, 680*, p. 193-205. https://doi.org/10.3354/meps13559

Paulay G., & Meyer C. (2006). Dispersal and divergence across the greatest ocean region: Do larvae matter? *Integrative & Comparative Biology, 46*(3), p. 269-281. https://doi.org/10.1093/icb/icj027

Pergl J., Brundu G., Harrower C.A., Cardoso A.C., Genovesi P., Katsanevakis S., Lozano V., Perglová I., Rabitsch W., Richards G., Roques A., Rorke S.L., Scalera R., Schönrogge K., Stewart A., Tricarico E., Tsiamis K., Vannini A., Vilà M., Zenetos A., & Roy H.E. (2020). Applying the Convention on Biological Diversity Pathway Classification to alien species in Europe. *NeoBiota, 62*, p. 333-363. https://doi.org/10.3897/neobiota.62.53796

Pettersen S.S., Aarnes Ø., Arnesen B., Pretlove B., Ervik A.K., & Rusten M. (2023). Offshore wind in the race for ocean space: A forecast to 2050. *Journal of Physics: Conference Series, 2507*. https://doi.org/10.1088/1742-6596/2507/1/012005

Phelps J.J.C., Polton J.A., Souza A.J., & Robinson L.A. (2015). Behaviour influences larval dispersal in shelf sea gyres: *Nephrops norvegicus* in the Irish Sea. *Marine Ecology Progress Series, 518*, p. 177-191. https://doi.org/10.3354/meps11040

Quell F., Schratzberger M., Beauchard O., Bruggeman J., & Webb T. (2021). Biological trait profiles discriminate between native and non-indigenous marine invertebrates. *Aquatic Invasions, 16*(4), p. 571-600. https://doi.org/10.3391/ai.2021.16.4.01

Rennau H., Schimmels S., & Burchard H. (2012). On the effect of structure-induced resistance and mixing on inflows into the Baltic Sea: A numerical model study. *Coastal Engineering, 60*, p. 53-68. https://doi.org/10.1016/j.coastaleng.2011.08.002

Rijnsdorp A.D., Hiddink J.G., van Denderen P.D., Hintzen N.T., Eigaard O.R., Valanko S., Bastardie F., Bolam S.G., Boulcott P., Egekvist J., Garcia C., van Hoey G., Jonsson P., Laffargue P., Nielsen J.R., Piet G.J., Sköld M., & van Kooten T. (2020). Different bottom trawl fisheries have a differential impact on the status of the North Sea seafloor habitats. *ICES Journal of Marine Science, 77*(5), p. 1772-1786. https://doi.org/10.1093/icesjms/fsaa050

Rumrill S.S. (1990). Natural mortality of marine invertebrate larvae. *Ophelia, 32*(1-2), p. 163-198. https://doi.org/10.1080/00785236.1990.10422030

Sams M.A., Warren-Myers F., & Keough M.J. (2015). Increased larval planktonic duration and post-recruitment competition influence survival and growth of the bryozoan *Watersipora subtorquata*. *Marine Ecology Progress Series, 531*, p. 179-191. https://doi.org/10.3354/meps11339

Schlenger A.J., Libralato S., & Balance L.T. (2019). Temporal Variability of Primary Production Explains Marine Ecosystem Structure and Function. *Ecosystems, 22*, p. 331-345. https://doi.org/10.1007/s10021-018-0272-y

Schourup-Kristensen V., Mohn C., Larsen J., Stæhr P.U., Buur H., Dahl K., & Maar M. (2024). Spredningsveje for ikke-hjemmehørende arter i Nordsøen. En modelanalyse. *Aarhus Universitet, DCE – Nationalt Center for Miljø og Energi*, 44 s. - Teknisk rapport nr. 307.

Seebens H., Gastner M.T., & Blasius B. (2013). The risk of marine bioinvasion caused by global shipping. *Ecology Letters, 16*(6), p. 782-790. https://doi.org/10.1111/ele.12111

Shanks A.L. (2009). Pelagic Larval Duration and Dispersal Distance Revisited. *Biological Bulletin, 216*(3), p. 373-385. https://doi.org/10.1086/BBLv216n3p373

Simpson J.H., & Bowers D. (1981). Models of stratification and frontal movement in shelf seas. *Deep Sea Research Part A. Oceanographic Research Papers, 28*(7), p. 727-738. https://doi.org/10.1016/0198-0149(81)90132-1

Smagorinsky I. (1963). General circulation experiments with the primitive equations I. The basic experiment. *Monthly Weather Review, 91*(3), p. 99-164. https://doi.org/10.1175/1520-0493(1963)091<0099:GCEWTP>2.3.CO;2

Smith S.D., & Banke E.G. (1975). Variation of the sea surface drag coefficient with wind speed. *Quarterly Journal of the Royal Meteorological Society, 101*(429), p. 665-673. https://doi.org/10.1002/qj.49710142920

Soto I., Balzani P., Carneiro L., Cuthbert R.N., Macêdo R., Tarkan A.S., Ahmed D.A., Bang A., Bacela-Spychalska K., Bailey S.A., Baudry T., Ballesteros-Mejia L., Bortolus A., Briski E., Britton J.R., Buřič M., Camacho-Cervantes M., Cano-Barbacil C., Copilaş-Ciocianu D., Coughlan N.E., Courtois P., Csabai Z., Dalu T., De Santis V., Dickey J.W.E, Dimarco R.D., Falk-Andersson J., Fernandez R.D., Florencio M., Franco A.C.S., García-Berthou E., Giannetto D., Glavendekic M.M., Grabowski M., Heringer G., Herrera I., Huang W., Kamelamela K.L., Kirichenko N.I., Kouba A., Kourantidou M., Kurtul I., Laufer G., Lipták B., Liu C., López-López E., Lozano V., Mammola S., Marchini A., Meshkova V., Milardi M., Musolin D.L., Nuñez M.A., Oficialdegui F.J., Patoka J., Pattison Z., Pincheira-Donoso D., Piria M., Probert A.F., Rasmussen J.J, Renault D., Ribeiro F., Rilov G., Robinson T.B., Sanchez A.E., Schwindt E., South J., Stoett P., Verreycken H., Vilizzi L., Wang Y-J, Watari Y., Wehi P.M., Weiperth A., Wiberg-Larsen P., Yapıcı S., Yoğurtçuoğlu B., Zenni R.D., Galil B.S., Dick J.T.A., Russell J.C., Ricciardi A., Simberloff D., Bradshaw C.J.A., & Haubrock P.J. (2024). Taming the terminological tempest in invasion science. *Biological Reviews, 99*(4). P. 1357-1390. https://doi.org/10.1111/brv.13071

Stæhr P.A.U., Carbonell A., Guerin L., Kabuta S. H., Tidbury H., & Viard F. (2022). Trends in New Records of Non-Indigenous Species (NIS) Introduced by Human Activities. In: OSPAR. (2023). Quality Status Report for the Northeast Atlantic. *OSPAR Commission, London*. Available via:

https://oap.ospar.org/en/ospar-assessments/quality-status-reports/qsr-2023/indicator-assessments/trends-new-records-nis

Stefaniak L.M., & Whitlatch R.B. (2014). Life history attributes of a global invader: factors contributing to the invasion potential of *Didemnum vexillum*. *Aquatic Biology, 21*, p. 221-229. https://doi.org/10.3354/ab00591

Sundelöf A., Jonsson P.R. (2011). Larval dispersal and vertical migration behaviour – a simulation study for short dispersal times. *Marine Ecology, 33*(2), p. 183-193. https://doi.org/10.1111/j.1439-0485.2011.00485.x

Sverdrup H.U. (1953). On Conditions for the Vernal Blooming of Phytoplankton. *Journal du Conseil, 18*(3), p. 287-295. On Conditions for the Vernal Blooming of Phytoplankton | ICES Journal of Marine Science | Oxford Academic

ter Hofstede R., Driessen F.M.F., Elzinga P.J., Van Koningsveld M., & Schutter M. (2022). Offshore wind farms contribute to epibenthic biodiversity in the North Sea. *Journal of Sea Research, 185*, 102229. https://doi.org/10.1016/j.seares.2022.102229

Thorson G. (1961). Length of Pelagic Larval Life in Marine Bottom Invertebrates as Related to Larval Transport by Ocean Currents. In: Sears M. (Ed.). Oceanography, American Association for the Advancement of Science. *Washington DC, 67,* p. 455-474.

Thrush S.F., & Dayton P.K. (2002). Disturbance to Marine Benthic Habitats by Trawling and Dredging: Implications for Marine Biodiversity. *Annual Review of Ecology, Evolution and Systematics, 33*, p. 449-473. https://doi.org/10.1146/annurev.ecolsys.33.010802.150515

Tomczak M.T., Heyman J.J., Yletyinen J., Niiranen S., Otto S.A., & Blenckner T. (2013). Ecological Network Indicators of Ecosystem Status and Change in the Baltic Sea. *PLoS ONE, 8*(10), e75439. https://doi.org/10.1371/journal.pone.0075439

Trifonova N., Scott B., De Dominicis M., & Wolf J. (2022). Use of Our Future Seas: Relevance of Spatial and Temporal Scale for Physical and Biological Indicators. *Frontiers in Marine Science, 8*, 769680. https://doi.org/10.3389/fmars.2021.769680

Tsirintanis K., Azzurro E., Crocetta F., Dimiza M., Froglia C., Gerovasileiou V., Langeneck J., Mancinelli G., Rosso A., Stern N., Triantaphyllou M., Tsiamis K., Turon X., Verlaque M., Zenetos A., & Katsanevakis S. (2022). Bioinvasion impacts on biodiversity, ecosystem services, and human health in the Mediterranean Sea. *Aquatic Invasions, 17*(3), p. 308-352. https://doi.org/10.3391/ai.2022.17.3.01

van Denderen P.D., Bolam S.G., Hiddink J.G., Jennings S., Kenny A., Rijnsdorp A.D., & van Kooten T. (2015). Similar effects of bottom trawling and natural disturbance on composition and function of benthic communities across habitats. *Marine Ecology Progress Series, 541*, p. 31-43. https://doi.org/10.3354/meps11550

Vandendriessche S., Vincx M., & Degraer S. (2007). Floating seaweed and the influences of temperature, grazing and clump size on raft longevity — A microcosm study. *Journal of Experimental Marine Biology and Ecology, 343*(1), p. 64-73. https://doi.org/10.1016/j.jembe.2006.11.010

Vasquez M., Ségea B., Cordingley A., Tilb E., Wilkström S., Ehrnsten E., Al Hamdani Z., Agnesi S., Andersen M.S., Annunziatellis A., Askew N., Bekkby T., Bentes L., Daniels E., Doncheva V., Ernsten V.B., Gonçalves J., Karvinen V. Laamanen-Nicolas L., Lillis H., Loukaidi V., Manca E., McGrath F., Mo G., Monteiro P., Muresan M., Nygard H., O'Keeffe E., Pelembe T., Radicioli M., Sakellariou D., Teaca A., Todorova V., Tunesi L., & Woods H. (2023) EUSeaMap 2023, A Europe-an broad-scale seabed habitat map, Technical Report. Ref. EASME/EMFF/2020/3.1.11/Lot3/SI2.843624 – MODnet Thematic Lot n° 3 – Seabed Habitats – D1.15. EMODnet. https://doi.org/10.13155/97116

Volker P.J.H., Hahmann A.N., Badger J., & Jørgensen H. E. (2017). Prospects for generating electricity by large onshore and offshore wind farms. *Environmental Research Letters, 12*, 034022. https://doi.org/10.1088/1748-9326/aa5d86

Vuorinen I., Hänninen J., Rajasilta M., Laine P., Eklund J., Montesino-Pouzols F., Corona F., Junker K., Meier H.E.M., & Dippner J.W. (2015). Scenario simulations of future salinity and ecological consequences in the Baltic Sea and adjacent North Sea areas—implications for environmental monitoring. *Ecological Indicators, 50*, p. 196-205. https://doi.org/10.1016/j.ecolind.2014.10.019

Warner J.C., Sherwood C.R., Arango H.G., & Signell R.P. (2005). Performance of four turbulence closure models implemented using a generic length scale method. *Ocean Modelling, 8*, p. 81-113. https://doi.org/10.1016/j.ocemod.2003.12.003

Werner K.M., Haslob H., Reichel A.F., Gimpel A., & Stelzenmüller V. (2024). Offshore wind farm foundations as artificial reefs: The devil is in the detail. *Fisheries Research, 272*, 106937. https://doi.org/10.1016/j.fishres.2024.106937

Wilhelmsson D., & Malm T. (2008). Fouling assemblages on offshore wind power plants and adjacent substrata. *Estuarine, Coastal and Shelf Science, 79*(3), p. 459-466. https://doi.org/10.1016/j.ecss.2008.04.020

Wiltshore K.H., & Manly B.F.J. (2004). The warming trend at Helgoland Roads, North Sea: phytoplankton response. *Helgoland Marine Research, 58*, p. 269-273. https://doi.org/10.1007/s10152-004-0196-0

Windolf J., Thodsen H., Troldborg L., Larsen S.E., Bøgestrand J., Ovesen N.B., & Kronvang B. (2011). A distributed modelling system for simulation of monthly runoff and nitrogen sources, loads and sinks for ungauged catchments in Denmark. *Journal of Environmental Monitoring, 13*, p. 2645-2658. https://doi.org/10.1039/C1EM10139K

Wood L.E., Silva T.A.M, Heal R., Kennerley A., Stebbing P., Fernand L., & Tidbury H.J. (2021). Unaided dispersal risk of *Magallana gigas* into and around the UK: combining particle tracking modelling and environmental suitability scoring. *Biological Invasions, 23*, p. 1719-1738. https://doi.org/10.1007/s10530-021-02467-x

Zenetos A., Tsiamis K., Galanidi M., Carvalho N., Bartilotti C., Canning-Clode J., Castriota L., Chainho P., Comas-González R., Costa A.C., Dragičević B., Dulčić J., Faasse M., Florin A-B., Gittenberger A., Jakobsen H., Jelmert A., Kerckhof F., Lehtiniemi M., Livi S., Lundgreen K., Macic V., Massé C., Mavrič B., Naddafi R., Orlando-Bonaca M., Petovic S., Png-Gonzalez L., Carbonell Quetglas A., Ribeiro R.S., Cidade T., Smolders S., Stæhr P.A.U., Viard F., & Outinen O. (2022). Status and Trends in the Rate of Introduction of Marine Non-Indigenous Species in European Seas. *Diversity, 14*(12), 1077. https://doi.org/10.3390/d14121077

Appendix A. Model validation and quality assurance

Validation of the applied models

Applied metrics

Model results of water level, temperature, salinity, nitrate, phosphate, Chl *a* and oxygen were validated against monitoring data. The correlation coefficient, *R*, was estimated using Pearson's with a type 2 error of 5%. A high correlation coefficient indicates a good agreement between observations and model results. *R* is sensitive to extreme values and seasonal timing, but not to a consistent bias between observations and model.

A cost function, *CF*, was used to assess the model performance:

$$CF = \frac{\sum_{i=1}^{N}|M_i - O_i|}{N \times STD_O} \quad \text{(eq. 1)}$$

Where *N*= number of data points, *M*= model data, *O*= observational data, STD_O = standard deviation of the observations (Radach & Moll 2006). According to the *CF* value, the model performance can be good (*CF* <1), reasonable (*CF* =1-2) or poor (*CF* >2) (Eilola et al. 2011). Hence, the model results are interpreted as good if the model mean deviates with less than plus or minus one standard deviation from the observed mean. The *CF* is sensitive to extreme values and consistent bias.

The normalized standard deviation, *nSTD*, was estimated as the ratio between the standard deviations of model data (STD_M) and observational data:

$$nSTD = \frac{STD_M}{STD_O} \quad \text{(eq. 2)}$$

The results are interpretated as good if the *nSTD* is within 1±0.25 (Eilola et al. 2011). The *nSTD* is a measure of the variability between observations and model results and is sensitive to extreme values.

North Sea validation

Model results from REF-NO-FARM were compared with tidal, remote sensing and monitoring data from 2020.

Water level measurements from tide gauge stations in Danish North Sea Waters are provided by the Danish Meteorological Institute (DMI) (https://www.dmi.dk/friedata/observationer) and the Danish Coastal Authority. The reference value for water level is DVR90 (Danish Vertical Reference 1990). DMI water level observations were compared with corresponding model data at three North Sea tide gauge stations — Hirtshals, Hanstholm,

and Thyborøn — for October 2020, which was selected arbitrarily for clarity (Figure A1.2).

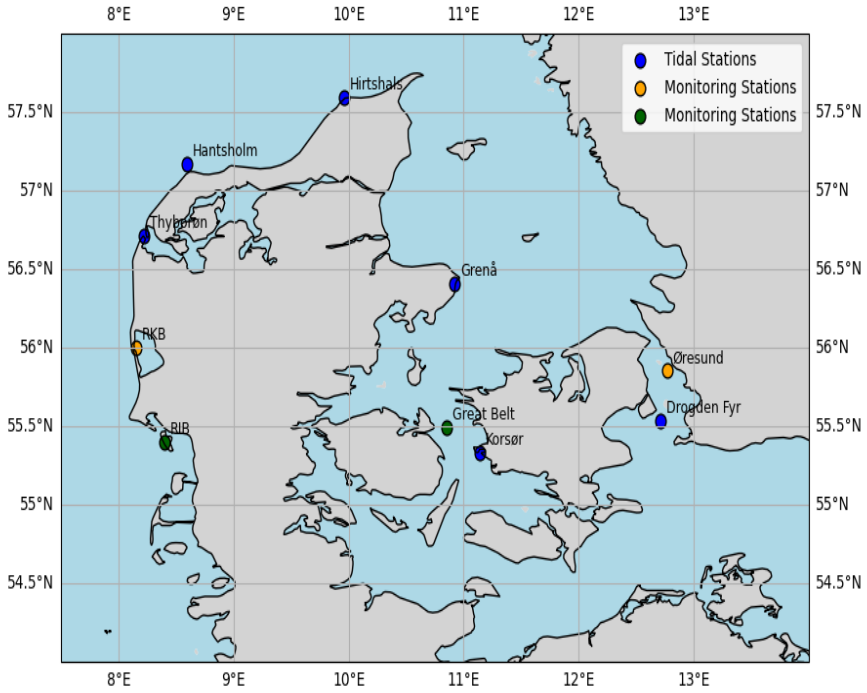

Figure A1.1. Map of tidal and monitoring stations used for model validation. The DMI tidal stations were used to validate water levels. The North Sea coastal monitoring stations, RKB (orange point) and RIB (green point) and the two Inner Danish waters stations Great Belt (green point) and Øresund (orange point) are used to validate biogeochemical parameters, temperature and salinity.

Table A1.1. Model validation against time-series of water level (SSH, 3-hourly) and SST observations (daily) at three different tidal station locations in the eastern North Sea along the Danish NW coast (see Figure A1.1 for an overview of station locations) in October 2020. CMEMS remote sensing locations for SST validation were extracted at the nearest DMI tidal station locations. The metrics used are *N* (number of data points), *R* (Pearson correlation), *p* value, normalized standard deviation (n*STD*) and cost function *CF*.

Tidal Station	**unit**	***N***	***R***	***p***	***nSTD***	***CF***
SSH						
Hirtshals	m	244	0.77	<0.01	1.26	0.66
Hanstholm	m	244	0.90	<0.01	0.96	0.36
Thyborøn	m	244	0.89	<0.01	0.82	0.50
SST						
Hirtshals	°C	366	0.98	<0.01	0.92	0.11
Hanstholm	°C	366	0.98	<0.01	0.92	0.08
Thyborøn	°C	366	0.97	<0.01	0.94	0.09

The model results for water levels showed a generally good model performance with strong agreement between simulated and observed water levels along the Danish North Sea coast. The Cost Function (*CF*) values were consistently below 0.7, and the normalized standard deviation (*nSTD*) values remained within 1±0.26, both indicating good model skill (Table A1.1). At the Thyborøn station (Figure A1.2c), the model slightly underestimated the observed water level amplitudes but accurately reproduced the temporal

variability. The discrepancies between the observed and simulated water levels at this particular location are most likely due to the complex interactions between the open-water tides and the entrance to the Limfjord. Good agreements between modelled and observed water levels were also obtained for other months in 2020, indicating a robust model performance.

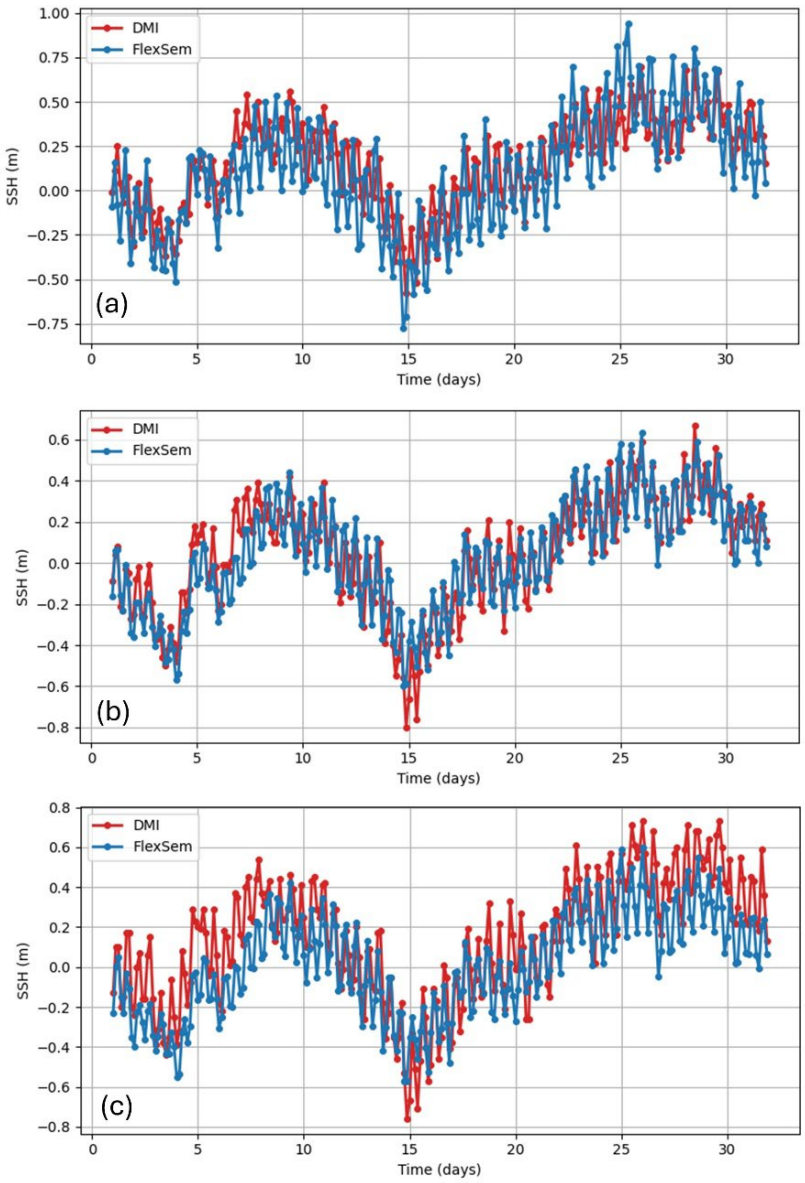

Figure A1.2. Comparison of 3-hourly model results (blue line) versus observed (red line) water level data at three North Sea DMI tidal stations (a) Hirtshals, (b)Hanstholm and (c) Thyborøn.

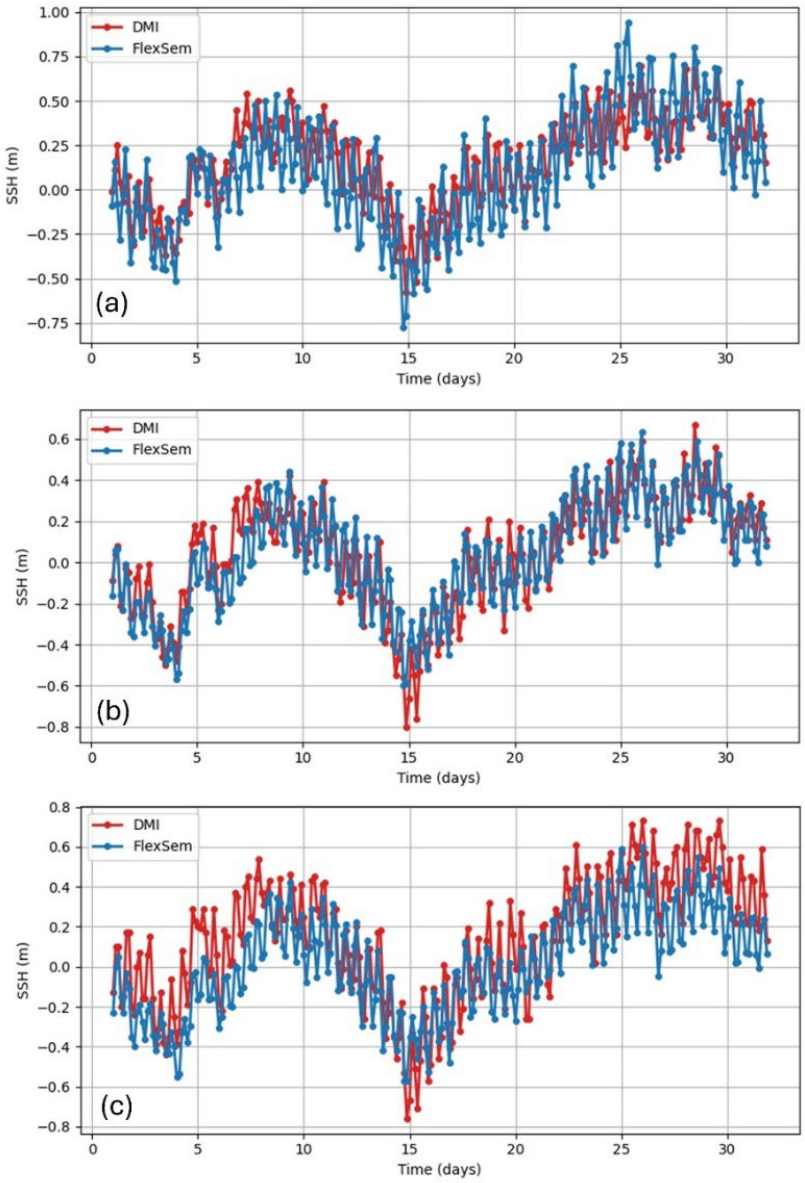

Figure A1.3. Comparison between daily modelled (blue line) and observed (red line) sea surface temperatures (SST) at locations nearest to three North Sea DMI tidal stations: (a) Hirtshals, (b) Hanstholm, and (c) Thyborøn.

Daily 2020 sea surface temperatures (SST) were extracted from the CMEMS North Sea / Baltic Sea remote sensing data set with corresponding model SSTs at the nearest tidal locations. The remote sensing data provide daily multi-sensor data at a 0.02° x 0.02° horizontal resolution, using satellite data from infra-red radiometers (Figure A1.3). The remote sensing data are available at: (https://data.marine.copernicus.eu/product/SST_BAL_SST_L3S_NRT_OBSERVATIONS_010_032/description). The SST model-data comparison showed a very good agreement between model and observations in both timing and magnitude of temperatures over most of the year with some underestimation of summer peak temperatures. However, the model performance metrics indicate generally good model performance at all station locations with *CF* values consistently below 0.2 (Table A1.1; Figure A1.3).

Two coastal stations, RIB and RKB, sampled with up to 19 samples per year, were also included in the analysis. The measured variables were surface temperature, salinity, nitrate, phosphate, Chlorophyll *a* (Chl *a*) and oxygen. Time-series data of surface temperature and salinity from RKB and RIB confirmed an overall good agreement between model and observations (Table A1.2, Figure A1.4). At both RIB and RKB, initial surface nitrate was underestimated causing a too low *nSTD* in the model. Model Chl *a* concentrations at RIB showed too high values during summer and there was no significant correlation with observations for both stations (Figure A1.4e). Phosphate and oxygen showed a high correlation between model results and observations. The cost functions indicated good model performance for all variables at both stations.

Table A1.2. Model validation against time-series of monitoring data from RIB and RKB coastal stations.

Variable	unit	*N*	*R*	*p*	*nSTD*	*CF*
RIB station						
Temperature	°C	12	0.99	<0.01	1.14	0.00
Salinity	psu	12	0.82	<0.01	0.91	0.94
Nitrate	mmol m^{-3}	16	0.93	<0.01	0.41	0.42
Phosphate	mmol m^{-3}	16	0.89	<0.01	0.85	0.00
Chl *a*	mg m^{-3}	15	0.23	ns	2.28	0.97
Oxygen	mmol m^{-3}	15	0.91	<0.01	1.26	0.14
RKB station						
Temperature	°C	19	0.97	<0.01	0.94	0.07
Salinity	psu	19	0.64	<0.01	1.13	0.24
Nitrate	mmol m^{-3}	19	0.96	<0.01	0.29	0.37
Phosphate	mmol m^{-3}	19	0.92	<0.01	0.88	0.19
Chl *a*	mg m^{-3}	19	0.20	Ns	2.03	0.27
Oxygen	mmol m^{-3}	15	0.93	<0.01	1.05	0.11

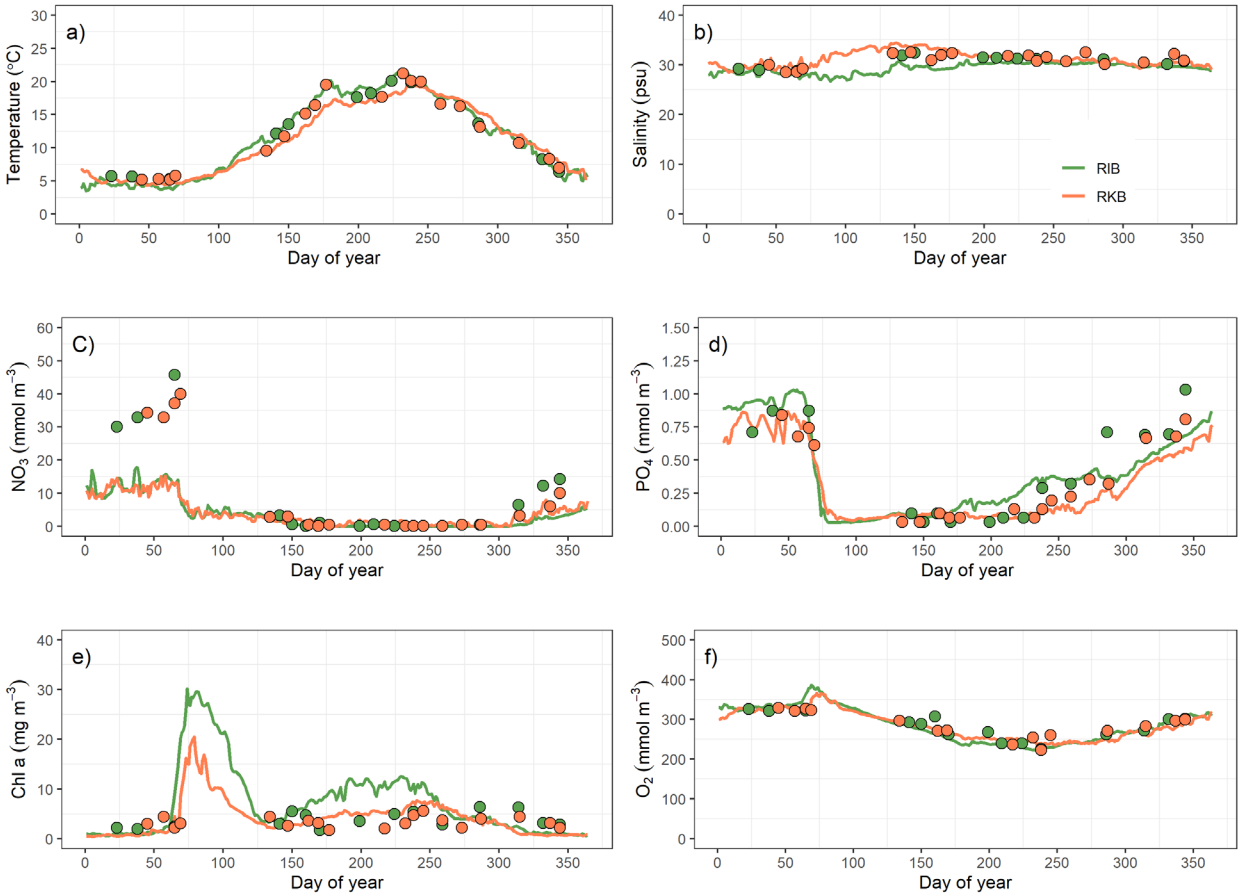

Figure A1.4. Comparison of model results (solid lines) versus monitoring data (points) from the two coastal stations RIB (green) and RKB (orange) of A) surface temperature, B) surface salinity, C) surface nitrate concentration, D) surface phosphate concentration, E) surface Chl *a* concentration, and F) surface oxygen concentration in 2020.

Inner Danish waters validation

Water level measurements from tide gauge stations in Inner Danish Waters are provided by the Danish Meteorological Institute (DMI) (https://www.dmi.dk/friedata/observationer) and the Danish Coastal Authority. The reference value for water level is DVR90 (Danish Vertical Reference 1990). DMI water level observations were compared with corresponding model data at three tide gauge stations — Grenå (Kattegat), Korsør (Great Belt), and Drogden Fyr (Øresund) — for October 2020, which was selected arbitrarily for clarity (Figure A1.5).

Figure A1.5. Comparison of model results (blue line) versus observed (red line) water level data from the three DMI tidal stations (a) Grenå (Kattegat), (b) Korsør (Great Belt) and (c) Drogden Fyr (Øresund).

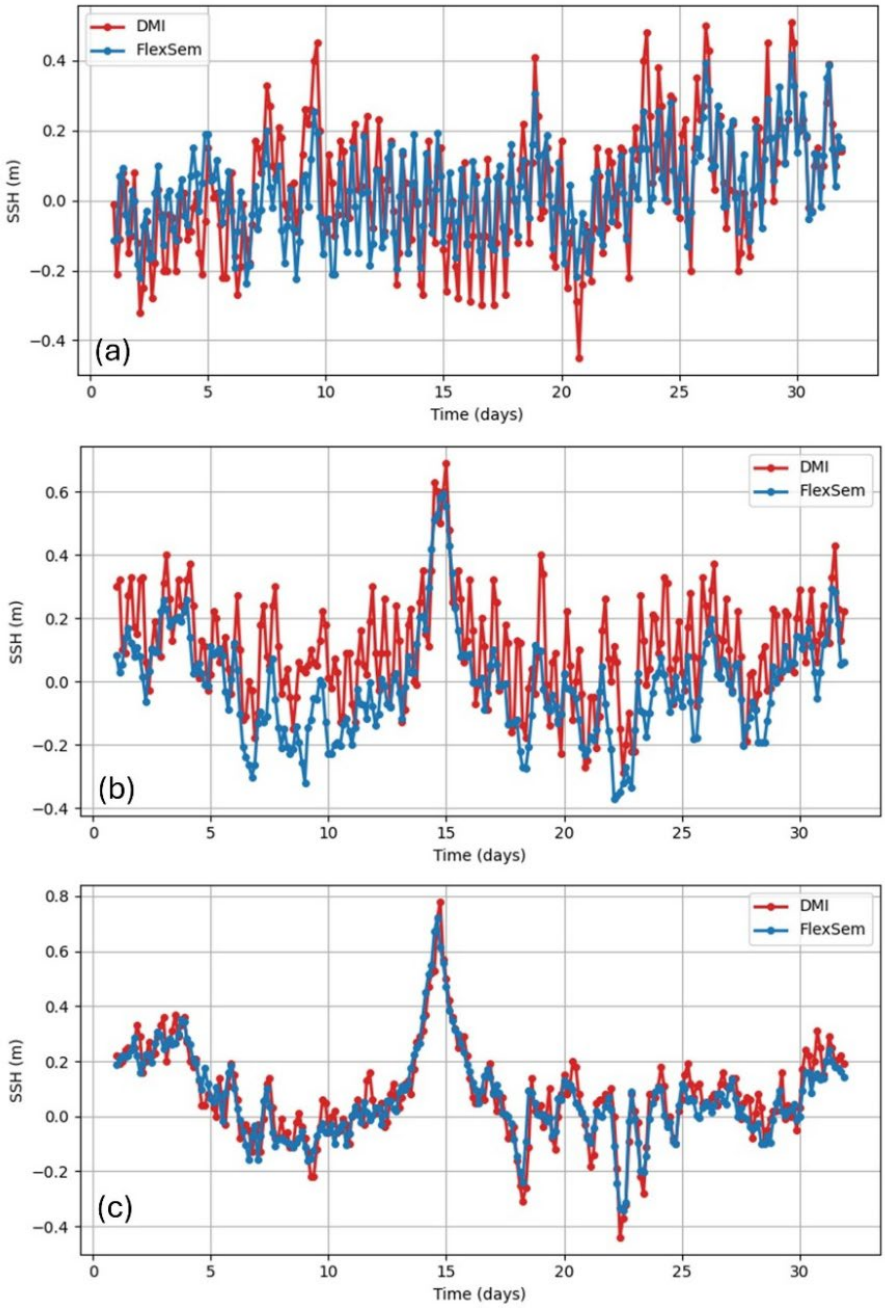

Table A1.3. Model validation against time-series of water level observations from three different tidal stations in the Kattegat, Great Belt and Øresund (see Figure A1.1 for an overview of station locations) for October 2020.

Tidal Station	unit	*N*	*R*	*p*	*nSTD*	*CF*
SSH						
Grenå (Kattegat)	m	244	0.73	<0.01	0.74	0.54
Korsør (Great Belt)	m	244	0.73	<0.01	1.00	0.79
Drogden Fyr (Øresund)	m	244	0.93	<0.01	0.95	0.29
SST						
Grenå (Kattegat)	°C	247	0.98	<0.01	0.93	0.16
Korsør (Great Belt)	°C	265	0.98	<0.01	0.97	0.13
Drogden Fyr (Øresund)	°C	258	0.97	<0.01	0.83	0.18

The FlexSem model demonstrated generally good performance, showing strong agreement between simulated and observed water levels. The Cost Function (CF) values were consistently below 0.8, and the normalized standard deviation (nSTD) values remained within 1±0.26, both indicating good model skill (Table A1.3). At the coastal stations Grenå and Korsør, the model slightly underestimated the observed water level amplitudes but successfully reproduced the temporal variability. The best agreement was observed at the more open-water station, Drogden Fyr (Figure A1.5c). Similar results were obtained for other months in 2020, indicating a robust model performance.

Daily 2020 SST data were obtained from the same CMEMS North Sea/Baltic Sea remote sensing dataset, with corresponding modelled SSTs extracted at the nearest IDW tidal station locations used for the comparison between model and observations. Once again, we observe a good agreement between the modelled and observed SSTs in both the magnitude and timing of temperature variations throughout most of the year, with an underestimation of summer peak temperatures only at the Øresund station. Model performance metrics similarly indicate good model performance across all station locations, with CF values again consistently below 0.2 (Table A1.3; Figure A1.6).

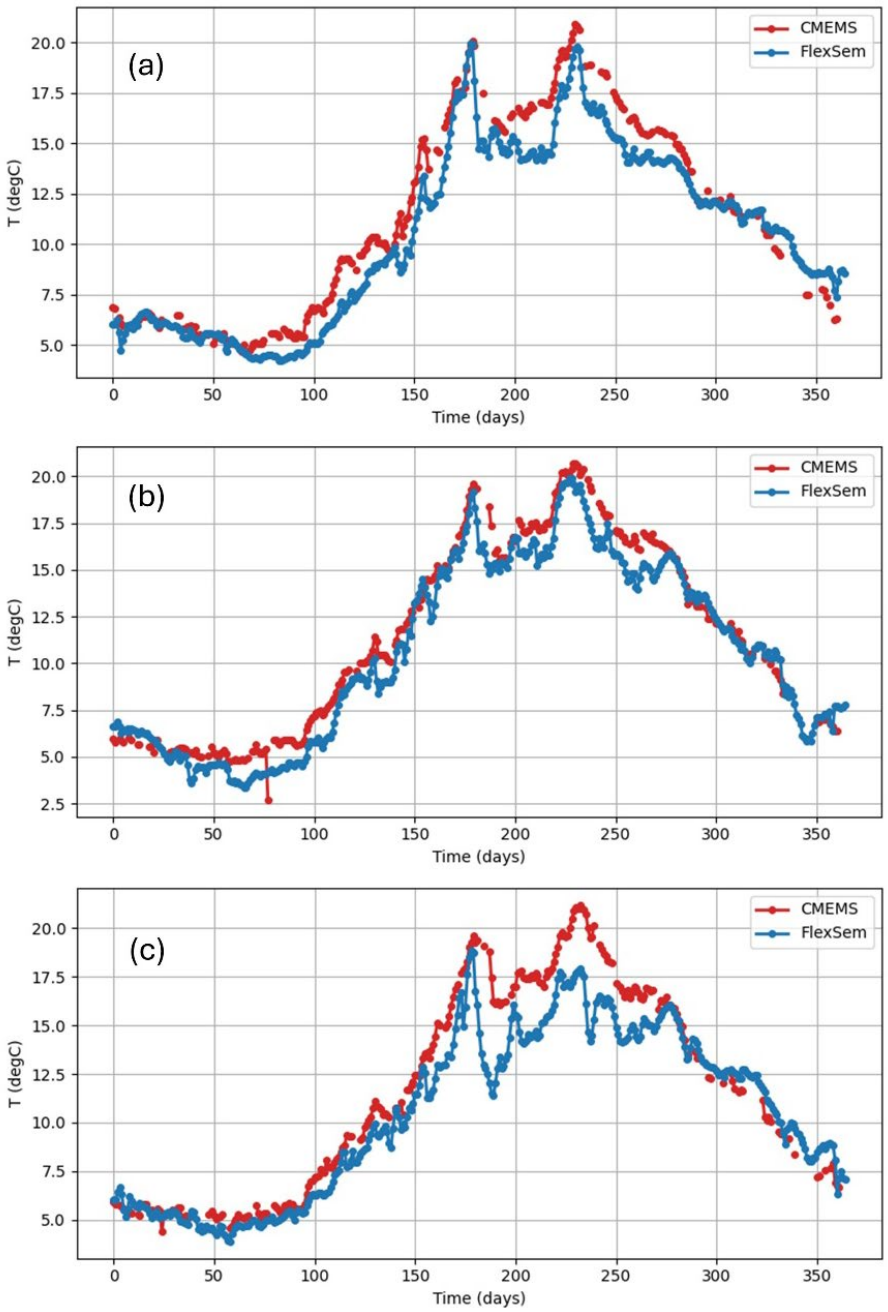

Figure A1.6. Comparison between daily modelled (blue line) and observed (red line) sea surface temperatures (SST) at locations nearest to three IDW DMI tidal stations: (a) Grenå (Kattegat, (b) Korsør (Great Belt), and (c) Drogden Fyr (Øresund).

In addition, model results in REF-NO-FARM from two stations in the Great Belt and the Øresund, in the Inner Danish waters were compared with monitoring data from 2020. The two stations were chosen because they are located at two important sites for the water exchange between the Kattegat and the Baltic Sea. The tested variables were surface temperature, salinity, nitrate, phosphate, Chl *a*, and surface- and bottom oxygen. The variables at the open water stations showed high correlations (R>0.50), except for Chl *a* concentrations (Table A1.4). The spring phytoplankton bloom started a bit too late and there was no autumn bloom in the model. The normalized standard deviation was too low for Chl *a* indicating too low seasonal variation in the model. The cost function indicated

good to reasonable model performance for all variables. Initial nitrate concentrations were too low in the model at both stations. Phosphate concentrations were generally too high during the summer months in Øresund. Overall, the main seasonal characteristics were reproduced by the model (Figure A1.7).

Table A1.4. Model validation against surface monitoring data for two stations in the Inner Danish waters.

Variable	Unit	*N*	*R*	*P*	*nSTD*	*CF*
Great Belt						
Temperature	Degree C	17	0.83	<0.0001	0.86	0.50
Salinity	Psu	17	0.64	<0.01	0.73	1.17
Nitrate	mmol m^{-3}	19	0.70	<0.0001	0.56	0.48
Phosphate	mmol m^{-3}	19	0.92	<0.0001	0.57	0.49
Chl a	mg m^{-3}	19	-0.1	0.68	0.49	1.4
Oxygen surf	mg L^{-3}	17	0.87	<0.0001	0.89	0.53
Oxygen bot	mg L^{-3}	17	0.68	<0.01	0.46	0.99
Øresund						
Temperature	Degree C	17	0.84	<0.0001	0.76	0.55
Salinity	Psu	17	0.66	<0.01	1.15	0.91
Nitrate	mmol m^{-3}	19	0.79	<0.0001	0.77	0.45
Phosphate	mmol m^{-3}	19	0.51	0.027	0.52	0.92
Chl a	mg m^{-3}	19	-0.06	0.8	0.45	0.69
Oxygen surf	mg L^{-3}	16	0.76	<0.001	0.88	0.59
Oxygen bot	mg L^{-3}	16	0.73	<0.01	0.58	1.1

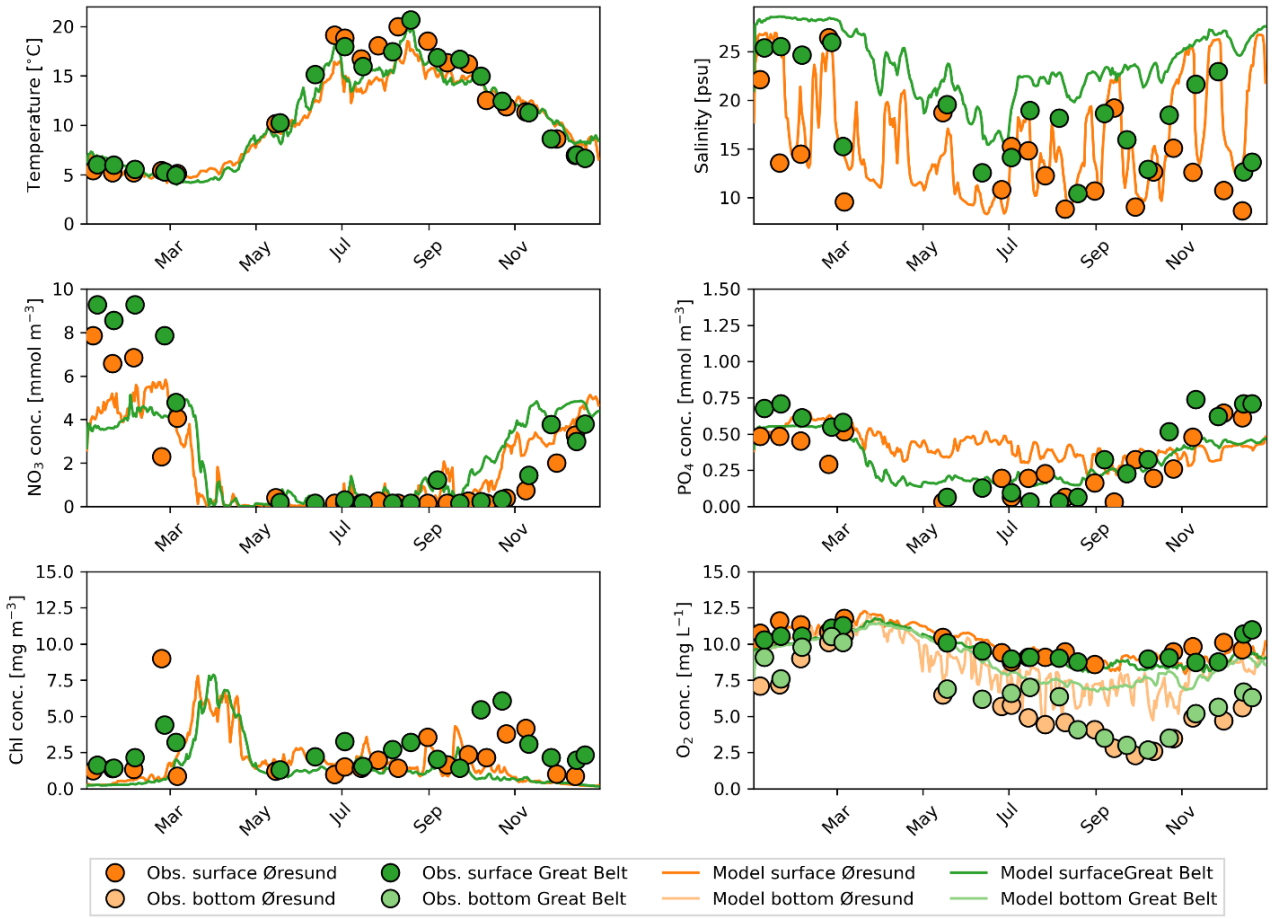

Figure A1.7. Comparison of model results (solid lines) versus monitoring data (points) from the two monitoring stations Great Belt (green) and the Øresund (orange) of A) surface temperature, B) surface salinity, C) surface nitrate concentration, D) surface phosphate concentration, E) surface Chl *a* concentration, and F) surface and bottom oxygen concentration in 2019.

Model quality assurance

The FlexSem model source code is open access and available on zenodo.org (Larsen 2025, Maar et al. 2025) and the FlexSem home page (FlexSem). The hydrodynamic and biogeochemical models have been described and validated in previous publications (Larsen et al. 2020, Maar et al. 2020, Schourup-Kristensen et al. 2024). The applied model versions were validated against monitoring data as described in the previous sections.

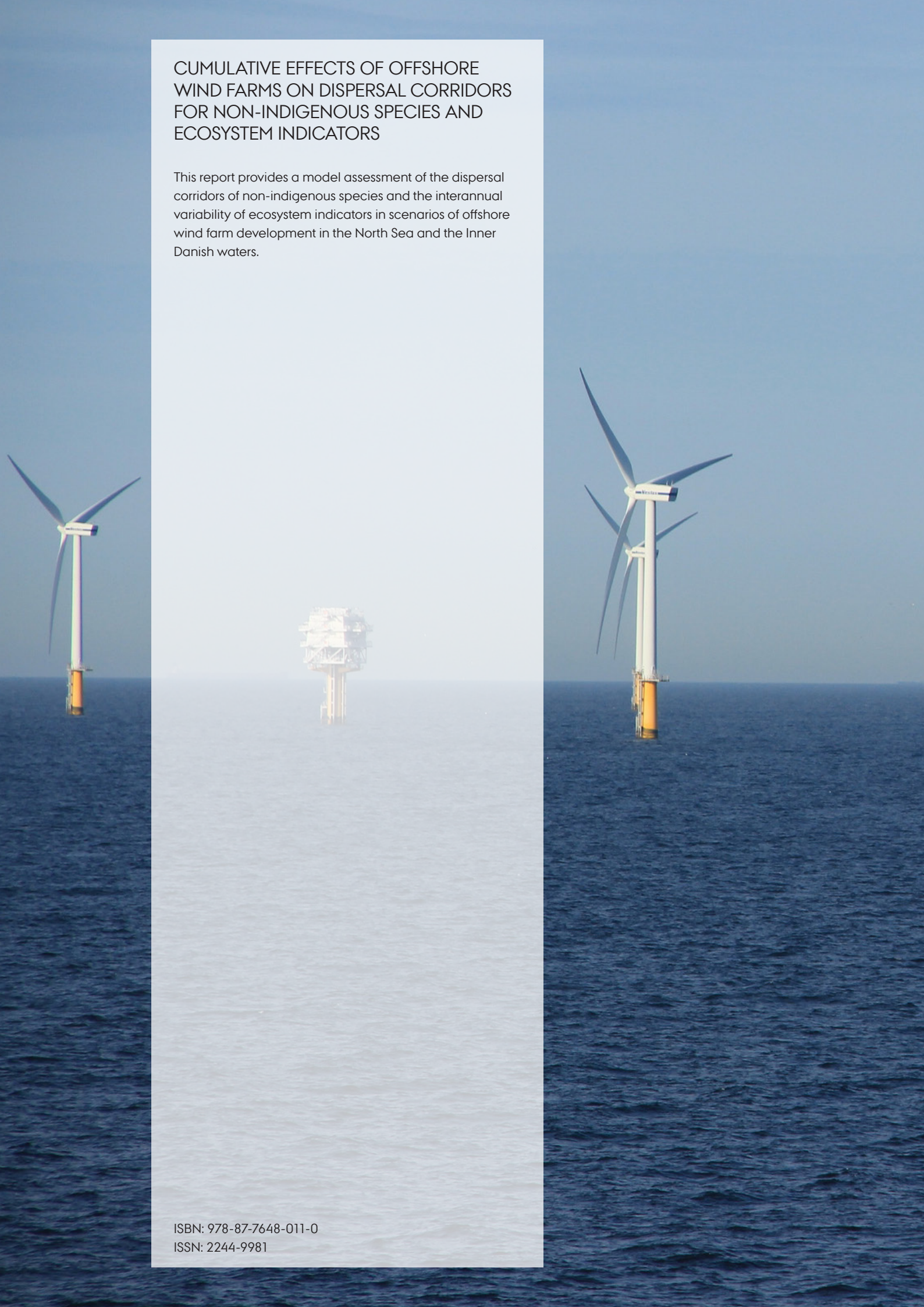

CUMULATIVE EFFECTS OF OFFSHORE WIND FARMS ON DISPERSAL CORRIDORS FOR NON-INDIGENOUS SPECIES AND ECOSYSTEM INDICATORS

This report provides a model assessment of the dispersal corridors of non-indigenous species and the interannual variability of ecosystem indicators in scenarios of offshore wind farm development in the North Sea and the Inner Danish waters.

ISBN: 978-87-7648-011-0
ISSN: 2244-9981